TUULIA TYNKKYNEN

¹H NMR Analysis of Serum Lipids

UNIVERSITY OF
EASTERN FINLAND

TUULIA TYNKKYNEN

^{1}H NMR Analysis
of Serum Lipids

Academic Dissertation

To be presented by permission of the Faculty of Science and Forestry for public examination in the Auditorium L22 in Snellmania Building at the University of Eastern Finland, Kuopio, on June, 28, 2012, at 12 o´clock noon.

School of Pharmacy

Author's address: University of Eastern Finland
                           School of Pharmacy
                           P.O. Box 1627
                           70211 KUOPIO
                           FINLAND
                           e-mail: tuulia.tynkkynen@uef.fi

Supervisors: Professor Reino Laatikainen, Ph.D.
                           University of Eastern Finland
                           School of Pharmacy
                           P.O. Box 1627
                           70211 KUOPIO
                           FINLAND
                           e-mail: reino.laatikainen@uef.fi

                           Pasi Soininen, Ph.D.
                           University of Eastern Finland
                           School of Pharmacy
                           P.O. Box 1627
                           70211 KUOPIO
                           FINLAND
                           e-mail: pasi.soininen@uef.fi

Reviewers: Bernd Diehl, Ph.D.
                           Spectral Service AG
                           Emil-Hoffmann-Str. 33
                           D-50996 KÖLN
                           GERMANY
                           e-mail: diehl@spectralservice.de

                           Docent Katariina Öörni, Ph.D.
                           Wihuri Research Institute
                           Kalliolinnantie 4
                           00140 HELSINKI
                           FINLAND
                           e-mail: kati.oorni@wri.fi

Opponent: Docent Hannu Maaheimo, Ph.D.
                             VTT Technical Research Centre of Finland
                             P.O. Box 65 (Viikinkaari 1)
                             00014 HELSINKI
                             FINLAND
                             e-mail: hannu.maaheimo@helsinki.fi

ABSTRACT

Many diseases, for example Alzheimer's disease and type 1 diabetes, alter lipid metabolism. The analysis of serum lipid composition by conventional methods is time-consuming and requires a combination of several analytical techniques such as thin-layer chromatography, gas chromatography, and high-performance liquid chromatography. Nuclear magnetic resonance (NMR) spectroscopy has become an alternative method that offers a rapid analysis of serum lipids requiring only a little sample preparation.

In the present thesis, ^{1}H NMR-based protocols for the analysis of serum lipids were developed and applied to clinical studies. The developed extraction and quantification protocol allows processing of about 100 samples per day. The protocol was applied to two clinical studies. The results from a study involving patients with mild cognitive impairment indicated that a low relative amount of ω-3 fatty acids is related to mild cognitive impairment. Another study revealed the association between sphingomyelin and kidney disease in type 1 diabetic patients. In addition, an NMR-based oxidation assay for serum was developed and applied to a dietary intervention study. The NMR assay was shown to be more sensitive than the commonly used spectrophotometric assay.

A part of the thesis was to perform quantum mechanical spectral analyses for short *n*-alkanes. It was proved that the proportion of the *trans* conformations increases when the hydrocarbon chain is lengthened, and the chemical environment has only a small effect on the conformational equilibrium.

It can be concluded that the developed protocols for serum lipid analyses provide valuable information about the lipid components of serum, as well as the oxidation susceptibility of serum lipids.

Preface

LIST OF ABBREVIATIONS

1D	one-dimensional
2D	two-dimensional
Aβ	amyloid-β
ACAT	acyl-CoA-cholesterol acyl transferase
ACP	acyl carrier protein
AD	Alzheimer's disease
AER	albumin excretion rate
ANOVA	analysis of variance
APP	amyloid precursor protein
BMI	body mass index
C1P	ceramide-1-phosphate
CDP-DAG	cytidine diphospho-DAG
CE	cholesteryl ester
CLA	conjugated linoleic acid
CoA	coenzyme A
CTLS	constrained total-line-shape
CYP4	cytochrome P450 4
DAG	diacylglyceride
DC	dark chocolate
DGLA	dihomo-γ-linolenic acid
DHA	docosahexaenoic acid
DHB	2,5-dihydroxybenzoic acid
DMSO	dimethylsulfoxide
EDTA	ethylenediaminetetraacetic acid
EPA	eicosapentaenoic acid
ER	endoplasmic reticulum
ESI	electrospray ionization
FA	fatty acid
FA-CoA	fatty acyl-coenzyme A-thioester
FAME	FA methyl ester
FAS	fatty acid synthase
FFA	free fatty acid
FID	free induction decay
FTICR-MS	Fourier transform ion cyclotron resonance MS

G-3-P	glycerol-3-phosphate
GC	gas chromatography
HDL	high-density lipoprotein
HMG-CoA	β-hydroxy-β-methylglutaryl-CoA
HPC	high-polyphenol chocolate
HPLC	high-performance liquid chromatography
HPTLC	high-performance TLC
HSL	hormone-sensitive lipase
IDL	intermediate-density lipoprotein
LCAT	lecithin-cholesterol acyl transferase
LDL	low-density lipoprotein
LPC	lysophosphatidylcholine
LSD	light scattering detector
MAG	monoacylglyceride
MALDI	matrix assisted laser desorption ionization
MCI	mild cognitive impairment
MOD-TLC	multi-one-dimensional TLC
MS	mass spectrometry
MS/MS	tandem MS
MTBE	methyl-*tert*-butyl ether
MUFA	monounsaturated fatty acid
m/z	mass-to-charge ratio
NCEP-ATP III	National Cholesterol Education Program's Adult Treatment Panel III
NMR	nuclear magnetic resonance
NP-HPLC	normal-phase HPLC
PAF	platelet-activating factor
PC	phosphatidylcholine
PE	phosphatidylethanolamine
PI	phosphatidylinositol
PL	phospholipid
PLA_2	phospholipase A-2
PPAR	peroxisome proliferator-activated receptor
ppm	parts per million
PS	phosphatidylserine
PUFA	polyunsaturated FA
R_F	retardation factor

RP-HPLC	reverse-phase HPLC
S1P	sphingosine-1-phosphate
S/N	signal-to-noise ratio
SFA	saturated FA
SM	sphingomyelin
SOM	self-organizing map
SPC	sphingosylphosphorylcholine
SPE	solid-phase extraction
SREBP	sterol regulatory element binding protein
TAG	triacylglyceride
TFA	*trans* fatty acid
TLC	thin-layer chromatography
TLS	total-line-shape
TOF	time-of-flight
UPLC	ultra-performance liquid chromatography
UV	ultraviolet
WC	white chocolate
VLDL	very-low-density lipoprotein

LIST OF ORIGINAL PUBLICATIONS

This thesis is based on data presented in the following articles*, referred to by the Roman numerals I–IV.

I   Tynkkynen T, Hassinen T, Tiainen M, Soininen P and Laatikainen R. ^{1}H NMR spectral analysis and conformational behavior of *n*-alkanes in different chemical environments. *Magnetic Resonance in Chemistry.* Submitted.

II   Tukiainen T, Tynkkynen T, Mäkinen V-P, Jylänki P, Kangas A, Hokkanen J, Vehtari A, Gröhn O, Hallikainen M, Soininen H, Kivipelto M, Groop P-H, Kaski K, Laatikainen R, Soininen P, Pirttilä T, Ala-Korpela M. A multi-metabolite analysis of serum by ^{1}H NMR spectroscopy: Early systemic signs of Alzheimer's disease. *Biochemical and Biophysical Research Communications 375: 356-361, 2008.*

III   Mäkinen V-P, Tynkkynen T, Soininen P, Forsblom C, Peltola T, Kangas AJ, Groop P-H and Ala-Korpela M. Sphingomyelin is associated with kidney disease in type 1 diabetes (The FinnDiane Study). *Metabolomics 8: 369-375, 2012.*

IV   Tynkkynen T, Mursu J, Nurmi T, Laatikainen R, Soininen P. NMR protocol for determination of oxidation susceptibility of serum lipids and application of the protocol to a chocolate study. *Metabolomics 8: 386-398, 2012.*

*Some unpublished data are also presented.

The publications are reproduced with kind permission of the copyright holders.

AUTHOR'S CONTRIBUTION

The author prepared all the study samples and acquired the spectra for the publication I. The author also performed most of the spectral analyses. In addition, the author contributed to the interpretation of the data and wrote a majority of the manuscript.

The author developed the extraction and quantification protocols for serum lipids that were used in the study II. In addition, the author extracted the serum lipids from the study samples, measured both the native and extracted serum samples, and quantified the ^{1}H NMR lipid spectra. The author also wrote the aforementioned sections to the manuscript, as well as revised the whole manuscript.

For the publication III, the author extracted serum lipids from the study samples, measured the ^{1}H NMR spectra of the lipid extracts, and quantified lipids from the spectra. In addition, the author contributed to the interpretation of the results, as well as writing of the manuscript.

The author planned the study IV together with the supervisors. The author performed all the experimental work in the development of the NMR oxidation assay and prepared, extracted, measured, and quantified all the study samples. The author also performed the SPSS data analysis and interpreted the random forest results. In addition, the author wrote the manuscript.

Contents

1 Review of the literature

1.1 STRUCTURE OF LIPIDS

There is a variety of biological lipids, and their common character is their insolubility in water (Nelson & Cox 2000). Lipids can be divided into eight categories including fatty acyls, glycerolipids, glycerophospholipids, sphingolipids, sterol lipids, prenol lipids, saccharolipids, and polyketides (Fahy et al. 2005). This thesis concentrates on the serum lipids, and thus, the three latter groups are not discussed.

1.1.1 Fatty acyls

Fatty acyls, or commonly fatty acids (FAs), are structurally the simplest lipids, and they are basic elements of many lipid groups. Natural FAs have hydrocarbon chains varying in length from 14 to 24 carbon atoms (Hu et al. 2009). These FAs have usually even number of carbon atoms in an unbranched chain (Otieno & Mwongela 2008). FAs can be either saturated (no double bonds) or unsaturated (1 to 6 double bonds) (Hu et al. 2009). The double bonds of polyunsaturated FAs (PUFAs) are separated by a methylene group (=CH-**CH2**-CH=), and conjugated double bonds are normally not present in natural PUFAs. In naturally occurring unsaturated FAs, the double bonds are usually in the *cis* configuration (Ratnayake & Galli 2009).

The nomenclature of FAs indicates the chain length and the number of double bonds (Nelson & Cox 2000). For example, 18-carbon linoleic acid with two double bonds is named as 18:2. The positions of double bonds can be reported in two ways. Firstly, the carbons where the double bonds are located are counted by starting from the carbonyl carbon and they are specified by superscript numbers following delta (Δ) (Ruiz-Rodriguez et al. 2010). E.g. for linoleic acid, $18:2(\Delta^{9,12})$. Secondly,

it is possible to use n-x, or ω-x nomenclature, where the first double bond is located at the xth carbon counting from the terminal methyl carbon of the FA molecule (Figure 1) (Ruiz-Rodriguez et al. 2010). Common names and structures of different types of FAs found in human serum are shown in Figure 1.
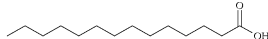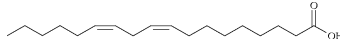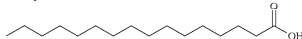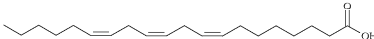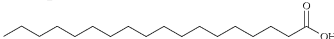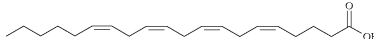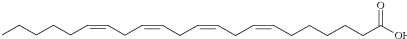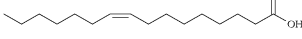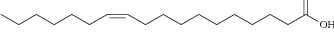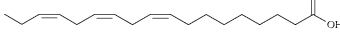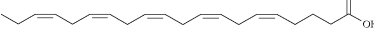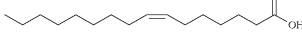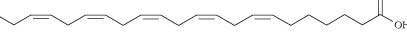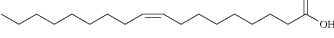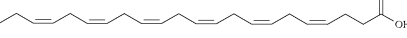
Figure 1. *Common names and structures of different types of fatty acids found in human serum (Assies et al. 2010). DGLA, dihomo-γ-linolenic acid; DHA, docosahexaenoic acid; DPA, docosapentaenoic acid; EPA, eicosapentaenoic acid; MUFA, monounsaturated fatty acid; PUFA, polyunsaturated fatty acid*

1.1.2 Glycerolipids

Glycerolipids are compounds in which one, two or three FAs are attached to a glycerol molecule, and they are called mono- (MAG), di- (DAG), or triacylglycerides (TAG) (Figure 2), respectively. Glycerolipids have various isomers since FAs can be attached in many different ways to *sn*-1, *sn*-2, and *sn*-3 positions of glycerol backbone (Hu et al. 2009). Usually, the FAs

20

attached to *sn*-1 carbon are saturated and those in *sn*-2 and *sn*-3 positions are unsaturated (Karantonis et al. 2009).
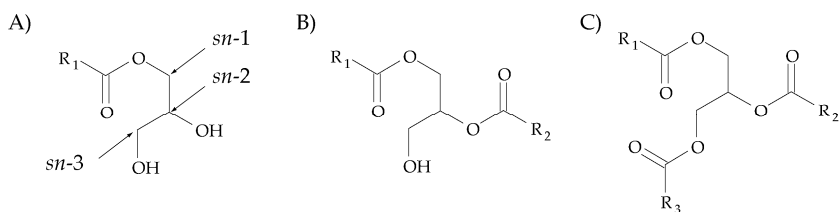
Figure 2. *Basic structures of monoacylglyceride (A), diacylglyceride (B) and triacylglyceride (C). R_1, R_2, and R_3 are hydrocarbon chains of fatty acid molecules. Three carbon atoms of the glycerol molecule are designated as sn-1, sn-2, and sn-3. Fatty acid chains in monoacylglyceride and diacylglyceride can be also in other positions than shown in structures (A) and (B).*

1.1.3 Glycerophospholipids

Glycerophospholipids (or phosphoglycerides) contain two FAs which are attached via an ester linkage to the *sn*-1 and *sn*-2 positions of glycerol backbone, and a highly polar or charged group that is attached through a phosphodiester linkage to the *sn*-3 position (Figure 3A,B) (Hu et al. 2009). Glycerophospholipids can be further subdivided based on the type of bond that links the FA chain to the *sn*-1 position (Figure 3C). Linkages can be ester, vinyl ether or alkyl ether that lead to phosphatidyl, plasmenyl, and plasmanyl subclasses, respectively (Figure 3C) (Peterson & Cummings 2006). At the *sn*-2 position there is always an ester bond, and monounsaturated or polyunsaturated FAs are preferred (Hodson et al. 2008). Essential ω-6 and ω-3 PUFAs are also preferentially stored in *sn*-2 position, from which they can be specifically and rapidly released by phospholipase A-2 (PLA2). Saturated (SFAs) and monounsaturated (MUFAs) FAs predominate at the *sn*-1 position (Leaf 2001). Also lyso-glycerolipids, where one hydroxyl group at the *sn*-1 or *sn*-2 position of the glycerol backbone is intact and the other is esterified to FA, belong to the group of glycerophospholipids (Hu et al. 2009).

Glycerophospholipids are named as derivatives of the parent compound phosphatidic acid, according to the polar alcohol in the head group (Nelson & Cox 2000). For example, phosphatidylcholine (PC) and phosphatidylserine (PS) have choline and serine as their polar head groups, respectively.
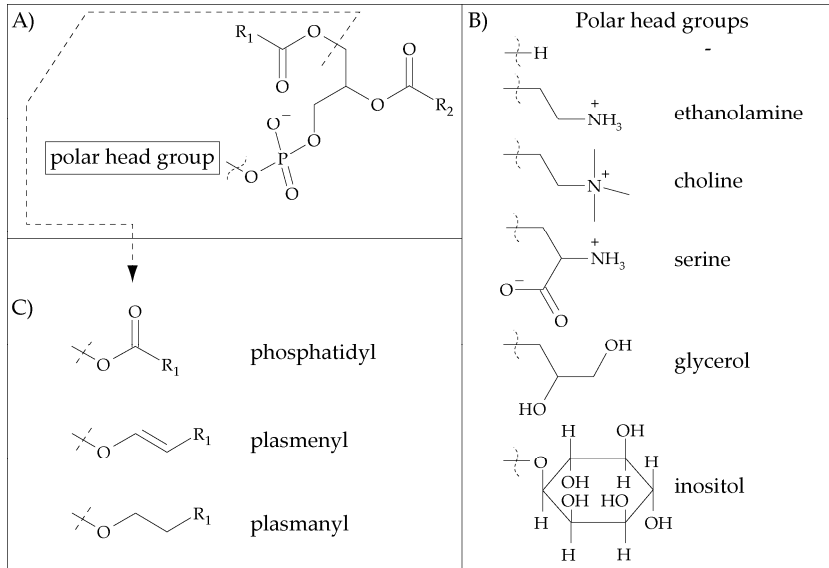
Figure 3. Basic structure of a glycerophospholipid (A) and structures of various polar head groups (B) that are attached to the phosphate group at the sn-3 position of the glycerol backbone (Nelson & Cox 2000; Peterson & Cummings 2006; Hu et al. 2009). Glycerophospholipids can be subdivided into phosphatidyl, plasmenyl, and plasmanyl subclasses depending on the linkage at the sn-1 position (C) (Peterson & Cummings 2006; Hu et al. 2009). R_1 and R_2 are hydrocarbon chains of fatty acid molecules.

1.1.4 Sphingolipids

Sphingolipids consist of sphingosine or one of its derivatives, one long-chain FA, and a polar head group that is attached either by a glycosidic or a phosphodiester linkage. Carbons C-1, C-2, and C-3 of the sphingosine molecule are structurally analogous to the three carbons of glycerol in glycerophospholipids (Figure 4) (Nelson & Cox 2000). Ceramide is the structural parent of all sphingolipids, and it has one FA

attached to the NH₂ group of a sphingosine molecule through an amide linkage (Figure 4) (Hu et al. 2009).

Sphingolipids can be divided into three subclasses: sphingomyelins (SMs), glycosphingolipids, and gangliosides (Fuller 2010). Sphingomyelins have a phosphocholine or phosphoethanolamine attached via an ether linkage to the 1-hydroxy group of a ceramide, and thus, belong together with glycerophospholipids to the group of phospholipids (PLs) (Nelson & Cox 2000). Glycosphingolipids contain one or more sugar molecules attached through a β-glycosidic bond to the ceramide structure (Ratnayake & Galli 2009). Gangliosides are the most complex group of sphingolipids and their polar head groups include at least three sugar molecules, of which one must be sialic acid (Fuller 2010).
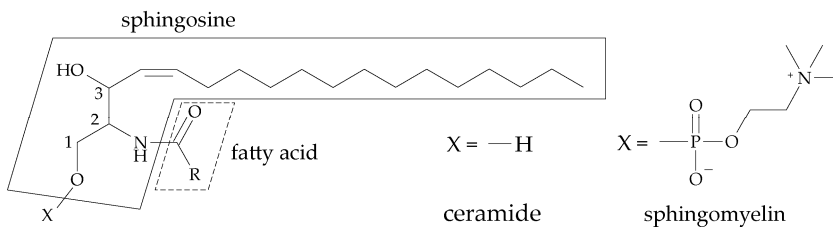
Figure 4. *Basic structure of sphingolipids and the structures of two important serum sphingolipids, ceramide and sphingomyelin.*

1.1.5 Sterol lipids

The characteristic structure of sterol lipids is the steroid nucleus consisting of four fused rings, three with six carbons and one with five (Figure 5). The steroid nucleus is relatively rigid whereas the alkyl side chain is flexible (Nelson & Cox 2000). Cholesterol is the most common sterol in human serum, and it is present as free (unesterified) cholesterol or as cholesteryl esters (CEs) (Quehenberger & Dennis 2011). Other examples of sterol lipids existing in serum are lathosterol, desmosterol, and 7-dehydrocholesterol but they are present only in small amounts (Quehenberger et al. 2010).
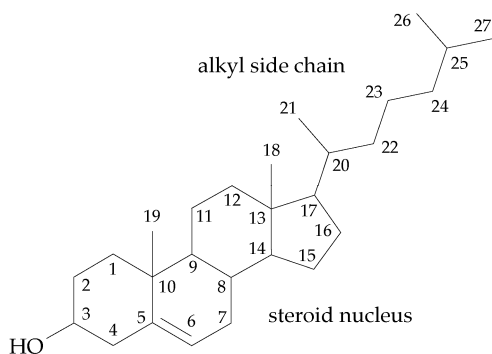
Figure 5. A structure of unesterified cholesterol with numbering of the carbon atoms. Polar hydroxyl group at C-3 can be esterified with a fatty acid yielding a cholesteryl ester.

1.2 SERUM LIPIDS

The whole blood is comprised of plasma (54% by volume) and various types of circulating cells (46% by volume), mainly erythrocytes (Hodson et al. 2008). Plasma consists of water (over 90%), small metabolites, electrolytes, lipids, and various proteins including fibrinogens, albumins, and globulins (Ala-Korpela 1995). The majority of plasma FAs are esterified in many lipid classes such as PLs, TAGs, and CEs, which are components of lipoproteins (Risé et al. 2007). To prepare plasma from whole blood sample, an anticoagulant (e.g. EDTA; ethylenediaminetetraacetic acid or heparin) needs to be added prior to the removal of blood cells. Serum is obtained when blood is allowed to clot and the clot is removed. Thus, serum lacks fibrinogens and related coagulation factors, as well as blood cells (Yu et al. 2011). Both serum and plasma can be used for lipid profiling studies, but for simplicity, mainly the term serum is used in this thesis.

1.2.1 Structure and function of lipoproteins

The main function of lipoproteins is to transport water-insoluble lipids in biological fluids (Kontush & Chapman 2010). Lipoproteins are composed of specific carrier proteins called apolipoproteins and varying amounts of TAGs, PLs, and free and esterified cholesterol (Nelson & Cox 2000). Lipoproteins contain also small amounts of fat-soluble antioxidants, such as

24

α-tocopherol and β-carotene (Ala-Korpela 1995). Apolipoproteins are characteristically distributed in the lipoprotein classes (Table 1), and they target lipoproteins to specific tissues or activate enzymes that act on lipoproteins (Ala-Korpela 1995; Nelson & Cox 2000).

Lipoprotein particles can be divided into five main classes (Table 1); chylomicrons, very-low-density lipoproteins (VLDLs), intermediate-density lipoproteins (IDLs), low-density lipoproteins (LDLs), and high-density lipoproteins (HDLs) on the grounds of amounts of protein and lipids they contain (Ala-Korpela 1995). Many of these groups can be further divided into several subpopulations based on the particle sizes or densities (Suna et al. 2007; Inouye et al. 2010). Hydrophobic TAGs and CEs are mainly located in the core of the lipoprotein particles, and hydrophilic PLs at the surface (Nelson & Cox 2000).

Table 1. Densities, radiuses, and main apolipoproteins of the human plasma lipoproteins (Ordovas 2003; Lusis & Pajukanta 2008; Vergès 2009a).

Lipoprotein	Density (g/ml)	Diameter (nm)	Apolipoproteins
Chylomicrons	<0.95	80–500	apoB-48, apoCs, apoE
VLDL	0.95–1.006	30–80	apoB-100, apoCs, apoE
IDL	1.006–1.019	25–35	apoB-100, apoE
LDL	1.019–1.063	18–28	apoB-100
HDL	1.063–1.210	5–12	apoAI–II, apoCs, apoE

VLDL, very-low-density lipoprotein; IDL, intermediate-density lipoprotein; LDL, low-density lipoprotein; HDL, high-density lipoprotein

Chylomicrons and VLDL particles contain a high proportion of TAGs and their function is to transport dietary (chylomicrons) or endogenously synthesized (VLDLs) TAGs to peripheral tissues (Ordovas 2003). IDLs transport endogenous TAGs and cholesterol to tissues and are precursors of LDL particles (Daniels et al. 2009). About half of the contents of LDL particles is cholesterol, and the function of LDL is to transport cholesterol to extrahepatic tissues that require extracellular

cholesterol (German et al. 2006; Daniels et al. 2009). The important function of HDL particles is the reverse cholesterol transport from extrahepatic tissues to liver (Ala-Korpela 1995; German et al. 2006).

1.2.2 Lipid composition of serum

The FA composition of diet affects physiological and pathophysiological processes in the body, such as gene expression, membrane properties, and energy expenditure (Vessby et al. 2002). The total FA pool of serum reflects both dietary intake and endogenous turnover, and it is composed of a mixture of all serum lipid fractions that contain FAs (Glaser et al. 2010). The most common FAs of serum are linoleic (18:2 ω-6), palmitic (16:0), and oleic (18:1 ω-9) acids (Table 2) (Hodson et al. 2008; Glaser et al. 2010). Approximately 35% of serum FAs are saturated, 25% are monounsaturated, and 40% are polyunsaturated (Assies et al. 2010).

Table 2. *Concentrations (μmol/l) and relative amounts (mol%) of serum fatty acids (FAs). The concentrations are expressed as means ± standard deviations from 65 samples of healthy human subjects (Assies et al. 2010).*

FA	c(μmol/l)	mol%	FA	c(μmol/l)	mol%
18:3 ω-3	63±40	0.61	16:1 ω-9	42±15	0.41
18:4 ω-3	1.5±1.9	0.01	18:1 ω-9	1975±722	19.05
20:5 ω-3	67±44	0.65	20:1 ω-9	14±6	0.14
22:5 ω-3	34±11	0.33	22:1 ω-9	12±8	0.12
22:6 ω-3	130±53	1.25	24:1 ω-9	64±20	0.62
18:2 ω-6	3040±685	29.32	20:3 ω-9	10±5	0.10
18:3 ω-6	47±20	0.45	14:0	146±74	1.41
20:2 ω-6	19±10	0.18	15:0	30±9	0.29
20:3 ω-6	156±94	1.50	16:0	2651±707	25.57
20:4 ω-6	554±165	5.34	18:0	741±174	7.15
22:4 ω-6	14±5	0.14	20:0	25.5±6.1	0.25
22:5 ω-6	9±4	0.09	22:0	58±12	0.56
14:1 ω-5	8.8±7.5	0.08	24:0	38±8	0.37
16:1 ω-7	242±124	2.33	SFAs	3660±942	35.30
18:1 ω-7	163±46	1.57	MUFAs	2527±881	24.37
20:1 ω-7	13±7	0.13	PUFAs	4145±837	39.98

MUFA, monounsaturated FA; PUFA, polyunsaturated FA; SFA, saturated FA

Approximately half of the serum FAs are in the TAG fraction (Hodson et al. 2008; Kotronen et al. 2010). Most of the TAG molecules are attached to VLDL particles in fasting serum, and they contain mainly oleic, palmitic, and linoleic acids (Table 3). The FA content of serum TAGs reflects a short-term dietary intake (last few meals) of FAs (Zeleniuch-Jacquotte et al. 2000; Hodson et al. 2008). The long-term qualitative dietary intake of FAs is seen from the FA composition of stored TAGs in adipose tissue (Ogura et al. 2010).

Table 3. Fatty acid composition in mol% (mol/100 mol total fatty acids) in different serum fractions (Hodson et al. 2008). For clarity, standard errors are not shown, but are within 5 and 15 mol% units for the most abundant fatty acids, and up to 3 mol% units for the fatty acids present in lower amounts.

Fatty acid	Abbreviation	TAG	PL	CE	FFA
myristic acid	14:0	3.3	0.5	0.8	3.0
palmitic acid	16:0	29.5	31.2	13.6	28.3
stearic acid	18:0	4.5	14.3	1.3	12.5
palmitoleic acid	16:1 ω-7	5.1	1.0	4.0	4.1
oleic acid	18:1 ω-9	37.7	10.1	19.3	32.7
linoleic acid	18:2 ω-6	15.0	21.9	52.0	13.5
DGLA	20:3 ω-6	0.2	2.4	0.5	0.1
arachidonic acid	20:4 ω-6	0.8	8.3	5.1	1.2
adrenic acid	22:4 ω-6	0.0	0.3	0.0	0.0
α-linolenic acid	18:3 ω-3	0.9	0.2	0.6	0.9
EPA	20:5 ω-3	0.1	1.0	0.7	0.1
DPA	22:5 ω-3	0.0	0.7	0.0	0.1
DHA	22:6 ω-3	0.4	3.3	0.4	0.4

CE, cholesteryl ester; DGLA, dihomo-γ-linolenic acid; DHA, docosahexaenoic acid; DPA, docosapentaenoic acid; EPA, eicosapentaenoic acid; FFA, free fatty acid; PL, phospholipid; TAG, triacylglyceride

Concentrations of selected glycerophospholipids and sphingolipids in serum are shown in Table 4, and it can be seen that phosphatidylcholine is the most abundant phospholipid. The most abundant FAs in serum PLs include palmitic and linoleic acids (Table 3). The FA composition of serum PLs reflects medium-term (weeks to months) dietary intake of FAs (Zeleniuch-Jacquotte et al. 2000; Hodson et al. 2008). Also the PL fraction of the erythrocyte membrane mirrors medium-term dietary intake of FAs (Patel et al. 2010).

Table 4. Total serum concentrations (μM) of selected glycerophospholipids and sphingolipids (Wiesner et al. 2009).

Lipid	Concentration (μM)
phosphatidylcholine	1986 ± 727
lysophosphatidylcholine	330 ± 168
phosphatidylethanolamine	35.6 ± 20.8
phosphatidylethanolamine-based plasmalogen	31.9 ± 13.9
sphingomyelin	415 ± 141
ceramide	8.1 ± 3.4

About two thirds of serum cholesterol is in esterified form, and approximately half of the CEs contain linoleic acid (Table 3). The benefit of the high amount of unsaturated FAs bound to cholesterol may be that they increase the fluidity of the molecule (Hodson et al. 2008). The FA composition of serum CEs mirrors medium-term dietary intake of FAs, as well as endogenous FA metabolism (Zeleniuch-Jacquotte et al. 2000; Kawashima et al. 2009).

The lowest amount of FAs, 6% or less, are as free fatty acids (FFAs) (Hodson et al. 2008). FFAs are very hydrophobic and generally toxic to cells, and therefore their concentrations in serum are kept at low nanomolar or micromolar range. About 99.9% of FFAs in serum are bound to proteins, mainly albumin (Leaf 2001). Oleic and palmitic acids are the most abundant FFAs in serum (Table 3).

Serum contains also low amounts of *trans* fatty acids (TFAs) that are obtained from diet. TFAs are produced during the bio-hydrogenation of PUFAs by ruminant animals or during the partial hydrogenation of vegetable oils (Gebauer et al. 2007; Mensink & Nestel 2009). Both of these mechanisms yield several different geometrical and positional TFA isomers of which *trans* octadecaenoic acids (18:1*t*) are the predominant products (Weggemans et al. 2004). Vaccenic acid (18:1 ω-11*t*) predominates in ruminant fat and elaidic acid (18:1 ω-9*t*) is the major TFA produced by industrial hydrogenation (Weggemans

et al. 2004; Gebauer et al. 2007; Thompson et al. 2011). Long-chain polyunsaturated TFAs, *trans* octadecadienoic acids (18:2*c*/*t*, 18:2*t*/*t*), and *trans* octadecatrienoic acids (18:3*c*/*t*) are produced in smaller amounts (Weggemans et al. 2004). The consumption of TFAs is advised to be kept as low as possible since some studies have shown that TFAs can increase the amount of LDL cholesterol and decrease HDL cholesterol (Mensink 2005; Ascherio 2006).

There are also small amounts of FAs with conjugated double bonds in serum. Conjugated linoleic acids (CLAs) are a group of linoleic acid isomers in which the double bonds are situated in positions 7, 9; 8, 10; 9, 11; 10, 12; or 11, 13 with *cis* or *trans* configuration. The most abundant isomer in nature is rumenic acid (*cis*-9, *trans*-11) which is formed in the rumen by the anaerobic bacteria (Zlatanos et al. 2008). CLAs are mainly obtained from dairy products and ruminant meat, and the amount of CLAs in human serum is relatively low (0.05-0.33% of total FAs) (Ratnayake & Galli 2009).

1.3 BIOLOGICAL FUNCTIONS OF LIPIDS

Biological lipids can serve as structural elements of biological membranes and a source of energy. In addition, lipids function as important signaling molecules.

1.3.1 Membranes

Biological membranes are composed of lipids and proteins. Sterols and PLs form a lipid bilayer where the non-polar FA parts are facing each other and the polar head groups are facing outward (Fernández-Quintela et al. 2007). Proteins are embedded in the bilayer by hydrophobic interactions between the membrane lipids and hydrophobic domains of the proteins (Nelson & Cox 2000; Eyster 2007). The interactions between the components of the membrane are non-covalent, and thus, the individual lipid and protein molecules can move in the plane of the membrane (Nelson & Cox 2000).

30

PLs are the most abundant class of membrane lipids, and they are unevenly distributed in the membrane: PC is situated primarily in the outer layer whereas PS, phosphatidylethanolamine (PE), and phosphatidylinositol (PI) are mainly present in the inner layer of the membrane. The transfer of PLs from layer to another is catalyzed by scramblases (Eyster 2007).

Also SM, sphingosine, and ceramide are abundant in membranes, and they can form hydrogen bonds with each other within the membrane (Eyster 2007). Cholesterol tends to fill the gaps among SM molecules, and the resulting membrane regions containing high amounts of SM and cholesterol are called lipid rafts (Simons & Vaz 2004; Gulati et al. 2010). The function of the lipid rafts is to segregate membrane components within the cell membrane, and they are assumed to have a role in the construction of signaling complexes (Bagatolli et al. 2010).

The amounts of saturated and unsaturated FAs in the membrane affect the physicochemical membrane properties such as fluidity. SFAs rigidify the lipid bilayer and the presence of PUFAs increases membrane fluidity (Fernández-Quintela et al. 2007; Eyster 2007). Some transport systems, for example insulin receptor, can be altered due to changes in the membrane viscosity: insulin binding increases with increasing content of PUFAs in membrane PLs (Fernández-Quintela et al. 2007).

1.3.2 Energy storage

FAs are mainly stored in adipose tissue as TAGs (Lafontan & Langin 2009). The TAG stores in the adipose tissue are in a dynamic state: TAGs are continuously formed by the intake of FAs from the TAG-rich lipoproteins and FFAs from circulation, and hydrolyzed to release the FAs back to the circulation (Connor et al. 1996; Henry et al. 2012). Nutritional states and endocrine factors have an effect on the relative rate of lipid deposition and lipid removal (Raclot 2003). For example, fasting enhances fat mobilization from adipose tissue to provide FAs as metabolic fuel (Henry et al. 2012).

Oleic, palmitic, and linoleic acids are the most abundant FAs in adipose tissue (Hodson et al. 2008). The FA composition of the diet reflects to the FA composition of adipose tissue TAGs, but the proportion of PUFAs in adipose tissue is lower than the proportion of PUFAs in the diet. This can be partly explained by the preferential release and the low re-uptake of some highly polyunsaturated FAs (Raclot 2003).

The mobilization of individual FAs from the adipose tissue depends on the molecular structure of the lipid and not the content of the particular FA in adipose tissue. In principle, SFAs are mobilized the least, PUFAs the most and MUFAs are intermediate. Especially eicosanoid precursors, arachidonic acid and eicosapentaenoic acid (EPA), are highly mobilized. On the contrary, docosahexaenoic acid (DHA), which is incorporated into the membrane PLs of cells and is not usually utilized for energy purposes or in prostaglandin synthesis, is among the most poorly mobilized FAs (Connor et al. 1996; Leaf 2001; Fernández-Quintela et al. 2007).

1.3.3 Signaling

Lipids have many different roles in signal transduction. For example, lipids are substrates of lipid kinases and lipid phosphatases, they act as ligands activating signal transduction pathways, and they function as mediators of signaling pathways. Furthermore, membrane lipids can serve as docking sites for cytoplasmic signaling proteins or give rise to cleavage products that act as ligands or substrates for other signaling molecules (Eyster 2007). Also, some proteins of signal transduction pathways have an affinity for lipid rafts (Cremesti et al. 2002). Lipid signaling pathways are interrelated and lipid mediators activate a significant amount of interaction among the signal transduction pathways (Eyster 2007). Since the lipid signaling is complex, this section will provide only a short introduction into this subject.

Signaling molecules cleaved by phospholipases

Phospholipases cleave membrane PLs at different positions of the molecule (Figure 6) and the cleavage products participate in signal transduction (Eyster 2007; Richmond & Smith 2011). Phospholipase A$_1$, and PLA$_2$ specifically hydrolyze FAs from the *sn*-1 and *sn*-2 positions, respectively (Richmond & Smith 2011). The resulting lysophosphatidylcholine (LPC) is a ligand e.g. for specific G protein-coupled receptors that induce increase in intracellular Ca^{2+} concentration, and thus, activate protein kinase C (Eyster 2007). Physiologically the most important cleavage product of PLA$_2$ is arachidonic acid, which is a precursor of inflammation mediators such as prostaglandins, leukotrienes, and thromboxanes (Eyster 2007; Richmond & Smith 2011). Platelet-activating factor (PAF), a mediator of inflammation, is formed when cytosolic PLA$_2$ cleaves one FA from PC and the resulting LPC is acetylated (Prescott et al. 2000).
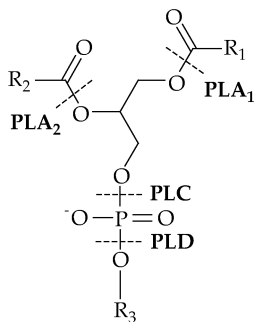
Figure 6. *Ester bond specificity of the phospholipases (Richmond & Smith 2011). Phospholipase A$_1$ and A$_2$ (PLA$_1$ and PLA$_2$, respectively) are acyl hydrolases, and phospholipases C and D (PLC and PLD, respectively) are phosphodiesterases.*

Phospholipase C catalyzes mainly the hydrolysis of the polar head phosphate from phosphatidylinositol (4,5)-bisphosphate (Bunney & Katan 2011; Richmond & Smith 2011). The resulting inositol-1,4,5-trisphosphate is released into the cytoplasm and it acts as a calcium-mobilizing second messenger, whereas DAG remains bound to the membrane and activates a variety of effector proteins, for example protein kinase C isoforms (Eyster 2007; Bunney & Katan 2011). Both inositol-1,4,5-trisphosphate and DAG participate in the regulation of several biological functions, e.g. fertilization (Bunney & Katan 2011).

Phospholipase D cleaves the polar head group mostly from PC to yield phosphatidic acid which activates a signaling cascade (Kang et al. 2011; Richmond & Smith 2011). Phosphatidic acid is an important second messenger that contributes to several cellular processes such as cell proliferation and cytoskeletal reorganization (Jang et al. 2012). Phosphatidic acid can be further degraded into lysophosphatidic acid by PLA$_2$ (Eyster 2007).

Signaling of sphingolipids

Sphingolipid signaling is complex and the signaling molecules are interconnected (Figure 7) (Hannun & Obeid 2008). Sphingomyelinase can hydrolyze sphingomyelin to ceramide, which may be further metabolized to sphingosine by ceramidase (Nixon et al. 2008; Gangoiti et al. 2010). Furthermore, ceramide and sphingosine can be phosphorylated to ceramide-1-phosphate (C1P) and sphingosine-1-phosphate (S1P), respectively (Chalfant & Spiegel 2005; Hannun & Obeid 2008). Sphingosylphosphorylcholine (SPC) is formed from sphingomyelin by sphingomyelin deacylase (Meyer zu Heringdorf et al. 2002; Nixon et al. 2008).

Sphingolipids have an important role in cell signaling, and they can act as both first and second messengers in several signaling and regulatory pathways (Hannun & Obeid 2008). Ceramide and sphingosine mainly stimulate cell cycle arrest and apoptosis whereas C1P and S1P stimulate cell survival and proliferation and are antiapoptotic (Figure 7) (Chalfant & Spiegel 2005). In addition, C1P and S1P participate in inflammatory reactions (Chalfant & Spiegel 2005; Eyster 2007). C1P appears to function only as an intracellular messenger, whereas S1P has intracellular messenger functions and can also be released from the cell and bind to G protein-linked receptors (Eyster 2007). The biological effects of SPC are not completely characterized, but it has been shown to participate in inflammatory reactions (Nixon et al. 2008).
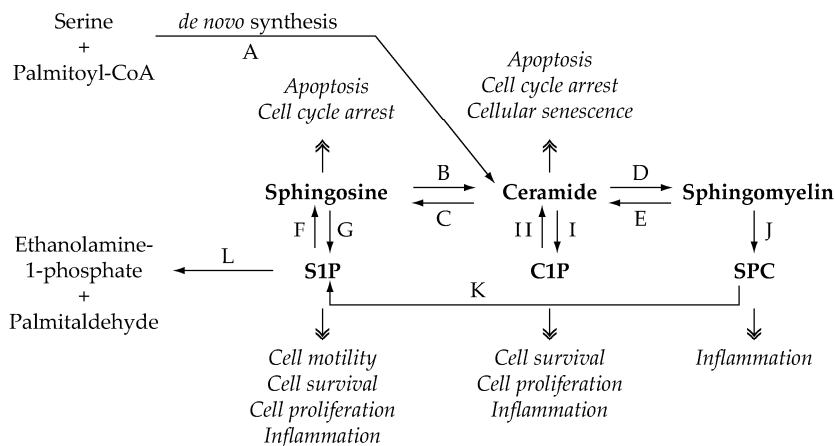
Figure 7. *The interconnectivity and the effects of the bioactive sphingolipid metabolites (Chalfant & Spiegel 2005; Nixon et al. 2008; Fuller 2010). C1P, ceramide-1-phosphate; S1P, sphingosine-1-phosphate; SPC, sphingosylphosphorylcholine. A) serine palmitoyl-CoA transferase, B) ceramide synthase, C) ceramidase, D) sphingomyelin synthase, E) sphingomyelinase, F) S1P phosphatase-1, G) sphingosine kinase, H) lipid phosphate phosphatases, I) ceramide kinase, J) sphingomyelin deacylase, K) autotoxin, L) S1P lyase*

Lipids as ligands

Lipids can bind to the receptors of the cell membrane, bind directly to the transcription factors, or indirectly affect the nuclear content of the transcription factors (Jump 2004; Eyster 2007). Prostaglandins, leukotrienes, lysophospholipids, and PAF are examples of lipid mediators that leave the cells of origin and bind to G protein-coupled receptors in the membranes of the same or neighboring cells. Cholesterol-derived steroid hormones estradiol, progesterone, and testosterone travel in the blood to distant sites where they bind to receptors and carry out their biological function (Eyster 2007).

Several nuclear receptors that belong to the steroid/thyroid superfamily bind FAs or their metabolites (Jump 2004). For example, peroxisome proliferator-activated receptor (PPAR) α controls the expression of genes involved in ketogenesis, gluconeogenesis, glycogen metabolism, and inflammation whereas PPAR γ regulates adipocyte differentiation (Schupp &

Lazar 2010). Liver X receptor family regulates the genes involved in the bile acid synthesis, reverse cholesterol transport, clearance of blood lipids, lipogenesis, and glucose uptake (Jump 2004).

Cholesterol and FAs have been shown to regulate the nuclear abundance of sterol regulatory element binding proteins (SREBPs) that are the transcription factors participating in the synthesis of cholesterol, FAs, and complex lipids. SREBP-1 regulates FA and TAG synthesis whereas SREBP-2 is a regulator of cholesterol synthesis (Jump 2004).

1.4 LIPID AND LIPOPROTEIN METABOLISM

The metabolism of lipids includes the digestion and absorption of dietary lipids, as well as the synthesis and degradation of lipids. In addition to the lipid metabolism, also lipoprotein metabolism is covered.

1.4.1 Digestion and absorption

Fats constitute approximately 40% of the energy intake in the Western diet (Mu & Høy 2004). To be able to utilize the energy content of fats, they have to be digested and absorbed. The digestion of lipids begins in the mouth and stomach but occurs mainly in the intestine (Goodman 2010). The absorption of lipids can be divided into three phases; absorption of lipids into enterocytes, intracellular processing, and export into mesenteric lymph (Mansbach & Gorelick 2007). The first two of these phases are discussed in this section and the synthesis and secretion of chylomicrons is described in the Lipoprotein metabolism section.

Digestion

The digestion of lipids begins in the mouth by lingual lipases which start the digestion of TAGs. Gastric and lingual enzymes continue the digestion process in the stomach (Iqbal & Hussain 2009). Dietary fat and fat-soluble vitamins form emulsions in the

stomach, and these lipid emulsions enter the duodenum and lead to the stimulation of the pancreatic enzyme secretion including lipases and esterases and the release of bile from the gallbladder (Iqbal & Hussain 2009; Goodman 2010). When the lipids arrive in the duodenum, only about 15% of fat has been digested and most of the lipids are intact (Goodman 2010). Bile and pancreatic juice contain bile salts, pancreatic lipase, and colipase which function cooperatively to ensure the efficient lipid digestion and absorption (Iqbal & Hussain 2009). In addition, colipase prevents the inactivation of lipase by the bile salts (Goodman 2010).

The majority of dietary lipids in human diet are TAGs, while PLs and sterols are only minor components (Niot et al. 2009). The digestion of TAGs occurs mainly in the upper segment of the jejunum by pancreatic lipase (Iqbal & Hussain 2009; Goodman 2010), that cuts the TAG molecule from the sn-1 and sn-3 positions yielding 2-MAG and FFAs (Mu & Høy 2004; Linderborg & Kallio 2005). Pancreatic lipase can further hydrolyze 2-MAG to glycerol and a FFA. PLs are digested primarily by pancreatic PLA$_2$ and other lipases secreted by the pancreas. These lipases cut FAs from the sn-2 position of PLs yielding FFAs and LPCs (Iqbal & Hussain 2009). Esterified cholesterol is hydrolyzed by cholesterol esterase, and only non-esterified cholesterol can be incorporated into bile acid micelles and absorbed by enterocytes (Goodman 2010). Approximately 50% of the cholesterol in the intestine is absorbed and the rest is excreted in feces (Iqbal & Hussain 2009).

Absorption

The initial step of absorption involves the transfer of digested lipids across the apical membrane of the enterocytes (Mansbach & Gorelick 2007). The products of TAG digestion, FFAs and 2-MAG, can cross the membrane via protein-independent diffusion or by a protein-dependent mechanism involving fatty acid transport proteins (Black 2007). Diffusion based and protein-dependent transport mechanisms have been suggested also for cholesterol (Hui et al. 2008; Iqbal & Hussain 2009).

The absorbed products of lipid digestion must traverse the cytoplasm to the endoplasmic reticulum (ER) where the resynthesis of complex lipids takes place (Black 2007). FAs and MAGs are reassemblied to TAGs, and there are two pathways for TAG formation in the intestine (Niot et al. 2009). The 2-MAG pathway involves the acylation of 2-MAG with two FAs (Mansbach & Gorelick 2007). Prior to acylation the FAs have to be transformed to fatty acyl-coenzyme A-thioesters (FA-CoAs) (Jump & Clarke 1999). The α-glycerophosphate pathway involves the acylation of glycerol-3-phosphate (G-3-P) to phosphatidic acid, dephosphorylation of the phospholipid to DAG, and the acylation of the DAG to form TAG (Mansbach & Gorelick 2007). The 2-MAG pathway predominates in the intestine and it produces only TAG whereas the α-glycerophosphate pathway can lead also to the synthesis of PLs (Niot et al. 2009). The absorbed and resynthesized lipids are then packed into chylomicron particles as discussed in the next section.

1.4.2 Lipoprotein metabolism

Lipoprotein metabolism includes the synthesis, remodeling, and clearance of different lipoprotein particles. This section provides a short introduction to these complex processes.

Chylomicrons are formed in the enterocytes of the intestine by the fusion of apolipoprotein B-48 and lipid droplets. The lipid pool of chylomicrons consists mainly of TAGs, but there are also small amounts of PLs and cholesterol in the particles (Mansbach & Gorelick 2007). When chylomicrons enter the circulation, they acquire apoCs and apoE from HDL particles (Daniels et al. 2009; Nakajima et al. 2011). The TAGs in the chylomicrons are hydrolyzed by endothelial-bound lipoprotein lipase to yield TAG-poorer remnant particles that are subsequently taken up by the liver (Rader & Daugherty 2008; Chatterjee & Sparks 2011). The lipids of chylomicron remnants are then hydrolyzed to FFAs and free cholesterol that can be used for the synthesis of VLDL particles (Redgrave 2004). Since

chylomicrons exist in the circulation only in the postprandial state, the fasting serum does not contain chylomicrons.

VLDLs are apoB-100 containing TAG-rich lipoproteins that are synthesized in the liver (Olofsson et al. 2000). The TAGs that are packed to the VLDLs can be derived from chylomicron and VLDL remnants, lipolysis of adipose tissue TAGs or *de novo* FA synthesis in the liver (Choi & Ginsberg 2011). Metabolic state and diet determine the relative proportions of TAGs and CEs in the particles, and thus, affect the size of VLDLs (German et al. 2006). VLDL particles are secreted continuously from the liver and the extent of the secretion depends on the metabolic state (Nakajima et al. 2011). In the circulation, VLDL particles release FFAs to muscle and adipose tissue through the action of lipoprotein lipase and exchange apoCs and apoE with HDL particles. The loss of TAGs and apoCs and enrichment with CEs generates IDL particles from VLDL (Ala-Korpela 1995; Daniels et al. 2009). Further removal of TAGs and apoE converts IDL to LDL (Vergès 2009a). In principle, the heterogenous sizes of LDL particles are mainly caused by the metabolic differences in the formation of these particles (German et al. 2006). About half of the VLDL remnants are taken up by the liver and the rest are transformed to LDL (Lusis & Pajukanta 2008). Also IDL and LDL remnants are subsequently cleared by the liver (Lusis et al. 2004).

HDL synthesis begins with the formation of nascent HDLs that contain two or more apolipoprotein molecules (only apoA-I or both apoA-I and apoA-II), PLs, and free cholesterol (Rye et al. 2009). Nascent particles are secreted from the liver or they can also be assembled in the serum from the individual components (Lusis & Pajukanta 2008; Rye et al. 2009). Lecithin-cholesterol acyl transferase (LCAT) converts free cholesterol molecules of nascent HDLs to CEs that partition into the center of the particles and more free cholesterol can be added to the particles (Daniels et al. 2009). This increases the particle size and transforms the nascent HDLs into the mature spherical HDLs (Ordovas 2003; Brufau et al. 2011). HDL particles are constantly remodeled in the circulation and they also interact with other

lipoproteins (Rye et al. 2009). Cholesteryl ester transfer protein exchanges CEs of HDL for TAGs of LDL and VLDL and remodels HDL into smaller particles (Daniels et al. 2009; Rye et al. 2009). Phospholipid transfer protein transfers mainly PLs from VLDL into HDL, as well as between individual HDL particles that results in either smaller or larger particles. Furthermore, endothelial lipase hydrolyzes PLs and hepatic lipase hydrolyzes TAGs and PLs of HDLs to yield smaller HDL particles (Rye et al. 2009). Apolipoprotein and PL composition of HDL affects the metabolic outcome of the lipoprotein and the HDL subclass distribution in serum is due to different clearance rates of these particles by the liver (German et al. 2006).

1.4.3 Biosynthesis of lipids

Since lipids have several roles, their biosynthesis is crucial for normal cellular function. This section describes the synthesis of FAs, glycerolipids, cholesterol, and sphingolipids.

Synthesis of fatty acids

The *de novo* synthesis of FAs from acetyl-CoA and malonyl-CoA is a cyclic process including a repeating four-step sequence (Figure 8). Each passage through the cycle extends the FA chain by two carbons. The reactions of the FA synthesis are catalyzed by a multi-enzyme complex called fatty acid synthase (FAS). After seven cycles, the final product is palmitic acid (Smith 1994; Nelson & Cox 2000).

The FA biosynthesis occurs in cytosol and begins with the conversion of acetyl-CoA into malonyl-CoA by acetyl-CoA carboxylase, which is the rate-limiting step in the synthesis process (Nelson & Cox 2000; Chan & Vogel 2010). Then, one acetyl-CoA and one malonyl-CoA are transferred to specific thiol sites of the FAS complex. The acetyl group binds to the β-ketoacyl-ACP synthase and the malonyl attaches to the acyl carrier protein (ACP) domain (Figure 8) (Smith 1994; Nelson & Cox 2000).
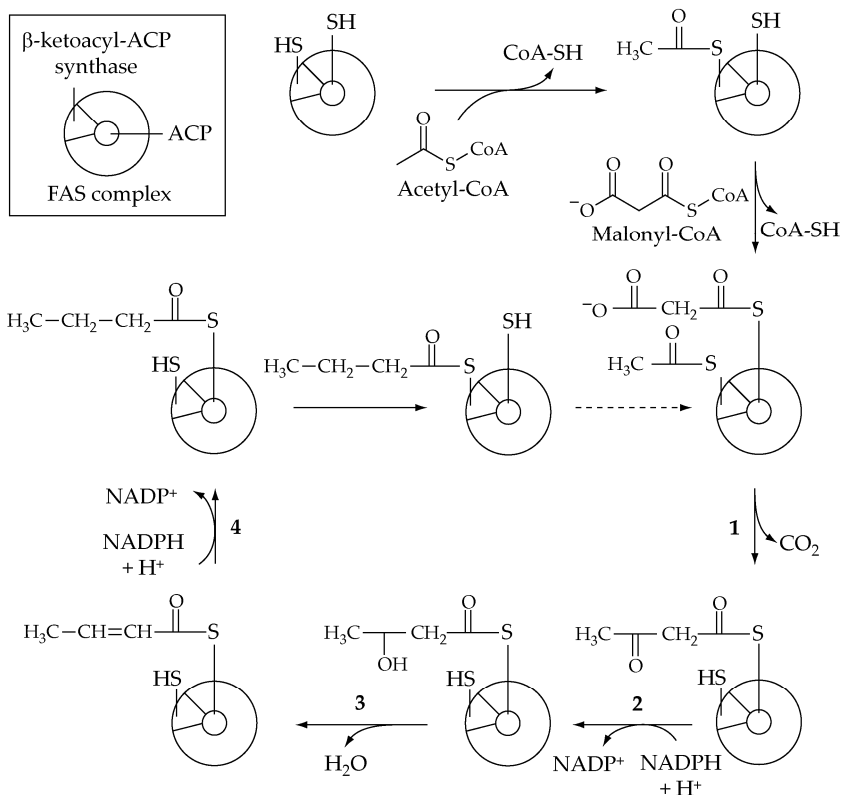
Figure 8. Reactions of the fatty acid biosynthesis (Smith 1994; Nelson & Cox 2000; Chan & Vogel 2010). Acetyl and malonyl groups are transferred to the β-ketoacyl-ACP synthase and acyl carrier protein (ACP) domains of the fatty acid synthase (FAS) complex, respectively. The four-step cycle involves the condensation of the malonyl and acyl groups (1), reduction of the β-keto group (2), dehydration (3), and reduction of the double bond (4). To initiate another cycle, the acyl group is transferred from the ACP domain to the β-ketoacyl-ACP synthase and a new malonyl group is attached to the ACP domain. CoA, coenzyme A

The first reaction in the four-step cycle is the condensation of the activated acetyl and malonyl groups by β-ketoacyl-ACP synthase to form acetoacetyl-ACP. Secondly, the acetoacetyl-ACP is reduced by β-ketoacyl-ACP reductase to yield D-β-hydroxybutyryl-ACP (Smith 1994; Nelson & Cox 2000). The third step involves the removal of water and the formation of a double bond to the molecule by β-hydroxyacyl-ACP

dehydratase. Finally, the double bond is reduced to form butyryl-ACP by the action of enoyl-ACP reductase. The butyryl group is then transferred from the phosphopantetheine SH group of ACP to the cysteine SH group of β-ketoacyl-ACP synthase. To start the next cycle, another malonyl group is attached to the phosphopantetheine SH group of ACP (Nelson & Cox 2000; Chan & Vogel 2010).

Synthesized or diet derived FAs can be further desaturated and/or elongated into long and very-long-chain FAs by specific membrane-bound enzymes in the ER (Figure 9) (Jakobsson et al. 2006; Guillou et al. 2010). The elongation involves the addition of two-carbon units (malonyl-CoA) to a FA-CoA (Wallis et al. 2002). Enzymatic steps involved in the elongation process are the same as for the synthesis of palmitic acid (Jakobsson et al. 2006). However, different enzyme systems are involved and CoA functions as the acyl carrier instead of ACP (Nelson & Cox 2000).

Desaturases add double bonds to specific positions of the FA chains. Mammals express Δ9-, Δ6-, and Δ5-desaturase activities. The number after delta indicates the position at which the double bond is introduced counting from the carboxylic end of the FA (Guillou et al. 2010). For example, Δ9-desaturase synthesizes palmitoleic and oleic acids from palmitic and stearic acids, respectively (Kawashima et al. 2009). However, mammals lack Δ12- and Δ15-desaturases, and thus, they cannot synthesize linoleic (18:2 ω-6) and α-linolenic acids (18:3 ω-3) and they have to be obtained from diet (Wallis et al. 2002; Poudyal et al. 2011). These two essential FAs serve as precursors for the synthesis of longer ω-6 and ω-3 PUFAs (Figure 9) (Hornstra et al. 1995; Smit et al. 2004; Das 2008). Since the ω-3 and ω-6 FAs compete for the same desaturases and elongases, the intake of these FAs determines the status of serum ω-3 and ω-6 FAs (Assies et al. 2010). For example, a high intake of linoleic acid promotes the endogenous synthesis of arachidonic acid (20:4 ω-6) and reduces the synthesis of ω-3 FAs deriving from α-linolenic acid (Warensjö et al. 2006). It has been proposed that an ω-6/ω-3 ratio of <4:1 in serum represents a healthy balance (Assies et al. 2010).

20:3 ω-9   ENDOGENOUS   DIET   22:2 ω-6
  ⇑ Δ5   SYNTHESIS   ↑
                                                          20:2 ω-6
  ⇑ Δ6   ↑
            14:0   18:3 ω-3   18:2 ω-6
16:1 ω-9   ⇓ Δ6
            16:0   ⇒   16:1 ω-7   18:4 ω-3   18:3 ω-6
                   Δ9   ⇓
18:1 ω-9   ⇐   18:0   18:1 ω-7   20:4 ω-3   20:3 ω-6
            Δ9   ⇓ Δ5   ⇓ Δ5
20:1 ω-9   20:0   20:1 ω-7   20:5 ω-3   20:4 ω-6
22:1 ω-9   22:0   22:5 ω-3   22:4 ω-6
24:1 ω-9   24:0   24:5 ω-3   24:4 ω-6
                                          ⇓ Δ6   ⇓ Δ6
                  26:0   24:6 ω-3   24:5 ω-6
                                          ⇓   ⇓
⇒ Desaturation   ⇨ β-oxidation   22:6 ω-3   22:5 ω-6
↠ Chain elongation
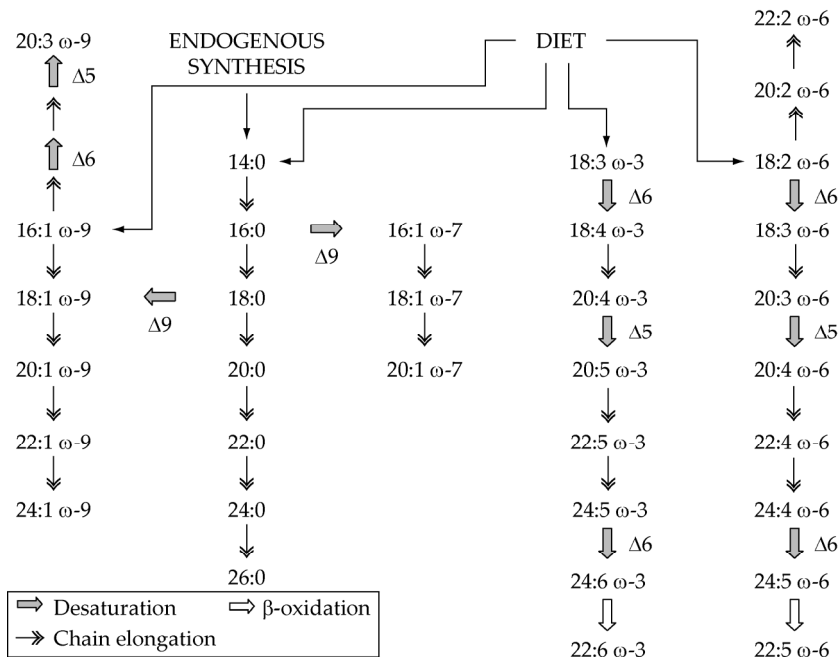
Figure 9. *Pathways of fatty acid chain elongation and desaturation (Wallis et al. 2002; Warensjö et al. 2006; Assies et al. 2010). Since mammals lack Δ12 and Δ15 desaturases, they have to obtain linoleic (18:2 ω-6) and α-linolenic acids (18:3 ω-3) from their diet.*

Synthesis of glycerolipids

The *de novo* synthesis of TAGs and glycerophospholipids are discussed together since their synthesis pathways share several reactions (Figure 10). More than 90% of TAGs are synthesized via the G-3-P pathway under normal physiological conditions in the liver (Coleman & Lee 2004). In the intestine, the major route for TAGs is the 2-MAG pathway, as discussed earlier.
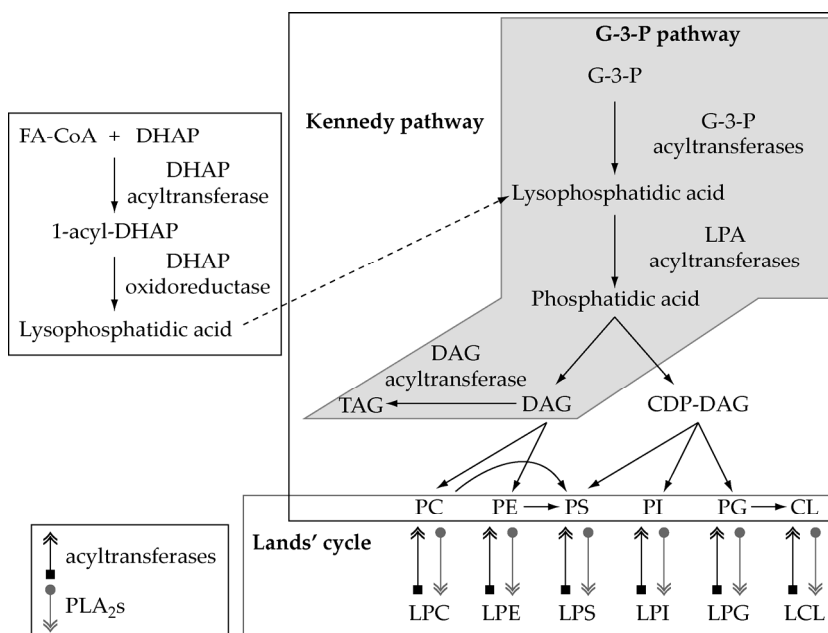
Figure 10. *Synthesis pathways of triacylglycerides (TAGs) and glycerophospholipids. Glycerophospholipids are synthesized through the de novo pathway (Kennedy pathway) and modified through the remodeling pathway (Lands' cycle) (Coleman & Lee 2004; Yen et al. 2008; Shindou & Shimizu 2009). TAGs are synthesized mainly via the glycerol-3-phosphate (G-3-P) pathway, which is a part of the Kennedy pathway. Some lysophosphatidic acid (LPA) is metabolized from dihydroxyacetone phosphate (DHAP). CDP-DAG, cytidine diphospho-diacylglyceride; CL, cardiolipin; LPC, lysophosphatidylcholine; LPE, lysophosphatidylethanolamine; LPG, lysophosphatidylglycerol; LPI, lysophosphatidylinositol; LPS, lysophosphatidylserine; PC, phosphatidylcholine; PE, phosphatidylethanolamine; PG, phosphatidylglycerol; PI, phosphatidylinositol; PLA2, phospholipase A-2; PS, phosphatidylserine*

Glycerophospholipids are synthesized by the *de novo* pathway (Kennedy pathway) and modified by the remodeling pathway (Lands' cycle) (Figure 10) (Shindou & Shimizu 2009). The first step in the Kennedy pathway (and also in the G-3-P pathway) involves the formation of lysophosphatidic acid from G-3-P (Coleman & Lee 2004). Lysophosphatidic acid is then metabolized into phosphatidic acid, which is subsequently converted either into DAG or cytidine diphospho-DAG (CDP-DAG). DAG can be transformed into TAG, PC or PE

44

whereas PS is synthesized from PC or PE (Coleman & Lee 2004). CDP-DAG can be converted to PI, PS or phosphatidylglycerol. After synthesis of glycerophospholipids, their FA composition at the *sn*-2 position is altered through the Land's cycle by actions of PLA$_2$s and lysophospholipid acyltransferases (Shindou & Shimizu 2009).

Synthesis of cholesterol

Cholesterol synthesis is a multi-step process including almost 30 enzymes, and the main reactions are shown in Figure 11 (Gulati et al. 2010). Briefly, acetoacetyl-CoA is formed from two acetyl-CoA molecules, after which acetoacetyl-CoA condenses with acetyl-CoA forming β-hydroxy-β-methylglutaryl-CoA (HMG-CoA) (Panda et al. 2011). HMG-CoA is then reduced to mevalonate by HMG-CoA reductase which is the rate-limiting step of the cholesterol synthesis (Gulati et al. 2010). Furthermore, mevalonate is converted to activated isoprene units through phosphorylation and decarboxylation reactions (Panda et al. 2011). Polymerization of isoprene units produces squalene, which undergoes cyclization to yield lanosterol (Nelson & Cox 2000; Gulati et al. 2010). Finally, 19 reactions are required to convert lanosterol to cholesterol (Gulati et al. 2010).

CEs can be synthesized from cholesterol and acyl-CoA by intracellular enzyme acyl-CoA-cholesterol acyl transferase (ACAT) that has specificity for oleic acid (Hodson et al. 2008; Gulati et al. 2010). CE formation may also occur in serum where LCAT transfers a FA from *sn*-2 position of PC to cholesterol (Nelson & Cox 2000; Hodson et al. 2008). The specificity of LCAT depends on the FA, and the order is linoleic acid > oleic acid > arachidonic acid > SFA which explains the high proportion of linoleic acid in CEs. Since serum contains more linoleic acid CE than oleic acid CE, most of the serum CEs must be derived from the LCAT pathway (Hodson et al. 2008).
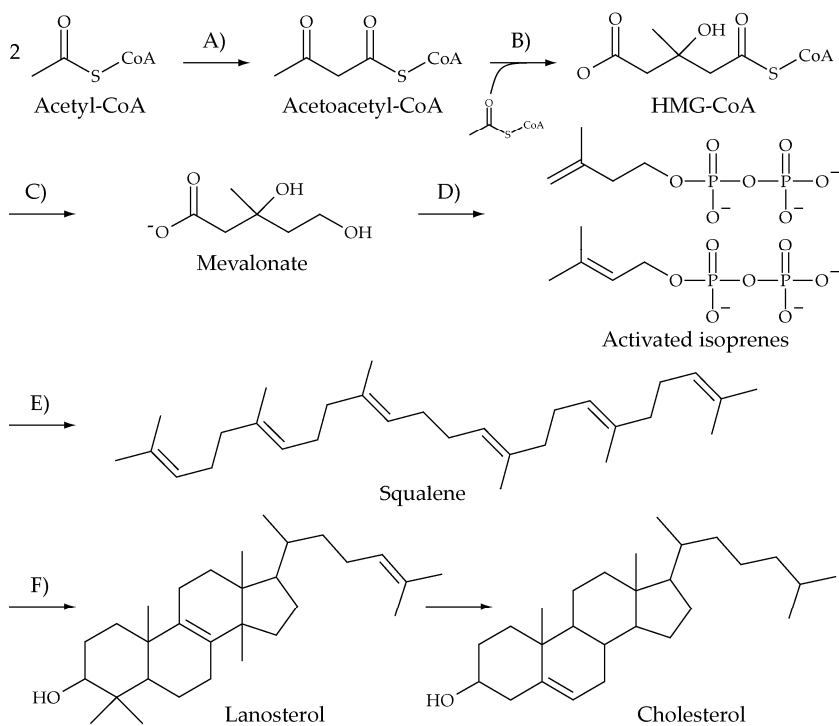
Figure 11. *Main reactions of the cholesterol synthesis with key enzymes (A–F) (Nelson & Cox 2000; Gulati et al. 2010; Panda et al. 2011). A) Acetoacetyl-CoA thiolase, B) β-hydroxy-β-methylglutaryl-CoA (HMG-CoA) synthase, C) HMG-CoA reductase, D) mevalonate kinase, phosphomevalonate kinase, mevalonate-5-pyrophosphate decarboxylase, E) geranyl pyrophosphate synthase, farnesyl pyrophosphate synthase, squalene synthase, F) squalene epoxidase, squalene epoxide cyclase. Conversion of lanosterol to cholesterol requires 19 reactions but they are not specified here. CoA, coenzyme A*

Synthesis of sphingolipids

The synthesis of ceramide begins at the cytosolic surface of the ER (Fuller 2010). The first and rate-limiting step of the sphingolipid synthesis involves a condensation of serine and palmitoyl-CoA to form 3-ketosphinganine (Figure 12). Then, 3-ketosphinganine is reduced to dihydrosphingosine which is acylated to yield dihydroceramide (Hannun & Obeid 2008; Gulati et al. 2010). Desaturation of dihydroceramide produces

ceramide that serves as a precursor for complex sphingolipids at the *trans*-Golgi (Gulati et al. 2010).

Sphingomyelin is formed when phosphocholine group of PC is transferred to the 1-hydroxyl group of ceramide. Glycosphingolipid synthesis begins with glucosylation of ceramide by glucosylceramide synthase to yield glucosylceramide which is then converted to lactosylceramide by the action of galactosyltransferase I. Lactosylceramide serves as a substrate for the synthesis of gangliosides (Fuller 2010).
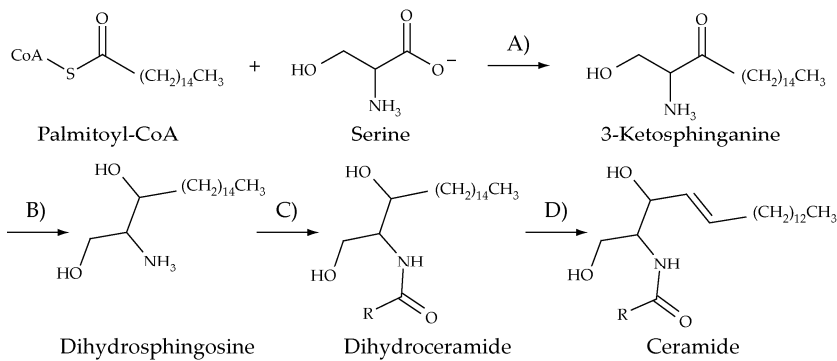
Figure 12. *The reactions of sphingolipid synthesis with key enzymes (A–D) (Gulati et al. 2010). A) serine palmitoyltransferase, B) ketosphinganine reductase, C) dihydroceramide synthase, D) dihydroceramide desaturase. Ceramide is a precursor of complex sphingolipids.*

1.4.4 Degradation of lipids

Oxidation rates of amino acids and carbohydrates are primarily determined by intakes of protein and carbohydrate, but the rate of fat oxidation is set mainly by the gap between the total energy expenditure and energy intake in the form of protein and carbohydrates (Fernández-Quintela et al. 2007). FA oxidation is an important metabolic pathway for energy homeostasis in the liver, heart, and skeletal muscles especially during fasting. Most of the tissues, excluding the brain, are able to use FAs directly to generate energy (Houten & Wanders 2010). In addition, the liver converts FAs into ketone bodies which can be used for energy production in all tissues including the brain (Rinaldo et al. 2002;

Houten & Wanders 2010). This section describes the catabolism of FAs, acylglycerides, PLs, cholesterol, and sphingolipids.

Catabolism of fatty acids

There are three mechanisms for the degradation of FAs including α-, β-, and ω-oxidation, of which β-oxidation is the principal pathway for the oxidation of serum FFAs or lipoprotein associated TAGs (Wanders et al. 2003; Wanders et al. 2011). Prior to β-oxidation, the TAGs must be first hydrolyzed by the endothelium-bound lipoprotein lipase (Houten & Wanders 2010).

There are mitochondrial and peroxisomal β-oxidation systems which are functionally complementary but have different roles (Reddy & Hashimoto 2001). Short- ($<C_8$) and medium-chain (C_8–C_{12}) FAs are exclusively and long-chain (C_{14}–C_{20}) FAs are predominantly β-oxidized in mitochondria (Reddy & Hashimoto 2001; Wanders & Waterham 2006). There are some FAs that cannot be β-oxidized in mitochondria including e.g. very long-chain FAs ($>C_{20}$), pristanic acid (2,6,10,14-tetramethylpentadecanoic acid), long-chain dicarboxylic acids, certain PUFAs such as tetracosahexaenoic acid (24:6), some prostaglandins and leukotrienes, and vitamins E and K, which are β-oxidized in peroxisomes (Wanders & Waterham 2006). However, peroxisomes are not able to β-oxidize FAs completely and the FAs are only chain-shortened to shorter chain FAs which are then transferred to mitochondria for full oxidation (Wanders et al. 2011). Only saturated unbranched FAs and 2-methyl-branched FAs can undergo direct β-oxidation in peroxisomes, other FAs need to be remodeled prior to the β-oxidation (Wanders & Waterham 2006).

The mitochondrial β-oxidation involves series of four enzyme reactions which sequentially remove an acetyl-CoA molecule per cycle from the carboxy-terminal of the initial FA substrate (Figure 13) (Houten & Wanders 2010). Each step of the cycle is catalyzed by multiple chain-length specific enzymes (Wanders et al. 2011). In addition to the acyl-CoA and an acetyl-CoA, the β-oxidation cycle yields also one nicotinamide adenine

dinucleotide and one flavin adenine dinucleotide as electron carriers (Houten & Wanders 2010). The acyl-CoA proceeds to another cycle of FA oxidation, and the acetyl-CoA can enter the citric acid cycle for further oxidation or condense to ketone bodies (Reddy & Hashimoto 2001). The electron carriers deliver electrons to the electron transport chain (Houten & Wanders 2010). The reactions of the β-oxidation cycle in peroxisomes are analogous but the reactions are catalyzed by different enzymes compared with the mitochondrial system (Mukherji et al. 2003; Wanders et al. 2011). Human peroxisomes have two β-oxidation systems of which one is an inducible pathway metabolizing long-chain FAs and the other is a constitutive pathway oxidizing pristanic and bile acids having (2S)-stereochemistry (Mukherji et al. 2003).
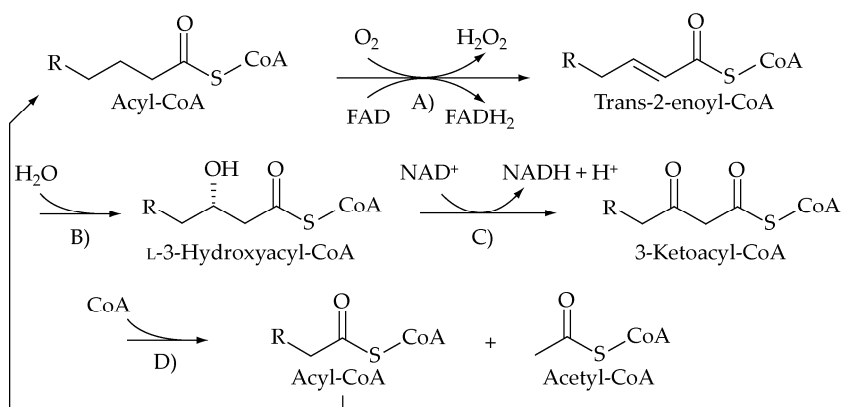
Figure 13. Mitochondrial fatty acid β-oxidation (Houten & Wanders 2010). The first step of the cycle involves the dehydrogenation of the acyl-CoA by acyl-CoA dehydrogenase (A) producing trans-2-enoyl-CoA. Then the formed double bond is hydrated by enoyl-CoA hydratase (B), and 3-hydroxyacyl-CoA dehydrogenase (C) dehydrogenates the resulting L-3-hydroxyacyl-CoA to yield 3-ketoacyl-CoA. In the final step, the thiolytic cleavage of the 3-ketoacyl-CoA catalyzed by 3-ketoacyl-CoA thiolase (D) forms an acyl-CoA shortened by two carbons and an acetyl-CoA. The peroxisomal β-oxidation cycle is analogous but the reactions are catalyzed by different enzymes compared with the mitochondrial system. CoA, coenzyme A; FADH2, flavin adenine dinucleotide; NADH, nicotinamide adenine dinucleotide

FAs having a methyl group or any other functional group attached to the carbon-3 cannot be degraded by β-oxidation, and they must first undergo α- or ω-oxidation (Wanders et al. 2003; Wanders et al. 2011). The α-oxidation of FAs is confined to peroxisomes and accepts only acyl-CoA esters as substrate. In the oxidation process, the FA is shortened by one carbon atom, and the functional group is then at carbon-2 (Wanders & Waterham 2006). For example, the α-oxidation of phytanoyl-CoA is illustrated in Figure 14.

(3R,S,7R,11R)-Phytanoyl-CoA

2-Hydroxyphytanoyl-CoA

Pristanal

(2R,S,6R,10R)-Pristanoyl-CoA
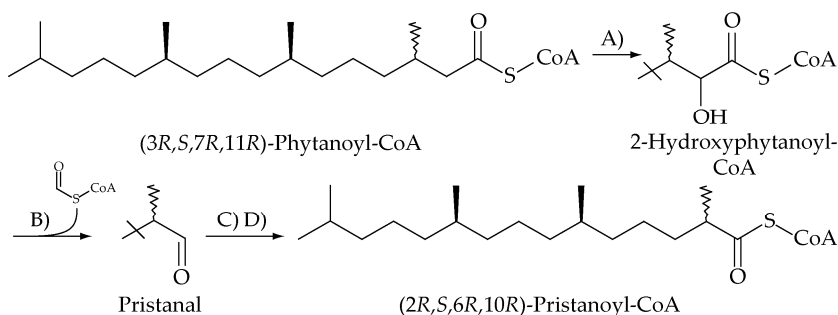
Figure 14. *Degradation of phytanoyl-CoA by α-oxidation (Mukherji et al. 2003). Phytanoyl-CoA is converted to 2-hydroxyphytanoyl-CoA by phytanoyl-CoA 2-hydroxylase (A). The resulting 2-hydroxyphytanoyl-CoA is converted into pristanal and formyl-CoA by phytanoyl-CoA lyase (B). Pristanoyl-CoA is formed in reactions catalyzed by pristanal dehydrogenase (C) and very-long-chain fatty acyl-CoA synthetase (D). Pristanoyl-CoA then undergoes three cycles of β-oxidation in the peroxisome and the resulting chain shortened FA-CoA is then transferred to mitochondrion for further oxidation (Wanders et al. 2011). CoA, coenzyme A*

FA ω-oxidation takes place almost exclusively in the smooth ER by cytochrome P450 4 (CYP4) family, and they ω-hydroxylate saturated, branched, and unsaturated FAs, as well as eicosanoids. Members of CYP4B, CYP4A, and CYP4F subfamilies metabolize FAs with chain lengths C_7–C_9, C_{10}–C_{16}, and C_{18}–C_{26}, respectively (Hardwick et al. 2009). The ω-oxidation involves ω-hydroxylation of the ω-carbon of a FA, and the sequential action of cytosolic alcohol and aldehyde dehydrogenases yield corresponding dicarboxylic acids (Nelson & Cox 2000; Hardwick et al. 2009).

Catabolism of acylglycerides

There are several lipases that degrade dietary or endogenous TAGs in different organs. Human gastric lipase and human pancreatic lipase catalyze the hydrolysis of dietary TAGs into DAGs and subsequently into MAGs in the stomach and intestine, respectively. Hepatic lipase is involved in the degradation of TAGs from HDL particles. Lipoprotein lipase hydrolyzes TAGs from the *sn*-1 and *sn*-3 positions of TAGs of chylomicrons and VLDLs, and is expressed in adipose tissue and muscles. TAG hydrolase degrades TAGs yielding DAGs and MAGs especially in the liver (Karantonis et al. 2009).

Adipose triacylglyceride lipase, hormone-sensitive lipase (HSL), and monoacylglycerol lipase degrade acylglycerides in the adipose tissue (Karantonis et al. 2009; Zechner et al. 2009). Adipose triacylglyceride lipase can hydrolyze both TAGs and DAGs but it exhibits 10-fold higher substrate specificity for TAGs. HSL is able to hydrolyze several lipids such as TAGs, DAGs, MAGs, and CEs, of which DAG is the preferable substrate. HSL slightly prefers unsaturated medium-chain FAs over saturated long-chain FAs in TAG substrates and it preferentially hydrolyzes FAs from *sn*-1 and *sn*-3 positions. Monoacylglycerol lipase specifically degrades MAGs and has no activity against DAGs or TAGs (Zechner et al. 2009).

Catabolism of phospholipids

PLs are degraded by the action of PLA_2 superfamily enzymes which catalyze the hydrolysis of the ester bond at the *sn*-2 position of a phospholipid yielding a FFA and a lysophospholipid. The superfamily consists of secreted, cytosolic, Ca^{2+} independent, and lysosomal PLA_2s, as well as PAF acetylhydrolases (Burke & Dennis 2009). The degradation products represent the first step in generating second messengers that have various physiological roles, as discussed earlier.

Catabolism of cholesterol

Bile acid biosynthesis is the main catabolic and non-reversible departure point of cholesterol. About 50% of the *de novo* synthesized cholesterol is converted to bile acids in human liver (Gulati et al. 2010). Primary bile acids (cholic acid and chenodeoxycholic acid) can be synthesized from cholesterol via the classic (neutral) pathway, which accounts for approximately 75% of the liver bile acid synthesis, or via the alternative (acidic) pathway (Li & Chiang 2009; Gulati et al. 2010). Secondary bile acids are formed from primary bile acids in the intestine by the action of bacterial enzymes (Li & Chiang 2009).

Catabolism of sphingolipids

The breakdown of complex sphingolipids occurs mainly in the lysosomes but the non-glycosylated sphingolipids such as ceramide and sphingomyelin can also be degraded in other sub-cellular locations (Fuller 2010; Kolter & Sandhoff 2010). Catabolism of sphingolipids prevents their accumulation and also generates and recycles intermediates and metabolites such as ceramide and sphingosine (Gulati et al. 2010).

Prior to the lysosomal degradation of sphingolipids, these lipids need to be transported to the lysosomes, and it occurs mainly by endocytosis, phagocytosis or autophagy (Kolter & Sandhoff 2006). Sphingomyelin is degraded to form ceramide and phosphocholine by sphingomyelinases (Gulati et al. 2010; Fuller 2010). The saccharide molecules of glycosphingolipids are sequentially removed from the non-reducing end of the oligosaccharide part by exohydrolases (Kolter & Sandhoff 2006; Fuller 2010). Glycosphingolipids having less than four sugar residues require the presence of sphingolipid activator proteins to be degraded. Sphingolipid activator proteins mediate the interaction between the membrane-bound lipid substrate and the water-soluble enzyme or activate the enzyme directly (Kolter & Sandhoff 2006). The degradation of gangliosides involves several steps in which the saccharide residues are removed and the final product is ceramide (Fuller 2010). Ceramide can be further degraded to sphingosine and a FA by

ceramidases (Hannun & Obeid 2008). The degradation of sphingolipids yields monosaccharides, sialic acid, FAs, ceramide, and sphingosine, which can leave the lysosome through the transporters of the membrane (Kolter & Sandhoff 2006).

1.5 LIPID PEROXIDATION

Oxidative stress is a condition in which the levels of oxidizing components and the relevant neutralizing substances are imbalanced leading to a potential damage to cells and organs (Opara 2006; Basu 2010). Especially the double bonds of PUFAs are susceptible to oxidation (Leopold & Loscalzo 2009). The interest for studying the oxidative stress is mainly due to its role in the development of chronic degenerative diseases such as coronary heart disease, cancer, and the degenerative processes associated with aging (Fernandez-Panchon et al. 2008).

1.5.1 Mechanisms of lipid peroxidation

There are three different lipid peroxidation mechanisms; free radical-mediated, free radical-independent, and enzymatic oxidation (Niki et al. 2005; Niki 2009). All the mechanisms result in specific products and different antioxidants inhibit each type of peroxidation mechanism (Niki 2009). PUFAs and cholesterol are oxidized both by the enzymatic and non-enzymatic pathways (Niki et al. 2005).

Free radical-mediated peroxidation of polyunsaturated fatty acids

Free radical is a molecule that has unpaired electrons in its atomic structure. This structure makes free radicals relatively unstable and very reactive, and they can oxidize proteins, DNA, and lipids (Opara 2006). Free radical-mediated lipid peroxidation proceeds by a chain mechanism meaning that one initiating free radical can oxidize several lipid molecules (Figure 15) (Niki 2009). There are five elementary reactions: (1) abstraction of a bisallylic hydrogen of PUFA by a chain

initiating radical or chain carrying peroxyl radicals to yield a pentadienyl carbon-centered radical (initiation reaction), (2) reaction of the lipid radical with molecular oxygen resulting in a lipid peroxyl radical (propagation reaction), (3) fragmentation of the lipid peroxyl radical to give oxygen and a lipid radical, which is a reverse of reaction (2), (4) rearrangement of the peroxyl radical to a more stable radical, and (5) cyclization of the peroxyl radical (Niki 2009; Yin et al. 2011). The cyclization reaction (5) takes place only during the oxidation of PUFAs having more than three double bonds (Niki et al. 2005). The oxidation process is terminated when two primary or secondary peroxyl radicals react together forming non-radical products (Yin & Porter 2005; Yin et al. 2011).

Initiation	$LH \longrightarrow L^{\bullet}$
Propagation	$L^{\bullet} + O_2 \longrightarrow LOO^{\bullet}$
	$LOO^{\bullet} + LH \longrightarrow LOOH + L^{\bullet}$
Termination	$L^{\bullet} + LOO^{\bullet} \longrightarrow$ non-radical products
	$L^{\bullet} + L^{\bullet} \longrightarrow$ non-radical products
	$LOO^{\bullet} + LOO^{\bullet} \longrightarrow$ non-radical products
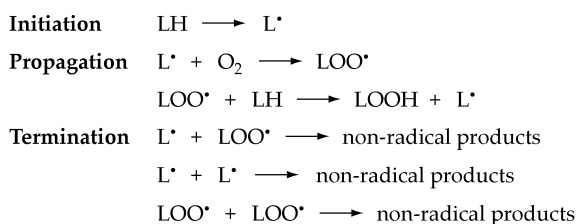
Figure 15. Reactions of the lipid peroxidation (Galleano et al. 2010). LH, lipid molecule; L·, lipid radical; LOO·, lipid peroxyl radical; LOOH, lipid hydroperoxide

Non-radical, non-enzymatic peroxidation of polyunsaturated fatty acids

Ozone and singlet oxygen oxidize lipids by non-radical mechanisms. Singlet oxygen oxidizes unsaturated lipids mainly by ene-reaction to yield hydroperoxide with simultaneous double bond migration. Minor side reactions include 1,4-addition to give 1,4-endoperoxide and 1,2-addition to yield dioxetane, which readily decomposes to result in chemiluminescent carbonyl compounds (Niki 2009). Oxidation induced by ozone results in ozonides and cleavage products (Uppu et al. 1995).

Enzymatic peroxidation of polyunsaturated fatty acids

There are enzymes such as lipoxygenase and cyclooxygenase that oxidize mainly arachidonic acid regio-, stereo-, and enantiospecifically (Schneider et al. 2007). Lipoxygenase enzymes produce hydroxyeicosatetraenoic acids which are then metabolized to leukotrienes. Cyclooxygenase enzymes oxidize arachidonic acid to prostaglandins, prostacyclin, and thromboxane. In addition, CYP enzymes metabolize arachidonic acid to dihydroxyeicosatetraenoic acids, as well as epoxyeicosatrienoic acids (Roman 2002).

Oxidation of cholesterol

Also cholesterol can be oxidized by all the three mechanisms described above, and the oxidation products are called oxysterols (Niki 2009). Major oxidation products from different cholesterol oxidation pathways are shown in Figure 16.
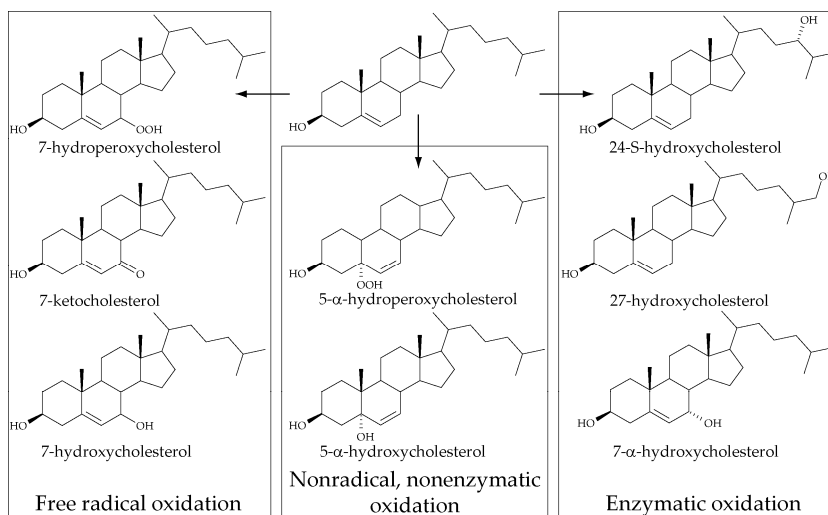
Figure 16. *Main oxysterols from free radical mediated, non-radical and non-enzymatic, as well as from enzymatic oxidation (Niki 2009).*

1.5.2 Defense mechanisms against oxidation
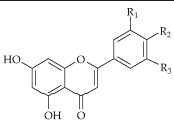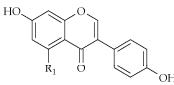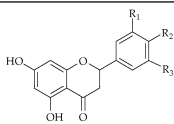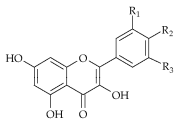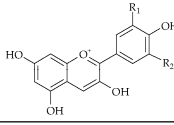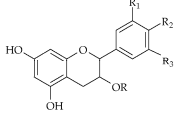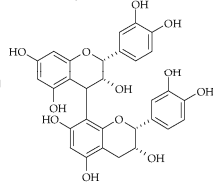
Organisms have various antioxidant defense mechanisms against oxidation including small antioxidant molecules and antioxidative enzymes. The actions of these different antioxidants are shortly discussed in this section.

Small antioxidant molecules

The group of small antioxidant molecules consists of several different components such as certain vitamins, trace elements, glutathione, uric acid, and polyphenols, and these compounds have a variety of antioxidant mechanisms. For example, vitamins (e.g. vitamin C and vitamin E) can act as donors and acceptors of reactive oxygen species, and trace elements such as selenium and zinc, act as cofactors regulating the activities of antioxidant enzymes (Opara 2006). Glutathione can scavenge free radicals and act as a reducing cofactor of glutathione peroxidase (Galleano et al. 2010). Uric acid is the end-product of enzymatic purine catabolism, and it functions both as a primary radical scavenger and an inhibitor of the iron-catalyzed oxidation of ascorbate (Nyyssönen et al. 1997).

Polyphenols are polyhydroxylated phytochemicals which are present mainly in plants (Lotito & Frei 2006). There are two subgroups of polyphenols including flavonoids and non-flavonoid compounds (Fraga et al. 2010). Flavonoids can be divided into several subclasses according to their structure; flavones, isoflavones, flavanones, flavonols, anthocyanidins, and flavanols (Table 5) (Mladenka et al. 2010). Stilbenes, phenolic acids, and lignans are non-flavonoid polyphenols, and examples of their structures are shown in Figure 17 (Fraga et al. 2010).

Table 5. *Chemical structures of flavonoid subclasses (Manach et al. 2004; Lotito & Frei 2006; Galleano et al. 2010).*

Flavonoid subclass	Basic structure	Examples
Flavones		$R_1=R_3=H$; $R_2=OH$: Apigenin $R_1=R_2=OH$; $R_3=H$: Luteolin
Isoflavones		$R_1=H$: Daidzein $R_1=OH$: Genistein
Flavanones		$R_1=R_3=H$; $R_2=OH$: Naringenin $R_1=R_2=OH$; $R_3=H$: Eriodictyol
Flavonols		$R_1=R_3=H$; $R_2=OH$: Kaempferol $R_1=R_2=OH$; $R_3=H$: Quercetin $R_1=R_2=R_3=OH$: Myricetin
Anthocyanidins		$R_1=R_2=H$: Pelargonidin $R_1=R_2=OH$: Delphinidin $R_1=OH$; $R_2=H$: Cyanidin
Flavanols		Monomers $R_1=R_2=OH$; $R_3=H$: Catechins $R_1=R_2=R_3=OH$: Gallocatechin Polymers Procyanidin dimer B2

57
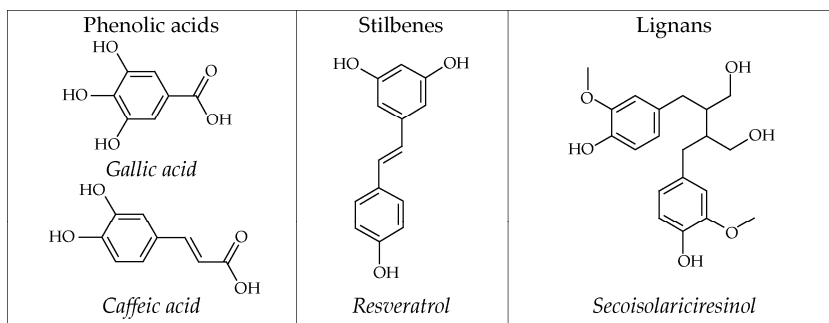
Figure 17. *Examples of the structures of non-flavonoid polyphenols (Manach et al. 2004).*

Several antioxidant mechanisms have been proposed for the compounds having a polyphenol structure (Fraga et al. 2010). In vitro studies suggest that polyphenols have a free radical scavenging activity and an ability to bind transition metal ions (Mladenka et al. 2010). However, the poor absorption and extensive metabolism of polyphenols does not allow high serum concentrations of polyphenols, and thus, limit the capacity of these compounds to act as direct antioxidants (Lotito & Frei 2006). Free radical scavenging function of polyphenols is relevant only in tissues that are directly exposed to flavonoids such as the gastrointestinal tract (Galleano et al. 2010). Indirect antioxidant mechanisms of polyphenols include interactions with membrane components and inhibition of free radical forming enzymes e.g. xanthine oxidase and lipoxygenases (Mladenka et al. 2010; Galleano et al. 2010).

Antioxidant enzymes

Glutathione peroxidase, catalase, and cytosolic superoxide dismutase are examples of antioxidant enzymes. Glutathione peroxidase catalyzes the reduction of hydroperoxides by using thiol cofactors (Bhabak & Mugesh 2010). Catalase decomposes hydrogen peroxide resulting in water and oxygen (O_2) (Nelson & Cox 2000; Khan et al. 2010). Superoxide dismutase can catalyze the dismutation of superoxide radical ($^{\cdot}O_2^-$) to hydrogen peroxide and oxygen (Khan et al. 2010; Torsdottir et al. 2010).

58

1.6 ALTERATIONS IN LIPID METABOLISM

FA composition is widely used as an indicator of disease risk since many disease states involve alterations in FA profiles. In this section, lipid alterations in some common metabolic states and diseases, such as obesity, diabetes, atherosclerosis, metabolic syndrome, and Alzheimer's disease (AD) are shortly discussed.

1.6.1 Obesity

Obesity is a state in which the storage capacity of adipose tissue is exceeded, and TAGs accumulate also in the liver and muscles (Langeveld & Aerts 2009). Body mass index (BMI) is used as a measurement of body fat, and it is calculated as weight (kg) divided by height squared (m^2) (Ahima 2011). Overweight is defined as a BMI ≥ 25 kg/m^2 and obesity as a BMI ≥ 30 kg/m^2 (Flegal et al. 2010; Ahima 2011). Environmental and lifestyle factors have a strong impact on the development of obesity but also genetic variation may determine the susceptibility of body fat accumulation and lipid disturbances (Pietiläinen et al. 2007). Obesity increases the risk for decreased insulin sensitivity which is characterized by reduced insulin-mediated glucose uptake and impaired suppression of lipolysis and hepatic glucose production (Langeveld & Aerts 2009). Furthermore, obesity is a risk factor for several diseases such as coronary heart disease, type 2 diabetes, stroke, and certain types of cancer (Holland & Summers 2008; Ahima 2011).

Obese individuals tend to have increased concentrations of serum TAGs, large VLDL particles, small dense LDL particles, and low amounts of HDL cholesterol compared to non-obese individuals (Pietiläinen et al. 2007). In addition, obesity involves decreased concentrations of ether PLs that have antioxidant activities, as well as increased amounts of LPCs that have proinflammatory and proatherogenic properties. These lipid

changes are associated with insulin resistance (Pietiläinen et al. 2007; Kontush & Chapman 2010).

Also sphingolipid metabolism is altered in obesity. Increased saturated FAs within circulating lipoprotein particles contribute to increased ceramide synthesis in peripheral tissues. Additionally, chronic low-level inflammation, which is associated with obesity, contributes to the induction of ceramide accumulation (Holland & Summers 2008). Excessive sphingolipids complicate insulin signaling and promote inflammation (Langeveld & Aerts 2009).

1.6.2 Diabetes

Diabetes is a complex metabolic disorder involving defects in glucose and insulin homeostasis. Type 1 diabetes is linked mostly to genetics and the production of autoantibodies that destroy pancreatic β-cells, and thus, the body stops making or makes only a tiny amount of insulin. Type 2 diabetes is caused mainly by insulin resistance and is related to obesity and age (Rains & Jain 2011). Type 2 diabetes is more common, and it accounts for 90–95% of diabetes diagnoses (Wright et al. 2006).

Lipid abnormalities in type 1 diabetes

Quantitative lipid abnormalities in untreated type 1 diabetes include decreased LDL and HDL cholesterol levels and increased amounts of TAG-rich lipoproteins (chylomicrons and VLDLs) that lead to hypertriglyceridaemia (Vergès 2009a). Patients with well-controlled blood glucose tend to have similar levels of serum lipids and lipoproteins as healthy controls (Sorensen et al. 2010). When considering the levels of individual lipid species, some sphingomyelin and ether phosphatidylcholine species have been suggested to decrease in type 1 diabetic individuals compared with controls (Orešic et al. 2008; Sorensen et al. 2010).

There are also qualitative lipid abnormalities that are common in type 1 diabetic patients both with poor and good glycaemic control (Vergès 2009a). VLDL particles are often enriched with CEs at the expense of TAGs, and the number of

small, dense LDL particles is increased (Skyrme-Jones et al. 2000; Vergès 2009a). Furthermore, the oxidation of LDL may be increased and HDL particles are commonly enriched with TAGs (de Castro et al. 2005; Vergès 2009a).

A part of patients with long-standing type 1 diabetes suffer from diabetic nephropathy (a leading cause of chronic kidney disease) involving increased urinary albumin excretion (Gross et al. 2005). Our study revealed that diabetic kidney disease consists of diverse phenotypes (Mäkinen et al. 2012a). According to the study, IDL and LDL lipids together with PLs and unsaturated FAs are increased in the early phase of the disease, but not in the late phase. Simultaneously, the patients express extensive metabolic diversity regarding SFAs, inflammation, and HDL metabolism, and this diversity may be one explanation to the variability in kidney disease onset (Mäkinen et al. 2012a). In the final phase, the sphingolipid pathway could be a mediator of lipotoxicity from SFAs on the path to end-stage renal disease and/or premature death (Mäkinen et al. 2012a; Mäkinen et al. 2012b).

Lipid abnormalities in type 2 diabetes

Type 2 diabetic patients have typically normal LDL cholesterol levels but HDL levels are decreased due to increased catabolism of these particles (Taskinen 2003; Adiels et al. 2008; Vergès 2009b; Betteridge 2011). In addition, overproduction of large VLDL particles, as well as accumulation of cholesterol-enriched remnant lipoprotein particles are common abnormalities (Taskinen 2003; Adiels et al. 2008; Betteridge 2011). Several atherogenic modifications including small, dense and TAG-rich LDL, oxidized LDL, and glycated LDL are typical in LDL particles of type 2 diabetic subjects. Also HDL particles are enriched with TAGs, or they can be glycated. Furthermore, the antioxidative and endothelium-dependent vasorelaxant properties of HDL particles are reduced (Vergès 2009b).

Increases in the levels of palmitic acid, palmitoleic acid, and dihomo-γ-linolenic acid (DGLA), as well as low amount of linoleic acid have been associated with insulin resistance

(Vessby et al. 2002; Risérus et al. 2009). The *trans* fatty acid intake is also positively correlated with the risk of diabetes (Risérus et al. 2009). It has been proposed that *trans* fatty acids increase inflammatory cytokines that are related to the risk of diabetes (Mozaffarian 2006).

1.6.3 Atherosclerosis

Atherosclerosis is a chronic inflammatory condition, and it is the most common cause of myocardial infarction, stroke, and cardiovascular disease (Shibata & Glass 2010; Adibhatla & Hatcher 2010). Accumulation and oxidation of LDL in the arterial intima and recruitment of monocytes to the developing lesion are two critical events in atherogenesis (Adibhatla & Hatcher 2010; Moore & Tabas 2011).

The first step in the atherosclerosis is endothelial dysfunction that is caused for example by elevated levels of LDL, hypertension, free radicals, or elevated homocysteine concentration. The endothelial dysfunction increases the adhesiveness and permeability of the endothelium and induces the production of cytokines and growth factors (Ross 1999). Inflammatory response then stimulates adhesion of monocytes to the endothelium (Mangge et al. 2010; Bornfeldt & Tabas 2011). Monocytes penetrate into the arterial intima, differentiate into macrophages and eventually become foam cells by binding and endocytosing oxidized LDL (Lusis 2000; Maxfield & Tabas 2005; Adibhatla & Hatcher 2010). The macrophage foam cells generate inflammatory mediators that recruit other cell types and contribute to the development of a complex lesion (Shibata & Glass 2010; Adibhatla & Hatcher 2010). The accumulation of mononuclear cells, migration and proliferation of smooth muscle cells, as well as the formation of fibrous tissue enlarge and restructure the lesion (Lusis 2000). Thickening of the artery wall can be compensated, to some extent, by dilatation of the blood vessel. However, at some point, the artery is no longer able to compensate the thickening and the blood flow of the artery is altered (Ross 1999). It is also possible that the lesion ruptures and causes thrombosis. The thrombus can block the

blood flow at the site of the thrombosis or, after erosion, the blood clot can move along the circulation and occlude a vein somewhere else (Lusis 2000).

Atherosclerotic patients have shown to have elevated serum levels of oxysterols. Oxysterols regulate lipid metabolism and inflammation and are toxic factors contributing to clinical complications of atherosclerosis (Shibata & Glass 2010).

Sphingolipids can promote atherosclerosis and thrombosis through several mechanisms. Ceramides of LDL particles tend to accumulate and self-aggregate to the artery walls (Holland & Summers 2008). This can induce foam cell formation. Ceramides are also able to induce apoptosis in vascular wall cells contributing to the erosion of plaques (Mallat & Tedgui 2001). S1P, the phosphorylated derivative of sphingomyelin, stimulates endothelial and smooth muscle cell proliferation that results in thickening of the vascular wall and plaque stabilization (Yatomi et al. 2000).

1.6.4 Metabolic syndrome

Metabolic syndrome is a collection of metabolic disorders and it is associated with an increased risk of development of type 2 diabetes and cardiovascular disease (Devaraj & Jialal 2012). Nutrition has a major impact on the development of metabolic syndrome (Kawashima et al. 2009). The National Cholesterol Education Program's Adult Treatment Panel III (NCEP ATP III) has defined metabolic syndrome as a state involving any three or more of the following risk factors: elevated TAGs, reduced HDL cholesterol, elevated fasting glucose, elevated blood pressure or obesity (Grundy et al. 2005; Gillingham et al. 2011).

Metabolic syndrome is usually associated with insulin resistance, and insulin resistance is related with a certain FA composition of serum (Vessby 2003). Patients with metabolic syndrome tend to have low concentrations of linoleic acid and high concentrations of DGLA, palmitic, and palmitoleic acids (Kawashima et al. 2009). It has been suggested that the increase of MUFA intake, especially as a substitute for dietary saturated

FAs, promotes the reduction of traditional risk factors defining metabolic syndrome (Gillingham et al. 2011).

Metabolic syndrome is also associated with disturbed lipoprotein metabolism (van Heyningen 2005; Suna et al. 2007). The level of HDL cholesterol is lower and HDL particles are smaller and denser than in healthy controls. Obesity and insulin resistance result in increased production of larger VLDL particles that leads to the formation of smaller and denser LDL particles (van Heyningen 2005).

1.6.5 Alzheimer's disease

AD is a progressive neurodegenerative disorder which is characterized by amyloid-β (Aβ) plaques, neurofibrillary tangles composed of abnormally hyperphosphorylated tau protein, and neuronal cell loss (Cunnane et al. 2009; Adibhatla & Hatcher 2010; Jicha & Markesbery 2010). Memory loss and cognitive decline are the clinical symptoms of AD (Hartmann et al. 2007). In sporadic late-onset AD (90–95% of all cases) the first symptoms appear after age of 65, and the presence of allele ε4 in the gene of apoE, which is the major carrier of cholesterol in central nervous system, is the main genetic risk factor. Familial early-onset AD starts approximately after 40 years of age and is associated with mutations in the genes coding amyloid precursor protein (APP) and presenilins 1 and 2. Several vascular problems such as atherosclerosis, hypercholesterolemia, diabetes, and obesity increase the risk of developing sporadic AD, whereas dietary antioxidants, B-vitamins, and ω-3 PUFAs may have potentially protective effects (Cunnane et al. 2009; Fonseca et al. 2010).

Cholesterol has a role in the development and progression of AD (Reid et al. 2007; Adibhatla & Hatcher 2010). High cholesterol content in lipid rafts, where the APP processing takes place, favors amyloidogenic processing of the APP whereas low cholesterol content yields mainly non-amyloidogenic Aβ production (Mathew et al. 2011). Furthermore, cholesterol is a precursor of neurosteroids of which many have neuroprotective functions. The levels of these

neurosteroids are decreased in AD brains (Adibhatla & Hatcher 2010).

Also sphingolipids have important functions in AD. Sphingomyelin inhibits γ-secretase leading to decreased Aβ production (Hartmann et al. 2007). Acid sphingomyelinase is activated in AD brain that leads to elevated ceramide levels, activation of ceramidases, and production of sphingosine. Ceramide promotes Aβ biogenesis, and thus, the reduction of ceramide levels reduces the secretion of APP and Aβ in human neuroblastoma cells. It has been suggested that elevated amounts of ceramide and sphingosine, as well as low S1P creates a "pro-apoptotic" environment in the AD brain leading to neuronal death (He et al. 2010). Additionally, some gangliosides bind Aβ peptides and alter their conformations from random coils to more ordered structures thus increasing their aggregation (Di Paolo & Kim 2011).

The nervous system is highly enriched with PUFAs, especially DHA (Hartmann et al. 2007; Jicha & Markesbery 2010). There has been evidence of the inverse correlation between the intake of DHA and AD incidence. For example, the daily administration of ω-3 FAs (DHA and EPA) resulted in positive effects in patients at very mild stage of AD, whereas no beneficial effects were observed in patients having mild-to-moderate AD (Hartmann et al. 2007). In addition, the low relative amount of ω-3 FAs has been proposed to be indicative of mild cognitive impairment (MCI) that is a transitional state with considerably increased risk for AD (Tukiainen et al. 2008). Some studies suggest that the beneficial effects of ω-3 FA supplementation may depend on the stage of the disease, other dietary mediators, and apoE status. Also several mechanisms how ω-3 PUFAs may prevent amyloidogenic processing have been presented. These include the facilitation of α-secretase actions that leads to the release of non-toxic amyloid peptides, the shielding of γ-secretase cleavage site and the dysregulation of γ-secretase yielding prevention of Aβ peptides, and the inhibition of fibrillation and aggregation of Aβ fragments (Jicha & Markesbery 2010).

Also progressive inflammation and increased oxidative stress may have an important role in the early development of Aβ plaque deposition and tangle formation (Jicha & Markesbery 2010). The accumulation of Aβ fragments induces inflammatory response and expression of pro-inflammatory cytokines. These cytokines again stimulate Aβ production and amyloid formation (Cunnane et al. 2009). EPA and DHA can protect from inflammation since the mediators formed from these FAs, such as leukotrienes and resolvins, are anti-inflammatory (Cunnane et al. 2009; Barberger-Gateau et al. 2011). The accumulation of Aβ peptides is also accompanied by increased free radical production and increased lipid peroxidation in the brain (Cunnane et al. 2009).

1.7 ANALYSIS OF SERUM LIPIDS

Prior to the analysis of lipids, they have to be extracted from serum to get rid of proteins and other non-lipid molecules. Since there are a lot of different lipids in serum, their analysis requires usually a combination of different fractionation and detection techniques. The following sections include descriptions of these commonly used methods used in lipid studies.

1.7.1 Lipid extraction techniques

There are four main extraction protocols for serum lipids. Extraction protocols of Folch (Folch et al. 1957), as well as the method of Bligh and Dyer (Bligh & Dyer 1959) use chloroform and methanol as solvents. The dichloromethane assay is based on the Folch method but chloroform is replaced by less carcinogenic dichloromethane (Cequier-Sánchez et al. 2008). The fourth protocol uses methyl-*tert*-butyl ether (MTBE) and methanol to extract lipids (Matyash et al. 2008).

Folch method
The Folch method is a widely known lipid extraction protocol that was initially developed to extract lipids from

various animal tissues (Folch et al. 1957). The method involves the homogenization of the tissue with a 2:1 chloroform-methanol (v/v) mixture after which the extract is washed by adding 0.2 of its volume of either water or an appropriate salt solution (NaCl, KCl, CaCl$_2$, or MgCl$_2$) (Figure 18). The mixture forms two separate phases of which the lower organic phase contains lipids. The purpose of the salt solution is to reduce the dissolution of lipids to the water-methanol phase.

Bligh and Dyer method

The Bligh and Dyer method was developed to extract lipids from tissues containing 80% water and about 1% lipids (Bligh & Dyer 1959). In the protocol, a tissue sample is homogenized with a mixture of 2:1 methanol-chloroform (v/v) after which chloroform and water are added (Figure 18). Final ratios of methanol, chloroform, and water are 2:2:1.8. The additions of chloroform and water produce a biphasic system, of which the lower chloroform layer contains lipids and the upper methanol-water phase non-lipid molecules. When extracting materials that do not contain 80% water, the size of the sample should be adjusted so that the volumes of chloroform, methanol, and water, before and after the final additions of chloroform and water, are in the proportions 1:2:0.8 and 2:2:1.8, respectively.

Dichloromethane method

The dichloromethane extraction method is based on the Folch protocol but chloroform has been replaced with dichloromethane (Cequier-Sánchez et al. 2008). The protocol involves the extraction of lipids with 2:1 dichloromethane-methanol (v/v) (Figure 18). The assessment of the dichloromethane assay with different tissue samples indicated that the protocol yields comparable results with the Folch method, and thus, dichloromethane can replace chloroform in lipid studies (Cequier-Sánchez et al. 2008).

MTBE method

In the extraction protocol of Matyash et al, lipids are extracted with 10:3:2.5 MTBE-methanol-water (v/v/v) (Figure 18) (Matyash et al. 2008). The solvent mixture forms two layers of which the upper one contains lipids. Using the MTBE protocol, the recovery of the lipid species of almost all major classes has been shown to be the same or better than is typically achieved by the Folch method (Matyash et al. 2008).

Comparison of the extraction protocols

Figure 18 shows the four extraction protocols described above. Even though the Folch and Bligh and Dyer extraction methods were initially developed for tissue samples, these protocols, or their variations, have been widely used also for the extraction of serum lipids (Burdge et al. 2000; Sommer et al. 2006; Beger et al. 2006; Pietiläinen et al. 2007; Ding et al. 2008; Sandra et al. 2010; Sorensen et al. 2010). However, it has been proposed that the use of chloroform should be avoided since it is toxic and carcinogenic. Dichloromethane is a good alternative for chloroform since it is less toxic but extracts lipids as well as chloroform (Cequier-Sánchez et al. 2008).

The biggest difference between the MTBE method and chloroform or dichloromethane based methods is that the density of MTBE is lower than that of water, and thus, it is the upper phase in the two-phase partitioning system whereas chloroform and dichloromethane are below the water phase (Figure 18). When the lower phase is collected, the glass pipette or the needle has to go through the protein layer which is between the two phases. Even minute amounts of insoluble precipitate can cause problems when using liquid chromatography or mass spectrometry (MS), and thus, when using these quantification methods, the MTBE protocol is preferred (Matyash et al. 2008).

Folch protocol

200 μl serum

4.5 ml 2:1 CHCl$_3$-CH$_3$OH

mixing

0.9 ml H$_2$O or salt solution

mixing

centrifugation

W
P
O

Bligh and Dyer protocol

30 μl serum + 1.2 ml H$_2$O

4.5 ml 2:1 CH$_3$OH-CHCl$_3$

mixing

1.5 ml CHCl$_3$

mixing

1.5 ml H$_2$O

mixing

centrifugation

W
P
O

Dichloromethane protocol

200 μl serum

4.5 ml 2:1 CH$_2$Cl$_2$-CH$_3$OH

mixing

0.9 ml 0.88% (w/v) KCl solution

mixing

centrifugation

W
P
O

MTBE protocol

200 μl serum

1.5 ml CH$_3$OH

mixing

5 ml MTBE

mixing

1.25 ml H$_2$O

mixing

centrifugation

O
W
P

Figure 18. Overview of the Folch, Bligh and Dyer, dichloromethane, and MTBE extraction protocols. For clarity, only one extraction cycle is presented. After removal of the organic phase, the water phase is usually extracted again with organic solvent to enhance the yield. CHCl$_3$, chloroform; CH$_2$Cl$_2$, dichloromethane; CH$_3$OH, methanol; MTBE, methyl-tert-butyl ether; O, organic phase; P, protein layer; W, water phase

1.7.2 Lipid fractionation techniques

After extraction, the lipid sample is often fractionated using chromatography. Chromatographic systems consist of a stationary and a mobile phase. The stationary phase can be solid or liquid, and the mobile phase is either gas or liquid. The separation of the sample components is based on their different physical and chemical properties since the molecules have different affinities for the two phases (Peterson & Cummings 2006). Thin-layer chromatography (TLC), gas chromatography (GC), high-performance liquid chromatography (HPLC), and solid-phase extraction (SPE) are common separation methods for lipid mixtures.

Thin-layer chromatography

Thin-layer chromatography is a simple, fast, and moderately cheap separation method that has been widely used in lipid research (Touchstone 1995; Fuchs et al. 2010). TLC utilizes a solid stationary phase and a liquid mobile phase (Peterson & Cummings 2006). In TLC method, a total lipid extract is dissolved usually in chloroform and applied to the origin of a TLC plate (Burdge et al. 2000). Silica gel, alumina, and kieselguhr are commonly used stationary phases for lipid separations, of which silica gel is the most popular (Fuchs et al. 2011). It is also possible to make chemical modifications to the silica gel to improve the separation of the lipid classes (Peterson & Cummings 2006).

Dried lipid spots are developed with appropriate mobile phase after which the plates are allowed to dry (Burdge et al. 2000). Solvent mixtures of chloroform, methanol and water are common as mobile phases (Peterson & Cummings 2006). Lipid spots can be detected by staining and collected by scraping the silica into a glass tube (Burdge et al. 2000). There are various non-destructive and destructive dyes available (Fuchs et al. 2011). Lipid spots are identified by calculating the retardation factor (R_f), which is the ratio of the distance moved by the analyte from the origin to the distance moved by the flowing solvent from the origin (Figure 19) (Peterson & Cummings 2006). To obtain reliable identification for the lipid spots, a reference sample should also be applied to the plate since R_f values depend on different parameters such as solvent composition, used TLC plates, relative humidity, and temperature. Additionally, TLC is possible to couple with matrix assisted laser desorption ionization (MALDI) mass spectrometer (Fuchs et al. 2009).

The separation of lipid classes can be improved by using two-dimensional (2D) chromatography in which the TLC plate is first developed in one direction, and after drying, it is developed in another solvent mixture and the plate is turned 90° compared to the first development direction (Figure 19) (Singh & Jiang 1995; Peterson & Cummings 2006). However, 2D TLC cannot be

used to analyze more than one sample per plate (White et al. 1998; Fuchs et al. 2011). Also, as only a single sample can be applied, the simultaneous application of standards is not possible which complicates spot assignments and quantitative data analysis (Fuchs et al. 2011).
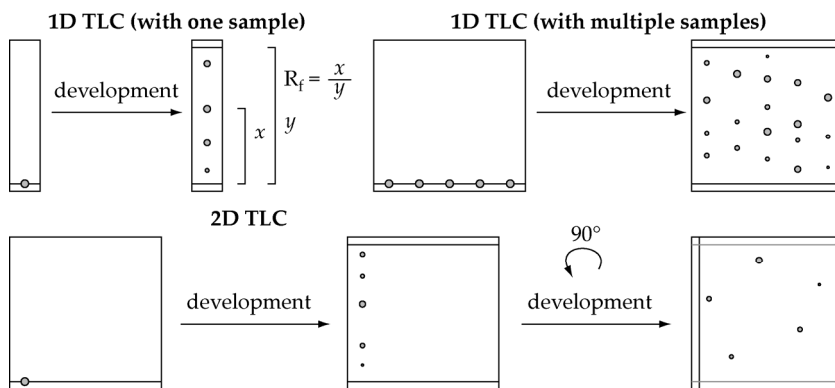
Figure 19. Overview of the one-dimensional (1D TLC) and two-dimensional (2D TLC) thin-layer chromatography runs. Retardation factor (R_f) is defined as the ratio of the distance moved by the analyte from the origin (x) to the distance moved by the flowing solvent from the origin (y).

An another variation of TLC, a multi-one-dimensional TLC (MOD-TLC) involves the separation of lipids by running the plate using several different solvent mixtures and drying the plate before changing the solvent (White et al. 1998). MOD-TLC allows for direct comparative analysis of multiple samples on a single TLC plate, and still provides good resolution for the quantification of most of the major lipid classes. There are MOD-neutral- and MOD-flip-flop-TLC methods which vary from each other by the used solvent mixtures and the place where the samples are applied on the plate. Additionally, in MOD-flip-flop-TLC, the TLC plate is rotated by 180° before the last solvent run (White et al. 1998).

High-performance TLC (HPTLC) is an advancement of TLC method which exploits finer gel grades than normal TLC and allows plates to be thinner and smaller, thus leading to faster separation times and better separation efficiency (Peterson &

Cummings 2006; Stübiger et al. 2009). Furthermore, HPTLC requires smaller sample amounts, as well as smaller detection limits can be achieved when compared with normal TLC (Fuchs et al. 2011).

Gas chromatography

Gas chromatography can be used to separate volatile organic compounds (Roberts et al. 2008). Some of the lipids are naturally volatile but most of them must be derivatized to increase their volatility (Nelson & Cox 2000; Roberts et al. 2008). Thus, prior to GC-analysis, lipids are hydrolyzed and methylated to corresponding FA methyl esters (FAMEs) (Bicalho et al. 2008).

GC includes a solid stationary phase and a gaseous mobile phase (Peterson & Cummings 2006). Polar stationary phases are usually used to separate complex FAME mixtures (Bicalho et al. 2008). Non-polar silicone phase allows separation of FAMEs according to their molecular weight whereas high molecular weight hydrocarbon phase separates FAMES based on their unsaturation (Roberts et al. 2008). Helium is commonly used as a mobile phase (Bicalho et al. 2008; Novgorodtseva et al. 2011; Liu et al. 2011). There are different detectors that can be coupled to GC but flame ionization detection and mass spectrometer are commonly used in lipid studies (Dodds et al. 2005; Quehenberger et al. 2011).

High-performance liquid chromatography

High-performance liquid chromatography is a widely used separation method for lipids, and it can also be used for quantification when internal standards are available (Schiller et al. 2004). HPLC utilizes a solid or a liquid-coated solid stationary phase and a liquid mobile phase (Peterson & Cummings 2006). Also ultra-performance liquid chromatography (UPLC) is applied to lipid analysis. With UPLC it is possible to obtain chromatographic separations in shorter analytical run than with HPLC without losing specificity and fidelity (Castro-Perez et al. 2010).

HPLC can be divided in two groups on the basis of the polarities of the stationary phase and the mobile phase: normal-phase HPLC (NP-HPLC) and reverse-phase HPLC (RP-HPLC). In NP-HPLC the stationary phase is more polar than the mobile phase whereas in RP-HPLC the mobile phase is more polar than the stationary phase (Peterson & Cummings 2006). For example, when separating phospholipids, NP-HPLC separates PLs according to their head group whereas RP-HPLC allows separation based on the hydrophobicity of the FA residues (Schiller et al. 2004; Castro-Perez et al. 2010; Khalil et al. 2010).

Common detectors coupled to HPLC that are used for lipid studies include ultraviolet (UV) detector, light scattering detector (LSD), and mass spectrometer (Roberts et al. 2008). UV detectors are highly sensitive but saturated FAs are under-represented since only carbonyl groups and double bonds are functional groups that absorb in the UV range (Peterson & Cummings 2006). LSD measures the intensity of light scattered by lipids that remain after the solvent has been evaporated (Wang et al. 2003). LSD is not dependent on the degree of saturation of the FAs in the sample like UV detectors but the detector is destructive and each lipid class needs to be calibrated separately to quantify lipids (Peterson & Cummings 2006). MS is nowadays the most popular detection method and it is further discussed later.

Solid-phase extraction

SPE is a column chromatography method in which the analytes form strong but reversible interactions with the stationary phase of the column and the compounds are separated by washing the column with different solvents (Ruiz-Gutiérrez & Pérez-Camino 2000). There is a wide range of chemically bonded stationary phases commercially available but the most suitable phases for the separation of lipid classes are aminopropyl bonded phases (Burdge et al. 2000; Bondia-Pons et al. 2006).

In SPE, the columns are placed in vacuum and activated with an appropriate solvent mixture. Lipid extracts dissolved in

chloroform are applied to the cartridges under vacuum and the solvent is pulled through, thus leaving the lipid mixture on the column (Bondia-Pons et al. 2006). The column is washed with different solvents to separate different lipid classes (Kaluzny et al. 1985; Bondia-Pons et al. 2006). In Figure 20 is shown how FFAs, PLs, and neutral lipids can be separated using SPE. Since the recovery of lipid classes is less than 100%, appropriate recovery standards should be included into the samples for the determination of lipid concentrations (Burdge et al. 2000).
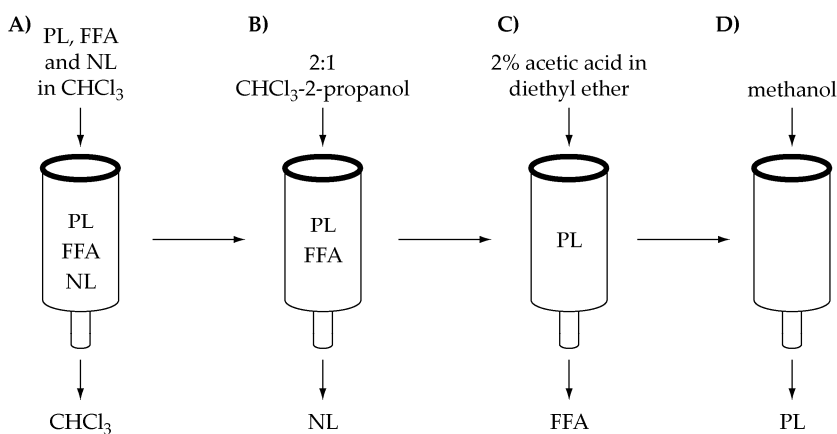
Figure 20. *Separation of phospholipids (PLs), free fatty acids (FFAs) and neutral lipids (NLs) including free cholesterol, esterified cholesterol, triacylglycerides, diacylglycerides, and monoacylglycerides by solid-phase extraction (Kaluzny et al. 1985). Lipid extract is first dissolved in chloroform, and then the mixture is applied to the column. Chloroform is pulled through thus leaving the lipids on the column (A). The column is eluted with 2:1 chloroform-2-propanol to separate neutral lipids (B). 2% acetic acid in diethyl ether is used to separate FFAs from PLs (C), and finally, PLs are removed from the column by adding methanol (D).*

Comparison of the fractionation methods

The advantages and drawbacks of TLC, GC, HPLC, as well as SPE are shown in Table 6. TLC is ecologically-friendly method since low amounts of solvents are needed especially in comparison with HPLC (Fuchs et al. 2010). SPE resembles TLC since both of them are able to separate lipid mixtures into different lipid classes (Bondia-Pons et al. 2006). HPLC is

74

relatively fast and it has high resolution (Schiller et al. 2004). GC requires the lipids to be volatile, and thus, polar lipids need to be derivatized (Wenk 2005). Both GC and HPLC can be automated and combined with mass spectrometer (Fuchs et al. 2011).

Table 6. *The advantages and drawbacks of thin-layer chromatography (TLC), gas chromatography (GC), high-performance liquid chromatography (HPLC), and solid phase extraction (SPE) (Wenk 2005; Khalil et al. 2010; Fuchs et al. 2011).*

Method	Advantages	Drawbacks
TLC	- inexpensive - low amounts of solvents - technically easy - suitable for complex mixtures - different staining - possible to couple with MALDI	- oxidation of unsaturated FAs may occur - not automated - relatively poor reproducibility - low lipid recoveries
GC	- highly established in FA analysis - automatic devices commercially available - coupling with mass spectrometer	- derivatization required since only volatile compounds can be analyzed - large amount of lipids required for derivatization - yield information on the hydrolysis products of lipids and not on the parent compounds
HPLC	- high quality separations achievable - separated fractions can be collected and used for further analysis - automated - coupling with mass spectrometer	- detection of saturated lipids difficult when using UV detector - post-column derivatization challenging
SPE	- quite inexpensive - versatile - technically easy	- recovery standards required for quantification - not automated

1.7.3 Lipid quantification techniques

TLC, GC, and HPLC are mainly lipid separation methods but they can also to some extent be used for quantification of lipids. However, MS and nuclear magnetic resonance (NMR) spectroscopy are preferable methods for lipid identification and quantification.

Mass spectrometry

Mass spectrometric analysis includes a production of gas-phase ions from analyte compounds, a separation of the formed ions according to their mass-to-charge ratio (*m/z*), and a detection of ions in proportion to their abundance (Roberts et al. 2008). It is also possible to fragment the precursor ion which is useful especially in identification of the compounds. This method is called tandem MS (MS/MS) (de Hoffmann & Stroobant 1999). There are many types of mass spectrometers that differ in the type of ionization source and mass analyzer (Peterson & Cummings 2006).

Ionization sources can be divided into hard and soft ionization methods based on the extent of fragmentation of the molecule. Hard ionization methods, such as electron ionization, yield a lot of fragments whereas soft ionization techniques, such as electrospray ionization (ESI) and MALDI, result in only a few fragmentations and usually the molecular ion is present in the mass spectrum (Peterson & Cummings 2006). The soft ionization methods are preferred in modern lipid analysis (Schiller et al. 2004).

ESI is an ion source which ionizes a sample at atmospheric pressure. The sample is directed through a narrow hole in the ion source creating a spray. The spray is ionized, and eventually the solvent evaporates and charge is applied to the sample (de Hoffmann & Stroobant 1999; Peterson & Cummings 2006). ESI generates usually protonated or deprotonated molecules depending on the polarity of the ionization mode utilized. It can also generate molecular adducts with cations such as Na^+, K^+ or NH_4^+ in positive ion mode which originate mainly from the mobile phase used for the analysis (Castro-Perez et al. 2010).

ESI is usually coupled to time-of-flight (TOF) (Sandra et al. 2010) or ion-trap (Hu et al. 2008; Pang et al. 2008; Ding et al. 2008; Sorensen et al. 2010) mass analyzers. ESI-MS is suitable for sensitive, quick, and high-throughput qualitative and quantitative determination of lipid mixtures (Table 7), especially PLs, since ESI-MS has a simple sample processing approach, good resolution, and it can be automated (Zhu et al. 2009). Using ESI-MS it is possible to characterize and quantify substances even in femtogram levels (Castro-Perez et al. 2010).

MALDI ion source requires that the sample is crystallized with a matrix that absorbs light at the laser wavelength (Fuchs et al. 2010). Small organic molecules are usually used as a matrix, and 2,5-dihydroxybenzoic acid (DHB) has proposed to be the most appropriate matrix for lipid analysis. By using DHB, both positive and negative ion mass spectra can be recorded from the same sample. Lipid analysis by MALDI is usually performed using N_2 lasers (Schiller et al. 1999; Schiller et al. 2004). When the vaporized gas cloud expands, ions (e.g. H^+ and Na^+) are exchanged between the matrix and the analyte, thus leading to the formation of charged analyte molecules which are called adducts or quasimolecular ions. Also anions can be generated by abstracting H^+ or Na^+ from the analyte. Positive and negative ions can be differentiated by inverting the direction of the applied electric field. To record positive-ion mode spectra is more common and it has been noted that MALDI mass spectrometers detect negative ions less sensitively than positive ions (Fuchs et al. 2009; Fuchs et al. 2010).

MALDI ion source is normally combined with a TOF mass analyzer since TOF has a nearly unlimited mass range and the pulsed ion generation of MALDI is most suitable for TOF (Fuchs et al. 2010). MALDI-TOF MS allows the analysis of lipids in nanomolar range (Schiller et al. 2004). The advantages of MALDI-MS are the speed of analysis and simplicity of operation (Zehethofer & Pinto 2008; Hu et al. 2009). However, the matrix molecules cause a lot of background in the lower mass range which is an important disadvantage of the method (Table 7). MALDI can be coupled also with Fourier transform ion

cyclotron resonance MS (FTICR-MS) which solves the problem arising from the matrix background because the matrix peaks and lipids are resolved due to the high resolution of FTICR. FTICR has also better mass accuracy, sensitivity, and MS/MS capabilities than MALDI-TOF MS but the acquisition time is slower. MALDI-MS-based methods have limitations such as quantification of complex mixtures, and when compared with ESI-MS, MALDI-MS is less quantitative (Table 7) (Hu et al. 2009).

Table 7. The advantages and drawbacks of electrospray ionization (ESI) and matrix assisted laser desorption ionization (MALDI) (Wenk 2005; Hu et al. 2009).

Ionization	Advantages	Drawbacks
ESI	- direct detection by *m/z*	- suppression of ionization
	- high sensitivity and resolution	- absolute quantification
	- direct profiling of complex lipid mixtures	laborious
	- ease of automation	
	- compatible with HPLC and GC	
	- quantification in femtogram level	
MALDI	- direct detection by *m/z*	- suppression of ionization
	- buffer and salt contaminants generally well tolerated	- matrix backgrounds
		- less quantitative than ESI-MS
	- can be combined with prior TLC separation	- quantification of complex mixtures difficult
	- fast	
	- simple	- quantification of lipids in nanomolar range

Before MS analysis the sample is usually pre-fractionated using liquid chromatography (Pang et al. 2008; Sandra et al. 2010; Sorensen et al. 2010), TLC (Fuchs et al. 2009), GC (Zhu et al. 2009) or SPE (Burdge et al. 2000) since different lipid classes have different desorption/ionization characteristics which cause suppression effects thus making the analysis difficult or the interpretation of the results complicated. The fractionation

significantly improves the lipid detection and allows more accurate peak assignments and easier quantification (Stübiger et al. 2009). However, the fractionation can weaken the accuracy since the yields of different lipid species obtained by using diverse fractionation methods may vary unless also yield standards are used.

There is also a direct infusion ESI-based MS approach that involves a direct infusion of a crude lipid extract or a fraction obtained after further sample preparation into the MS without pre-fractionation (Han et al. 2012). A drawback of this method is that the resolution of the lipids with the same molecular weight (isobaric lipids) is limited if MS/MS experiments are not used and there is a risk of ion suppression of very low abundant lipids (Hu et al. 2009).

The quantification with MS requires the use of internal standards. Especially when using MALDI, there is a direct relation between signal intensity and analyte concentration only in a small concentration range. Thus, similarly concentrated analyte solutions should be used and all the measurements should be performed in the presence of internal standards (Fuchs et al. 2010). The internal standard should belong to the same lipid class as the compound that is investigated and have a comparable molecular weight (Schiller et al. 2004). Isotopically labeled compounds or lipids with odd numbered fatty acyl chains are commonly used as internal standards in lipid samples. It is also possible to use relative peak intensity ratios for the quantification but it does not reveal whether only one or both concentrations are changing, and thus, the use of internal standards is recommended (Fuchs et al. 2010). Lipids can also be quantified by using a signal-to-noise ratio (*S/N*) that is calculated according to Eq. 1 (Müller et al. 2001).

$$S/N = 2.5[(S_H - 0.5N_{PP})/N_{PP}], \qquad (1)$$

where S_H is the signal height at the center of a certain mass peak over the lower limit of noise (Figure 21). N_{PP} is the peak-to-peak

noise amplitude, determined from the maximum and minimum values of 250 points of pure noise (Figure 21).
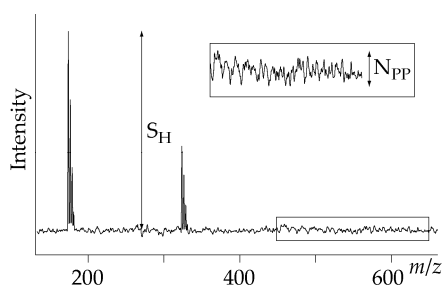
Figure 21. Hypothetical mass spectrum showing the signal height of a certain peak over the lower limit of noise (S_H) and the peak-to-peak noise amplitude (N_{PP}) that are used for the calculation of the S/N ratio from the MS spectrum as shown in Equation 1.

NMR spectroscopy

NMR spectroscopy is based on the behavior of magnetically active nuclei in magnetic field (Günther 1995). The nuclei are excited with a radiofrequency pulse after which they start to return to their ground state and the emission signal i.e. free induction decay (FID) is detected (Fessenden et al. 1998; Claridge 1999). FID describes the intensity of the detected signal as a function of time. FID is then Fourier transformed to give a spectrum in which the signal intensities are presented as a function of frequency (Claridge 1999). Chemical shifts of the resonance signals are usually reported in δ values, which are expressed as parts per million (ppm) of the applied radiofrequency (Fessenden et al. 1998). For example, at 500 MHz, 1.0 ppm is 500 Hz.

Prior to NMR measurement, the sample has to be dissolved in a deuterated solvent that serves as a lock signal to maintain the field stability. Normally a chemical shift reference compound is added to the sample (Claridge 1999). In the NMR spectrum, the area under a resonance signal is proportional to the number of nuclei that give rise to the signal (Figure 22) (Beyer et al. 2010; Srivastava et al. 2010a). The signal areas can be transformed to concentrations by using an internal or external concentration reference compound. If a concentration reference is not used, the relative quantification can be performed by using ratios of selected resonances (Kriat et al.

1993). The acquisition parameters, such as pulse width, acquisition time, relaxation delay, spectral width, transmitter offset, and number of scans and dummy scans should be selected in a way that the spectrum provides quantitative information (Beyer et al. 2010).

NMR spectroscopy has several advantages over MS-based approaches (Oostendorp et al. 2006). NMR does not require many different standard compounds, the identification and quantification of lipids are almost unequivocal if at least one distinct resonance is resolved and the sample preparation is simple (Oostendorp et al. 2006; Srivastava et al. 2010a). In addition, NMR spectroscopy does not require extensive optimization of instrumental parameters that are often needed in mass spectrometry. However, the quantification of metabolites from complex mixtures can be difficult if the signals are severely overlapping. Additionally, NMR is less sensitive (quantification in micromolar range) than MS-based approaches (Hu et al. 2009).
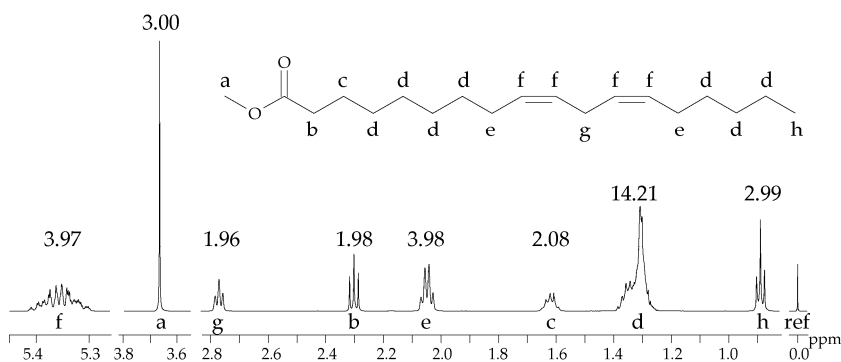
Figure 22. ^{1}*H NMR spectrum (500 MHz) of methyl linoleate in deuterated chloroform with signal assignments. Chemical shifts (ppm) are referenced to tetramethylsilane (ref). The signal areas are shown on the top of each signal.*

^{1}H, ^{13}C, and ^{31}P are the most useful nuclei in the biological NMR studies, and ^{1}H is the most sensitive naturally occurring NMR nucleus due to its high gyromagnetic ratio and 100% abundance (Claridge 1999; Srivastava & Govil 2001). Tritium has even higher gyromagnetic ratio than proton but its natural

abundance is negligible (3×10^{-16}%) (Yuen et al. 2010). The one-dimensional (1D) ^{1}H NMR spectrum of untreated serum does not provide much information on lipid molecules since they are mainly situated in the lipoprotein particles, and broad protein signals obscure their resonances (Oostendorp et al. 2006). However, this kind of spectrum can be used to quantify lipoprotein subclasses (Ala-Korpela et al. 2007). ^{1}H NMR-based method for the quantification of lipoprotein subclasses was developed in 1990s (Otvos et al. 1992; Ala-Korpela et al. 1994). There is a commercial protocol called NMR LipoProfile® (by LipoScience Inc.) which provides information on 9 lipoprotein subclasses (Jeyarajah et al. 2006). There is also a corresponding assay that is able to quantify 14 lipoprotein subclasses (chylomicrons and extremely large VLDL particles, very large VLDL, large VLDL, medium VLDL, small VLDL, very small VLDL, IDL, large LDL, medium LDL, small LDL, very large HDL, large HDL, medium HDL, and small HDL) (Inouye et al. 2010). Additionally, concentrations of several lipid groups in the lipoprotein subclasses (e.g. VLDL-TAGs, LDL-cholesterol, and HDL-cholesterol) can be determined (Vehtari et al. 2007; Kettunen et al. 2012). The quantification of both lipoprotein subclasses and the lipids in lipoproteins are obtained by a quantification protocol utilizing regression models. The models are cross-validated against NMR-independent HPLC data (Kettunen et al. 2012).

The extraction of the lipids from serum makes it possible to quantify individual lipid species. 1D ^{1}H NMR spectrum of a serum lipid extract provides, for example, concentrations of free and esterified cholesterol, TAGs, glycerophospholipids, PC, and SM (Tukiainen et al. 2008). Also, at least two FAs, linoleic acid and DHA, can be quantified (Willker & Leibfritz 1998; Tukiainen et al. 2008). Furthermore, methyl (CH_3), methylene (-CH_2-), allylic (=CH-CH_2-), olefinic (-CH=CH-), and bisallylic (=CH-CH_2-CH=) signals can be identified (Oostendorp et al. 2006). The ratios of these signals have been used to estimate the mean FA chain length (methylene/bisallylic) (Kriat et al. 1993), the number of double bonds (methylene/olefinic) (Kriat et al.

1993), and the presence of branched chain FAs (methylene/methyl) (Oostendorp et al. 2006). It should be noted that the contribution of cholesterol protons have to be taken into account whenever they overlap with other signals (Roncalli et al. 2007).

[13]C has low abundance (1.1%), and its gyromagnetic ratio is one-quarter of that of ^{1}H, and thus, the overall sensitivity of a ^{13}C NMR measurement is approximately 0.01% of a proton spectrum of the same sample (Srivastava & Govil 2001). However, ^{13}C NMR spectra are useful especially in identification of lipids since carbon chemical shifts are spread about 200 ppm range compared with narrow range of proton chemical shifts (approximately 10 ppm) (Pollesello et al. 1996; Srivastava & Govil 2001). Furthermore, the resonances that are severely overlapping in the 1D spectrum can be resolved and identified by homonuclear ([1]H-^{1}H) or heteronuclear (^{1}H-^{13}C) 2D NMR (Srivastava & Govil 2001).

[31]P is naturally abundant nucleus (100%), and the assignment of ^{31}P resonances is quite simple since the chemical shift range of biological phosphates is large (approximately 40 ppm) (Srivastava & Govil 2001). In lipid studies, ^{31}P NMR is suitable for PL analysis (Kriat et al. 1993; Wenk 2005; Srivastava et al. 2010b; Fuchs et al. 2011). The main PLs of serum include PC, SM, and LPC, and they give separate resonance signals to a ^{31}P NMR spectrum. Less abundant phospholipids, such as PS and PE, are usually not detected in a reasonable time (Kriat et al. 1993). When measuring ^{31}P NMR spectra, a suitable detergent can be added to the sample to suppress the aggregation of PLs that would cause line-broadening and loss of resolution (Fuchs et al. 2011).

2 Aims of the study

This thesis introduces novel protocols for ^{1}H NMR analysis of serum lipids. The development of the protocols was performed in the NMR metabonomics laboratory at the University of Eastern Finland, and the developed protocols have already been applied to numerous studies. The specific aims of this thesis were:

1. To learn to perform modern quantum mechanical spectral analyses by analyzing the ^{1}H NMR spectra of *n*-alkanes, as well as to understand the conformational behavior of CH_2-fragments, common structural units in lipids, in a solution state via the NMR spectral parameters of *n*-alkanes (Paper I)

2. To develop and optimize an extraction protocol for serum lipids that allows the extraction of about 100 samples per day

3. To develop a constrained total-line-shape (CTLS) fitting protocol to be used in the quantification of the ^{1}H NMR spectra of serum lipid extracts (Paper II)

4. To apply the lipid extraction and quantification protocols to clinical studies. The first study included patients with MCI (Paper II), and the second type 1 diabetic patients with concomitant kidney disease (Paper III)

5. To develop an NMR-based protocol for the assessment of the serum lipid oxidation susceptibility (Paper IV)

6. To apply the NMR oxidation protocol to serum samples from a chocolate consumption study (Paper IV)

3 Materials and methods

3.1 SAMPLE POPULATIONS

The extraction protocol for serum lipids was developed using fasting serum obtained from healthy volunteers. The serum samples were stored at -70°C. The study populations of the MCI, diabetes, and oxidation studies are defined below.

3.1.1 Sample population of the MCI study (II)

A total of 806 elderly individuals were recruited from Kuopio, Finland, between October 1997 and November 1998 to determine the prevalence of MCI among elderly population (Hänninen et al. 2002). The participants without dementia were followed-up at approximately 3, 5, and 6 years after the baseline visit. Altogether 45 individuals completed the full 6 years of follow-up and this group was included in the study. On each visit the participants underwent a structured interview including demographic and medical information, as well as an extensive neuropsychological assessment. The diagnosis of MCI was based on the diagnostic criteria proposed by Mayo Clinic Alzheimer's Disease Research Center (Hänninen et al. 2002). At baseline two of the participants had MCI, and on the following visits the number of MCI subjects was 18, 16, and 18. At the last visit one of the subjects received a dementia diagnosis. Weight, height, and blood pressure were measured, and fasting blood samples were drawn at each visit.

3.1.2 Sample population of the diabetes study (III)

Altogether 326 type 1 diabetic patients (218 men and 108 women) as part of the Finnish Diabetic Nephropathy Study were included in the study (Mäkinen et al. 2008). Type 1 diabetes was defined as an age of onset below 35 years. About half (56%) of the study population did not have kidney disease and the rest

had microalbuminuria (17%) or overt kidney disease (26%). Serum and urine samples were collected from each study subject.

The normal range of urinary albumin excretion rate (AER) was defined as AER < 20 µg/min for night urine or AER < 30 mg/24h for a timed circadian collection. The limits for overt kidney disease were: AER ≥ 200 µg/min or AER ≥ 300 mg/24h (macroalbuminuria). The intermediary range (microalbuminuria, 20 ≤ AER < 200 µg/min or 30 ≤ AER < 300 mg/24h) is a clinically challenging borderline with no clear pathological changes. In this study, microalbuminuria was regarded as not having kidney disease, since reduced kidney function could not be seen. Since there can be a large daily variance in the AER values, the kidney diagnosis was based on at least two out of three consecutive albumin tests. Urinary albumin was measured also centrally from a single 24 h collection to obtain a continuous renal status (denoted by 24 h-AER).

3.1.3 Sample population of the chocolate study (IV)

The study population consisted of 45 non-smoking subjects (12 men and 33 women) who had consumed 75 g of white chocolate (WC), dark chocolate (DC) or high-polyphenol chocolate (HPC) daily for three weeks (Mursu et al. 2004). There were 15 subjects in each chocolate group. The study subjects had to fulfill following criteria: (i) BMI < 32 kg/m^2; (ii) no regular use of any drugs or supplements with antioxidative (β-carotene, vitamins C or E) or lipid-lowering properties; (iii) no chronic diseases such as diabetes, coronary heart disease, or other major illnesses; and (iv) willingness to consume 75 g of study chocolate daily for 3 weeks. Fasting blood samples were taken before and after the chocolate consumption. The serum samples were stored at -70°C and not thawed before.

3.2 SAMPLE PREPARATION

3.2.1 Preparation of the *n*-alkane samples (I)

Approximately 5% (w/v) samples of liquid *n*-pentane, *n*-hexane, and *n*-heptane were prepared by dissolving the alkanes in deuterated chloroform. The *n*-butane sample was prepared by dissolving gaseous *n*-butane in deuterated chloroform. In addition, both *n*-pentane and *n*-hexane were dissolved in deuterated benzene, acetone, methanol, and dimethylsulfoxide (DMSO). For *n*-pentane, also acetonitrile and dichloromethane were used as solvents, and *n*-hexane was dissolved in hexane-d$_{14}$. The samples were filtered through cotton wool to 5 mm NMR tubes in order to get rid of possible solid particles, and oxygen in the NMR tubes was replaced with nitrogen. The solvents contained 0.03% of tetramethylsilane that served as an internal chemical shift reference.

3.2.2 Preparation of the lipid samples

Approximately 5% (w/v) samples of hexanoic acid (6:0), palmitic acid, oleic acid, palmitoleic acid, linoleic acid, DGLA, arachidonic acid, α-linolenic acid, EPA, DHA, PC, SM, TAG, as well as free and esterified cholesterol were prepared by dissolving the lipids in deuterated chloroform. Tetramethylsilane was used as an internal chemical shift reference.

3.2.3 Extraction of lipids (II, III, IV)

Serum lipids were extracted by using a dichloromethane (Cequier-Sánchez et al. 2008) method with some in-house modifications. Briefly, 1:2 (v/v) methanol-dichloromethane solution and an equal amount of 0.15 M NaCl solution were added to a serum sample. The sample was mixed and centrifuged (2200×*g* 20 min (II and III), or 2400×*g* 10 min (IV)) after which the lower dichloromethane layer was recovered. The remaining aqueous phase was extracted again with dichloromethane. The separated organic phases were combined and evaporated to dryness. The lipids were dissolved in 0.6 ml

of deuterated chloroform containing 0.03% tetramethylsilane for chemical shift reference.

3.2.4 Oxidation of lipids (IV)

First, 0.3 ml of serum, 0.3 ml of NMR buffer (75 mM Na_2HPO_4 in 80%/20% H_2O/D_2O, pH 7.4; including also 0.08% sodium 3-(trimethylsilyl)propionate-2,2,3,3-d_4 and 0.04% sodium azide) (Soininen et al. 2009), and 0.3 ml of 0.15 M sodium chloride solution were combined in a 2 ml eppendorf tube after which the solution was warmed in an incubator at 37°C for 10 min. Oxidation reaction was initiated by adding 0.1 ml of 5, 10, 20 or 40 mM $CuSO_4$ to the prewarmed solution to yield a copper concentration of 0.5, 1.0, 2.0 or 4.0 mM, respectively. In order to determine the initial concentration of PUFAs in each sample, also a reference sample without copper was prepared. The copper containing samples were incubated in an end-over-end mixer at 37°C for 1.5, 3, 4.5 or 6 h. The optimized oxidation protocol included 0.5 M $CuSO_4$ and 6 hour incubation. The oxidation reaction was terminated by extracting the lipids as described above.

To be able to evaluate the repeatability of the method, five replicate samples were prepared within a period of two months in random order. The chocolate study samples were analyzed in triplicates (WC and HPC groups) or duplicates (DC group).

3.3 NMR SPECTROSCOPY (I, II, III, IV)

The ^{1}H NMR measurements of all the studies were performed on a Bruker AVANCE 500 DRX spectrometer operating at 500.13 MHz. Some of the spectra of the *n*-alkane study were measured with a Bruker AVANCE III spectrometer operating at 500.36 MHz. Shimming of the *n*-alkane samples was performed manually paying attention to both linewidth and lineshape. The *n*-alkane spectra were measured with spinning the sample. The samples of the other studies were shimmed automatically

without spinning the sample. Acquisition parameters used in each study are shown in Table 8.

Table 8. Acquisition parameters used in the measurements of n-alkanes (I), hexanoic acid, individual lipid species, as well as MCI (II), diabetes (III), and chocolate (IV) studies.

Parameter	I and hexanoic acid	individual lipid species	II and III	IV
T (K)	300	293	293	295
pulse sequence	zg	zg	zg	zg
pulse angle (°)	90	90	90	90
sw (Hz)	5530	3230	5340	4400
td	262144	65536	65536	65536
ds	0	0	4	2
ns	8	1	64	64
aq (s)	23.7	10.1	6.1	7.5
d1 (s)	10.0	3.9	3.9	0.5

aq, acquisition time; d1, relaxation delay; ds, number of dummy scans; ns, number of scans; sw, spectral width; td, number of data points

All the spectra were processed using PERCH NMR Software (Laatikainen et al. 2011). The measured FIDs were zero-filled and multiplied by an exponential window function with a 0.3 Hz (II and III) or a 0.5 Hz (IV and individual lipid species) line-broadening. The FIDs of the *n*-alkanes (I) and hexanoic acid were multiplied by a sinusoidal ($A\sin^2 x + Be^y$) window function prior to Fourier transformation to narrow the linewidths in order to be able to reveal the information arising from small coupling constants.

3.4 QUANTUM MECHANICAL SPECTRAL ANALYSIS

3.4.1 Spectral analysis of the ^{1}H NMR spectra of *n*-alkanes (I)

The spectral analyses of *n*-butane, *n*-pentane, *n*-hexane, and *n*-heptane were performed with PERCH NMR Software

(Laatikainen et al. 2011) using total-line-shape (TLS) fitting (Laatikainen et al. 1996a) mode of the PERCHit iterator. The geminal (^2J) coupling constant of *n*-butane could not be obtained from the spectrum, and therefore, the value was estimated on the basis of the analysis of *n*-pentane spectrum and the value was kept fixed during the iteration. The spectral analyses of *n*-hexane and *n*-heptane were performed including only ^2J, ^3J, and ^4J coupling constants since the spectra did not contain enough information about ^5J and ^6J couplings.

Also baseline parameters were optimized during the iteration. The baseline correction compensates mainly lineshape artifacts that are due to the resolution enhancement which reduces the relative intensity of the central parts of the CH_2 signals. Since essential information on the coupling constants is carried by weak lines, some of the fittings were performed using a weighting function that gives higher weight for the smaller signals than for bigger ones.

The spectral analyses of *n*-butane, *n*-pentane, and *n*-heptane were performed allowing different linewidths for each spin particle. In the case of *n*-hexane, the ^2J coupling constants correlated with linewidths and had only a weak effect on the spectrum, and hence, the following approach was used. The geminal coupling constants were estimated on the basis of the spectral analysis of *n*-pentane and were kept fixed during the iteration. The fitting was started using the same linewidth for each spin particle and after convergence was achieved, the linewidths were released.

3.4.2 Spectral analysis of the ^1H NMR spectrum of hexanoic acid

The spectral analysis of hexanoic acid was performed with PERCH NMR Software (Laatikainen et al. 2011) using both integral transform (Laatikainen et al. 1996a) and TLS fitting (Laatikainen et al. 1996a) modes of the PERCHit iterator. The starting values for the analysis were estimated based on the analyses of the *n*-alkane spectra. The ^5J and ^6J coupling constants were set to zero since the spectrum did not contain enough

information to solve them. The spectral analysis was started using integral transform mode, and the spectral parameters were finalized using TLS fitting mode.

3.5 QUANTIFICATION OF SERUM LIPIDS BY TOTAL-LINE-SHAPE FITTING (II, III, IV)

The areas of the lipid resonances were determined using TLS fitting mode of PERCH NMR software (Laatikainen et al. 2011). The structures of some multiplets, which were defined by the intensity ratios, coupling constants, and frequencies of individual signals forming the multiplet, were used as constraints that enabled the quantitative analysis of severely overlapping peaks (Soininen et al. 2005). More detailed description of the analysis is provided in the Results and discussion section.

3.6 CALCULATION OF THE NMR OXIDATION SUSCEPTIBILITY (IV)

The NMR oxidation susceptibility was determined from the signal areas of the bisallylic protons of PUFAs (A_{PUFA}) at 2.74–2.88 ppm. First, the difference between the amounts of PUFAs before (REF) and after (OX) the oxidation reaction was calculated. Then, the difference was divided by the signal area of PUFAs from the spectrum of non-oxidized sample and converted to a percentage value ((A_{PUFA}(REF)-A_{PUFA}(OX))/A_{PUFA}(REF)×100%). The obtained value describes the amount of oxidized PUFAs, and hence, the oxidation susceptibility of serum lipids. The signal areas were scaled so that the signal area of total cholesterol C(18)H$_3$ protons was the same both in the spectra of non-oxidized and oxidized serum. Also cholesterol oxidizes slightly and many of the cholesterol oxidation products can be identified from the spectrum of oxidized serum since their C(18)H$_3$ signals resonate at 0.61–

0.69 ppm, next to the non-oxidized cholesterol C(18)H$_3$ signals (0.676 and 0.678 ppm) (Bradamante et al. 1992). These oxysterol signals were taken into account when the total cholesterol amount was calculated.

3.7 DATA ANALYSIS

3.7.1 Statistics of the oxidation study (IV)

The results are expressed as means (± standard deviations). A paired t-test was used to test the changes between the baseline and end-point values within the study groups. Means were compared across the study groups by the analysis of variance (ANOVA), and post hoc Tukey's test was used when a statistically significant heterogeneity between the groups was shown by the ANOVA. Correlations were estimated by Pearson's or Spearman's correlation coefficients. Differences with p values of 0.05 or less were considered significant. The statistical analyses were performed with SPSS software (version 14.0; SPSS, Inc., Chicago, IL, USA).

Random forest classification was used to study the chocolate induced metabolic effects and random forest regression was used to explore the descriptors for the oxidation susceptibility. Random forest analysis involves a build-in cross-validation that uses out-of-bag data (usually 30% of the samples). For classification, there are two ways to measure variable importance, mean decrease in classification accuracy and mean decrease in Gini index. These usually provide slightly different results, and there is no common agreement which one should be preferred. For regression, the corresponding performance measures are increase in mean square error and increase in node purity. The calculations were performed with the R (R Development Core Team 2008) program package randomForest (Liaw & Wiener 2002).

4 Results and discussion

4.1 ^{1}H NMR SPECTRA OF _N_-ALKANES

Alkyl chains are important structural units in many compounds, for example in lipids. Even though the structures of _n_-alkanes are simple, they yield quite complex spectra. This chapter presents the quantum mechanical spectral analyses of _n_-butane, _n_-pentane, _n_-hexane, _n_-heptane, and hexaenoic acid in chloroform. In addition, solvent effects on the conformational equilibrium of _n_-alkanes are discussed.

4.1.1 Quantum mechanical spectral analysis of _n_-alkanes (I)

The difficulty in the analysis of _n_-butane was that the spectrum (Figure 23A) does not contain much information about the geminal coupling constant, and thus, its accurate value cannot be obtained from the spectral analysis. This problem could be solved by estimating the value of the geminal coupling constant on the basis of the analysis of _n_-pentane spectrum since the values of other coupling constants did not depend significantly on the ^2J coupling. The spectral parameters of _n_-butane in chloroform are shown in Table 9.

The spectral analysis of the ^{1}H NMR spectrum of _n_-pentane in chloroform (Figure 23B) was straightforward and all the spectral parameters could be determined (Table 9). The spectral analysis of _n_-hexane (Figure 23C) appeared to be more complex and there were problems with all the other coupling constants except ^3J couplings. First, the small ^5J and ^6J couplings could not be solved unambiguously, and they were set to zero. Since these couplings and their variations can be assumed to be small, this approximation does not cause significant bias to other couplings. Second, the spectrum does not contain enough information about the ^2J couplings since only their difference ($^2J_{2,2}$ - $^2J_{3,3}$) seemed to be well defined. The ^2J couplings also

correlated with $^4J_{2,4'}$ and $^4J_{2,4}$ couplings and linewidths. Thus, the analysis was performed by fixing the ^2J couplings to the values that were estimated on the basis of the spectral analysis of *n*-pentane. Third, the $^4J_{2,4'}$ and $^4J_{2,4}$ couplings remained inaccurate since only their sum was rather well defined. The spectral parameters of *n*-hexane in chloroform are shown in Table 9.

The challenge in the spectral analysis of *n*-heptane was the size of the spin system ($A_3A_3'B_2B_2'C_2C_2'D_2$) that yields a lot of non-degenerate transitions whereas the spectrum (Figure 23D) contains only little details. The spectral analysis was simplified by including only ^2J, ^3J, and ^4J coupling constants into the analysis. The spectral data was inadequate for the $^3J_{3,4'}$ and $^3J_{3,4}$ couplings, and hence, the values of these coupling constants are not accurate. The chemical shifts and coupling constants of *n*-heptane in chloroform are shown in Table 9.

Error analysis

The error analysis of PERCH NMR Software (Laatikainen et al. 2011) yields confidence limits for the spectral parameters but they are too optimistic since the error analysis does not take into account all the uncertainties arising from lineshape, baseline, and resolution enhancement. To be able to estimate the real uncertainties of the coupling constants, some spectra of *n*-pentane were analyzed in different ways; by using a weighting function that decreases the predominance of the strong methyl signals, without weighting or by analyzing only the CH_2 signals. The FID was also multiplied in different ways using window functions resulting in different lineshapes. These analyses suggested that the confidence limits for the the ^3J, ^4J, ^5J, and ^6J coupling constants are up to 0.02 Hz and for the ^2J couplings they are ca. 0.10 Hz.
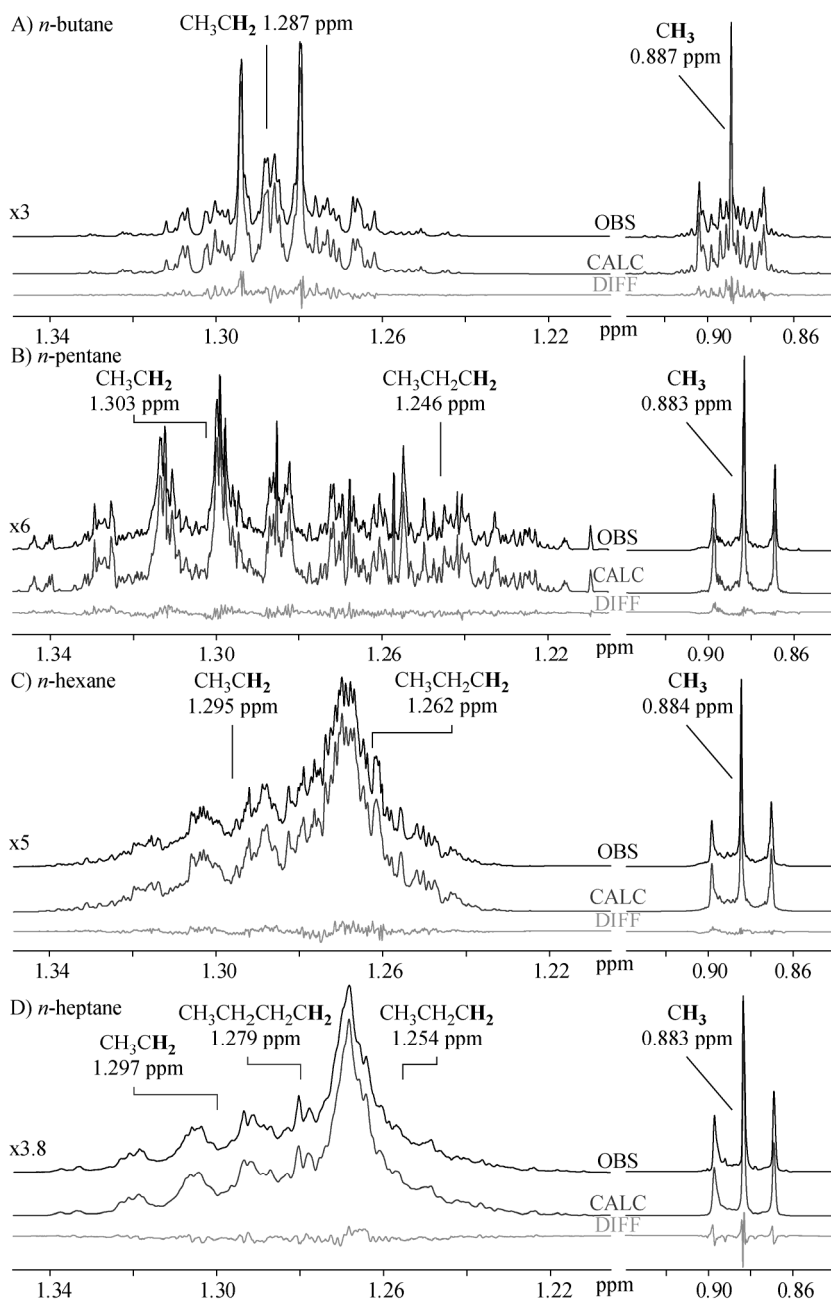
Figure 23. *¹H NMR spectra (500 MHz) of n-butane (A), n-pentane (B), n-hexane (C), and n-heptane (D) in chloroform together with the chemical shifts of the assigned protons. The observed (OBS), calculated (CALC), and the difference of these two spectra (DIFF) are presented with black, dark grey, and light grey lines, respectively.*

97

Table 9. *Chemical shifts (ppm) and coupling constants (Hz) of n-butane, n-pentane, n-hexane, and n-heptane in chloroform (at 300 K).*

Parameter	*n*-butane	*n*-pentane	*n*-hexane	*n*-heptane
$\delta(C\mathbf{H_3})$	0.8870	0.8834	0.8844	0.8833
$\delta(CH_3C\mathbf{H_2})$	1.2865	1.3033	1.2950	1.2967
$\delta(CH_3CH_2C\mathbf{H_2})$	-	1.2456	1.2616	1.2539
$\delta(CH_3CH_2CH_2C\mathbf{H_2})$	-	-	-	1.2788
$^3J_{1,2}$	7.389	7.393	7.403	7.401
$^4J_{1,3}$	-0.207	-0.212	-0.229	-0.236
$^5J_{1,4}$	-0.047	-0.001	$-^b$	$-^b$
$^6J_{1,5}$	-	0.044	$-^b$	$-^b$
$^2J_{2,2}$	-13.200[a]	-13.285	-13.283[a]	-13.264[c]
$^3J_{2,3}$	6.118	5.922	5.935	5.803
$^3J_{2,3'}$	8.664	9.173	9.169	9.167
$^4J_{2,4}$	-	-0.339	-0.363	-0.433
$^4J_{2,4'}$	-	-0.346	-0.285	-0.250
$^2J_{3,3}$	-	-13.164	-13.193[a]	-13.188[c]
$^3J_{3,4}$	-	-	5.717	5.654
$^3J_{3,4'}$	-	-	9.644	9.778
$^4J_{3,5}$	-	-	-	-0.313
$^4J_{3,5'}$	-	-	-	-0.212
$^2J_{4,4}$	-	-	-	-13.094[c]
$^3J_{2,3'}/^3J_{2,3}$	1.42	1.55	1.54	1.58
$^3J_{3,4'}/^3J_{3,4}$			1.69	1.73

The estimates of the 90% confidence limits for the coupling constants are between 0.02–0.10 Hz.

[a]The value of ^2J coupling was kept fixed during the iteration; the value was estimated on the basis of the spectral analysis of *n*-pentane.

[b]For the spectra of *n*-hexane and *n*-heptane the ^5J and ^6J coupling constants were set to zero.

[c]The spectrum of *n*-heptane did not contain much information about ^2J couplings, and thus, these values should be considered with some reservation.

Approximate analysis of n-alkane spectra

In order to obtain accurate spectral parameters, the linewidths must be as narrow as possible to reveal all the fine structures from the spectrum. On the contrary, when ^{1}H NMR spectra are measured for quantitative analyses the FIDs are usually multiplied with a window function that increases the signal-to-noise ratio, and at the same time, the linewidths are broadened. In our *n*-alkane analyses, the linewidths were 0.2–0.5 Hz when in quantitative analysis they are more often 0.7–1.0 Hz.

The purpose of this approximate analysis was to test how well the spectrum can be described if some coupling constants are set to zero. To imitate the conditions in quantitative analysis, an *n*-pentane spectrum was prepared in which the linewidth was approximately 0.7 Hz. When all the coupling constants were included, the rrms fit was 0.45% (from maximum intensity). The elimination of only ^6J, or both ^5J and ^6J coupling constants did not change the rrms value. When all the ^4J, ^5J, and ^6J coupling constants were set to zero, the rrms fit increased to 0.55%. The ignorance of the coupling constants induced small changes to the ^2J and ^3J couplings. The values of the geminal coupling constants changed 0.01–0.12 Hz whereas the vicinal coupling constants changed up to 0.05 Hz. To conclude, the *n*-pentane spectrum could be described reasonably well even though the ^4J, ^5J, and ^6J coupling constants were ignored, which simplifies the analysis. However, the ignorance of the couplings does not much reduce the simulation time of the spin system.

4.1.2 *Trans-gauche* equilibrium of *n*-alkanes in chloroform (I)
The $^3J_{2,3'}/^3J_{2,3}$ and $^3J_{3,4'}/^3J_{3,4}$ ratios provide information about the *trans-gauche* (*t-g*) equilibrium of C2-C3 and C3-C4 junctions, respectively. The $^3J_{2,3'}/^3J_{2,3}$ ratios for *n*-butane, *n*-pentane, *n*-hexane, and *n*-heptane in chloroform (Table 9) suggest that the proportion of the *t* conformer is clearly lower in *n*-butane than in *n*-pentane but in *n*-pentane and *n*-hexane it is almost the same. In *n*-heptane, the proportion of the *t* conformer is slightly increased compared to *n*-pentane. The *t/g* ratios in C3-C4

junction for *n*-hexane and *n*-heptane (Table 9) propose that the proportion of the *t* conformer is higher in C3-C4 junctions than in C2-C3 torsions. All these observations are in accordance with the average *trans* conformer populations obtained with Monte Carlo simulations (Thomas et al. 2006).

The four-bond $^4J_{2,4'}$ and $^4J_{2,4}$ coupling constants reflect the populations of the *gauche⁺gauche⁺* (g^+g^+) helix in which the sum of these couplings should be even positive. Since the sums of $^4J_{2,4'}$ and $^4J_{2,4}$ couplings for *n*-pentane, *n*-hexane, and *n*-heptane are very similar (vary between -0.65 and -0.69 Hz), the proportion of g^+g^+ type conformations in chloroform is not varied significantly with the chain length.

4.1.3 Solvent effects on conformational equilibrium (I)

To find out how chemical environment affects the conformations of *n*-alkanes, the spectra of *n*-pentane and *n*-hexane were measured in different solvents (Tables 10 and 11). In the case of *n*-pentane, only DMSO seems to have a small effect on the conformational equilibrium; it favors the *gauche* conformer in C2-C3 torsion that can be seen from the decreased ratio of $^3J_{2,3'}/^3J_{2,3}$ (Table 10).

There is a bit more variation in the $^3J_{2,3'}/^3J_{2,3}$ ratios of *n*-hexane than in *n*-pentane proposing that the chemical environment has slightly stronger effect on the conformational equilibrium of *n*-hexane. The $^3J_{2,3'}/^3J_{2,3}$ ratios (Table 11) show that the proportion of the *t* conformer in C2-C3 junction is slightly increased in acetone, methanol, and hexane-d₁₄ compared with chloroform (Table 9) but only hexane-d₁₄ of these solvents favors the *t* conformation also in C3-C4 junction. Benzene favors the *t* conformation only in C3-C4 torsion compared with chloroform. As in *n*-pentane, DMSO is the only solvent that increases the proportion of the *gauche* conformers in *n*-hexane (Table 11).

Also the four-bond coupling constants propose that the solvent effects are minor. The sums of $^4J_{2,4'}$ and $^4J_{2,4}$ of *n*-pentane and *n*-hexane are negative and almost equal in different solvents (vary from -0.63 to -0.69 Hz). Only in the case of *n*-hexane in hexane-d₁₄ the sum of $^4J_{2,4'}$ and $^4J_{2,4}$ is slightly different (-0.39 Hz).

However, due to the uncertainties in the spectral analysis, these couplings should be considered with some reservation. Thus, these results suggest that none of the solvents used in this study favors the g^+g^+ helix.

In summary, the chemical environment seems to have only small effects on the conformational equilibrium. Polar DMSO favors slightly the *gauche* conformations whereas hydrophobic hexane-d₁₄ increases the proportion of the *trans* conformations. These observed solvent effects are probably caused by packing effects (Lounila et al. 1999).

Table 10. *Chemical shifts (ppm) and coupling constants (Hz) of n-pentane in different solvents.*

Parameter	C_6D_6	CD_2Cl_2	acetone	CD_3OD	CD_3CN	DMSO
$\delta(C\mathbf{H_3})$	0.8738	0.8824	0.8772	0.8959	0.8869	0.8599
$\delta(CH_3C\mathbf{H_2})$	1.2629	1.3049	1.3051	1.3207	1.3116	1.2778
$\delta(CH_3CH_2C\mathbf{H_2})$	1.2012	1.2479	1.2490	1.2619	1.2558	1.2247
$^3J_{1,2}$	7.395	7.395	7.401	7.410	7.402	7.393
$^4J_{1,3}$	-0.235	-0.213	-0.217	-0.211	-0.214	-0.200
$^5J_{1,4}$	0.004	0.001	0.001	-0.007	0.004	0.005
$^6J_{1,5}$	0.079	0.047	0.047	0.031	0.048	0.025
$^2J_{2,2}$	-13.349	-13.264	-13.290	-13.292	-13.265	-13.267
$^3J_{2,3}$	5.917	5.926	5.914	5.926	5.935	5.975
$^3J_{2,3'}$	9.185	9.160	9.212	9.194	9.170	9.034
$^4J_{2,4}$	-0.372	-0.334	-0.337	-0.330	-0.342	-0.317
$^4J_{2,4'}$	-0.292	-0.342	-0.343	-0.342	-0.343	-0.348
$^2J_{3,3}$	-13.240	-13.138	-13.160	-13.158	-13.127	-13.135
$^3J_{2,3'}/^3J_{2,3}$	1.55	1.55	1.56	1.55	1.55	1.51

The estimates of the 90% confidence limits for the coupling constants are between 0.02–0.10 Hz.

C_6D_6, benzene; CD_2Cl_2, dichloromethane; CD_3CN, acetonitrile; CD_3OD, methanol; DMSO, dimethylsulfoxide

Table 11. *Chemical shifts (ppm) and coupling constants (Hz) of n-hexane in different solvents.*

Parameter	hexane-d_{14}	C_6D_6	acetone	CD_3OD	DMSO
$\delta(C\mathbf{H_3})$	0.8970	0.8862	0.8816	0.8973	0.8622
$\delta(CH_3C\mathbf{H_2})$	1.3179	1.2700	1.3016	1.3132	1.2709
$\delta(CH_3CH_2C\mathbf{H_2})$	1.2884	1.2295	1.2722	1.2813	1.2421
$^3J_{1,2}$	7.423	7.402	7.453	7.437	7.376
$^4J_{1,3}$	-0.180	-0.234	-0.280	-0.235	-0.165
$^2J_{2,2}$[a]	-13.285	-13.285	-13.285	-13.285	-13.285
$^3J_{2,3}$	5.830	5.939	5.894	5.870	6.089
$^3J_{2,3'}$	9.065	9.151	9.227	9.190	8.831
$^4J_{2,4}$[b]	0.263	-0.159	-0.382	-0.292	-0.353
$^4J_{2,4'}$[b]	-0.651	-0.519	-0.243	-0.341	-0.297
$^2J_{3,3}$[a]	-13.150	-13.150	-13.150	-13.150	-13.150
$^3J_{3,4}$	5.335	5.585	5.735	5.785	5.654
$^3J_{3,4'}$	9.727	9.711	9.650	9.652	9.610
$^3J_{2,3'}/^3J_{2,3}$	1.55	1.54	1.57	1.57	1.45
$^3J_{3,4'}/^3J_{3,4}$	1.82	1.74	1.68	1.67	1.70

The estimates of the 90% confidence limits for the coupling constants are between 0.02–0.10 Hz. C_6D_6, benzene; CD_3OD, methanol; DMSO, dimethylsulfoxide

[a]The ^2J couplings were estimated on the basis of the spectral analysis of *n*-pentane and they were kept fixed during the iteration.

[b]The sum of $^4J_{2,4'}$ and $^4J_{2,4}$ is well defined but their difference is not, and therefore, the values should be considered with some reservation.

4.1.4 Quantum mechanical spectral analysis of a short fatty acid

Saturated FAs contain alkyl chains and their spectra resemble partly the spectra of *n*-alkanes. However, since FAs contain a carbonyl group, the chemical shifts of the CH2 protons are more separated than in *n*-alkanes. Figure 24 shows the ^{1}H NMR spectrum of hexanoic acid in chloroform. The starting values for the analysis were estimated on the basis of the spectral analyses of *n*-alkanes, and it can be seen from Table 12 that the optimized coupling constants of hexanoic acid are very similar to those of *n*-alkanes (Table 9).
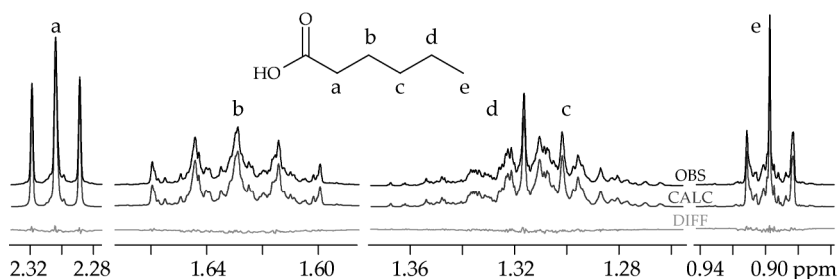
Figure 24. ¹*H NMR spectrum (500 MHz) of hexanoic acid in chloroform with signal assignments. The observed (OBS), calculated (CALC), and the difference of these two spectra (DIFF) are presented with black, dark grey, and light grey lines, respectively.*

Quantum mechanical spectral analysis slows down when the number of spin particles increases. For example, the spectral analysis of hexanoic acid can be performed within hours but for octanoic acid, that contains eight carbons, the analysis is remarkably slower. However, the increase of the analysis time is not the only challenge. When the alkyl chain is lengthened, there are more protons that resonate at 1.25–1.40 ppm, and it is difficult to obtain spectral parameters from these severely overlapping CH_2 signals. Already the analysis of palmitoleic acid (16:1) took several days and all the ^3J couplings and chemical shifts could not be defined.

Table 12. *Chemical shifts (ppm) and coupling constants (Hz) of hexanoic acid in chloroform. Naming of the protons is the same as in Figure 24.*

Parameter		Parameter		Parameter	
$\delta(a)$	2.3034	$^3J_{a,b'}$	8.635	$^4J_{b,d'}$	-0.329
$\delta(b)$	1.6292	$^4J_{a,c}$	-0.289	$^2J_{c,c}$	-13.183
$\delta(c)$	1.2997	$^4J_{a,c'}$	-0.278	$^3J_{c,d}$	5.920
$\delta(d)$	1.3253	$^2J_{b,b}$	-13.488	$^3J_{c,d'}$	9.162
$\delta(e)$	0.8972	$^3J_{b,c}$	5.724	$^4J_{c,e}$	-0.191
$^2J_{a,a}$	-15.569	$^3J_{b,c'}$	9.783	$^2J_{d,d}$	-13.296
$^3J_{a,b}$	6.529	$^4J_{b,d}$	-0.356	$^3J_{d,e}$	7.375

The estimates of the 90% confidence limits for the coupling constants are between 0.02–0.10 Hz.

4.2 ¹H NMR SPECTRA OF INDIVIDUAL LIPID SPECIES

The lipid fraction of human serum consists of several different lipid species. ¹H NMR spectra of some common serum FAs, glycerolipids, and sphingolipid, as well as free and esterified cholesterol are presented in Figures 25–27.
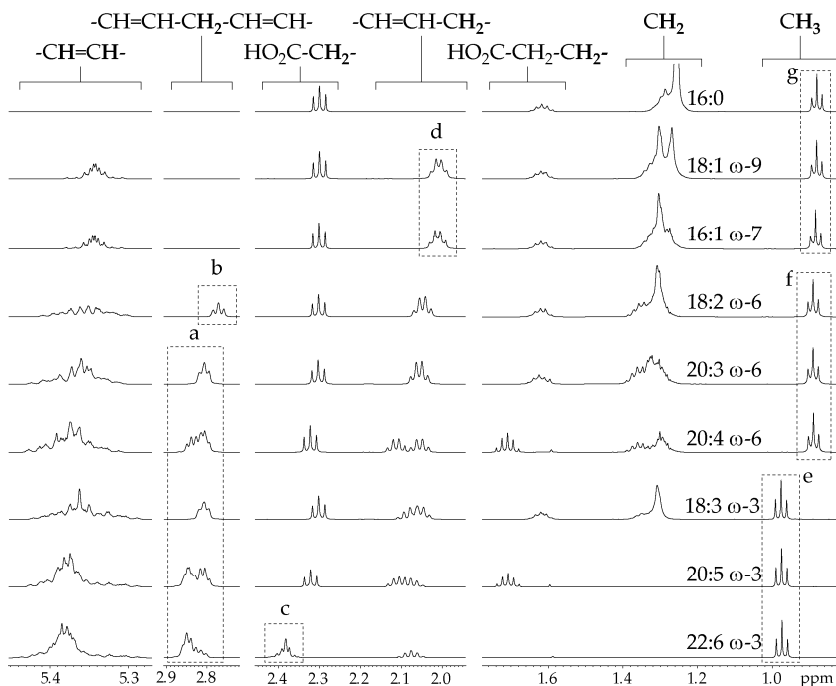
Figure 25. *¹H NMR spectra of palmitic acid (16:0), oleic acid (18:1 ω-9), palmitoleic acid (16:1 ω-7), linoleic acid (18:2 ω-6), dihomo-γ-linolenic acid (20:3 ω-6), arachidonic acid (20:4 ω-6), α-linolenic acid (18:3 ω-3), eicosapentaenoic acid (20:5 ω-3), and docosahexaenoic acid (22:6 ω-3) in chloroform (500 MHz) with signal assignments. The boxes indicate the signals arising from (a) other PUFAs than linoleic acid, (b) linoleic acid, (c) docosahexaenoic acid, (d) monounsaturated fatty acids (FAs), (e) ω-3 FAs, (f) ω-6 FAs, and (g) ω-7,9, and saturated FAs.*

The ω-3 (0.97 ppm), ω-6 (0.89 ppm), and ω-7, ω-9, as well as SFAs (0.88 ppm) can be distinguished from the spectrum of a

lipid mixture on the basis of their methyl resonances (Figure 25). Linoleic acid and DHA can be directly quantified since they both have one distinguishable signal in the spectra of lipid mixtures. Other PUFAs than linoleic acid, except DHA, can be determined only as a sum since their signals arising from the bisallylic protons overlap at 2.8–2.9 ppm. The quantification of MUFAs is possible by using the quartet signal at 2.0 ppm arising from the protons attached to the carbons next to the double bond carbons (Figure 25).
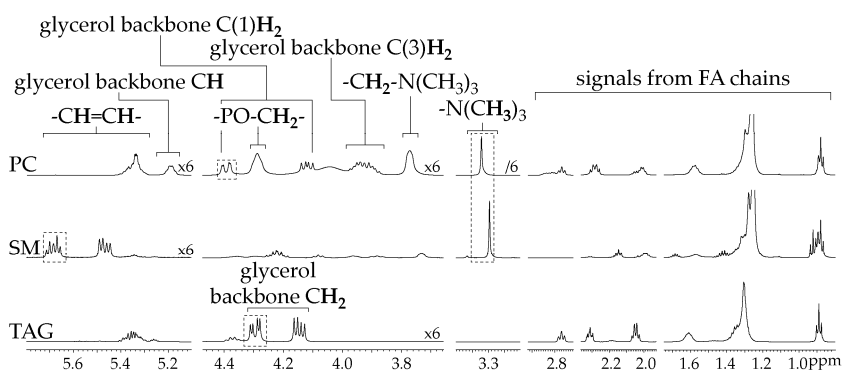
Figure 26. *^{1}H NMR spectra of phosphatidylcholine (PC), sphingomyelin (SM), and triacylglyceride (TAG) in chloroform (500 MHz) with signal assignments. The characteristic signals for PC, SM, and TAG that can be used for their quantification from lipid mixtures are indicated with boxes.*

About half of the spectra of PC, SM, and TAG are composed of the signals from the FA chains (Figure 26). Lipids containing a choline group, such as PC and SM, have a characteristic singlet at approximately 3.3 ppm arising from three methyl groups. The most characteristic signal for SM is the one from a double bond proton at 5.7 ppm. TAGs and phosphoglycerides give signals from the glycerol backbone at 4.1–4.4 ppm that can be used for their quantification from a lipid mixture.

^{1}H NMR spectra of free and esterified cholesterol are presented in Figure 27. Free and esterified cholesterol can be easily identified by looking at the signals at 3.5 and 4.7 ppm arising from a proton attached to carbon-3 (Figure 5). The singlet

at 0.7 ppm from $C(18)H_3$ protons is the best signal for the quantification of total cholesterol.
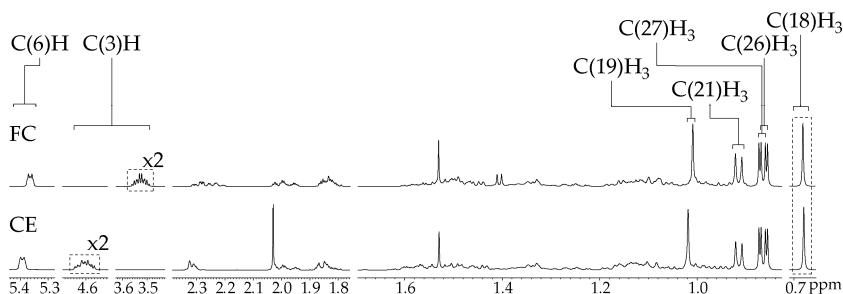
Figure 27. *^1H NMR spectra of free cholesterol (FC) and cholesteryl ester (CE) in chloroform (500 MHz) with some signal assignments. The numbering of the cholesterol protons is the same as in Figure 5. The characteristic cholesterol signals that can be used for their quantification from lipid mixtures are indicated with boxes.*

4.3 EXTRACTION PROTOCOL FOR SERUM LIPIDS

The extraction protocol used in this study is based on the dichloromethane extraction method (Cequier-Sánchez et al. 2008). Our aim was to optimize the extraction yield, as well as to enable the extraction of about 100 samples per day.

The effect of different mixing methods, as well as the most effective way for the addition of the extraction solvents was tested. Four variations from the dichloromethane extraction protocol (methods 1–4 in Table 13) were performed and the results are presented in Figure 28. It appeared that the best yields are obtained by mixing at a vertical shaker or by using sonication. Vortexing seemed to be the less effective mixing method. Also, the addition of methanol dropwise and dichloromethane and sodium chloride solution slowly by a glass pipette did not increase the yield. Thus, all the extraction solvents can be added by pouring.

Table 13. Different variations from the extraction protocol.

Method	Extraction procedure
1	- 5 ml CH_3OH + 10 ml CH_2Cl_2 + 15 ml 0.15 M NaCl (all poured)
	- mixing at a vertical shaker 5 min, centrifugation 2400 × g 10 min, phase separation
	- 10 ml CH_2Cl_2 (poured)
	- mixing, centrifugation, and phase separation as in the previous step
2	- 5 ml CH_3OH (poured) + 10 ml CH_2Cl_2 (poured)
	- sonication 5 min
	- 15 ml 0.15 M NaCl (poured)
	- sonication 5 min, centrifugation 2400 × g 10 min, phase separation
	- 10 ml CH_2Cl_2 (poured)
	- sonication, centrifugation, and phase separation as in previous step
3	- 5 ml CH_3OH + 10 ml CH_2Cl_2 + 15 ml 0.15 M NaCl (all poured)
	- vortex 45 s, centrifugation 2400 × g 10 min, phase separation
	- 10 ml CH_2Cl_2 (poured)
	- vortex 45 s, centrifugation 2400 × g 10 min, phase separation
4	- 5 ml CH_3OH dropwise + 10 ml CH_2Cl_2 (with a glass pipette) + 15 ml 0.15 M NaCl (with a glass pipette) under magnetic stirring
	- vortex 45 s, centrifugation 2400 × g 10 min, phase separation
	- 10 ml CH_2Cl_2 (with a glass pipette)
	- vortex 45 s, centrifugation 2400 × g 10 min, phase separation
5	- 10 ml 1:2 CH_3OH:CH_2Cl_2 mixture + 10 ml 0.15 M NaCl (all poured)
	- mixing at a vertical shaker 5 min, centrifugation 2400 × g 10 min, phase separation
	- 5 ml CH_2Cl_2 (poured)
	- mixing, centrifugation, and phase separation as in the previous step
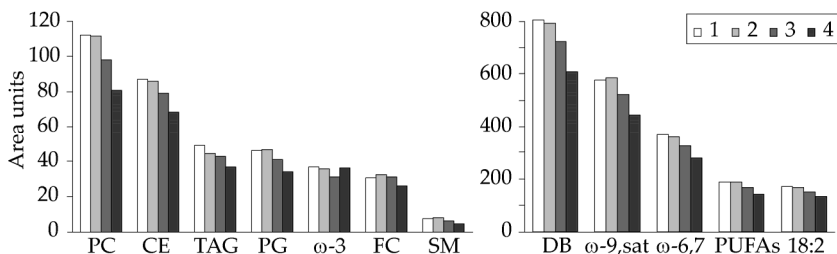
Figure 28. Signal areas (in area units) of the selected lipid species from the ¹H NMR spectra of serum lipid extracts using different mixing methods. The numbering of the columns refers to the extraction procedures in Table 13. 18:2, linoleic acid; CE, cholesteryl ester; DB, double bond protons; FC, free cholesterol; PC, phosphatidylcholine; PG, phosphoglyceride; PUFAs, polyunsaturated fatty acids; SM, sphingomyelin; TAG, triacylglyceride; ω-3, ω-3 fatty acids; ω-6,7, ω-6 and ω-7 fatty acids; ω-9,sat, ω-9 and saturated fatty acids

The repeatabilities of the extraction methods 1 and 2 (Table 13) were examined by extracting three serum samples. As can be seen from Figure 29, the standard deviations are smaller when the samples are mixed at a vertical shaker.

Figure 29. Average signal areas (in area units) and standard deviations of the selected lipid species from the ¹H NMR spectra of serum lipid extracts calculated from triplicate samples. The numbering of the columns refers to the extraction procedures in Table 13. For the abbreviations, see Figure 28.

To find out how many extraction steps are required to extract at least ca. 95% of the serum lipids, some serum samples were extracted using the extraction procedure 1 (Table 13) with three extraction steps. In each step, the dichloromethane phase was collected to a separate tube. Figure 30 illustrates that 80–90% of

the lipids are recovered in the first extraction step. The second step yields 7–13%, and only 0.3–6% of the lipids remains after two extraction steps. Thus, it can be concluded that two extraction steps are enough to extract 95–99% of the serum lipids.
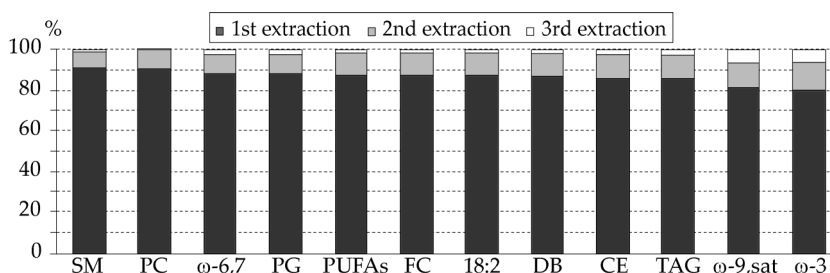
Figure 30. *Extraction yields (%) of the selected lipid species after first, second, and third extraction. For the abbreviations, see Figure 28.*

Finally, it was tested whether methanol and dichloromethane could be combined since it would fasten the extraction procedure. The experiment showed that there is no remarkable difference between the extraction yields if the two solvents are combined or added separately (Figure 31). Thus, the extraction procedure 5 in Table 13 was selected to be the most efficient taking into account both the yield, as well as the speed.
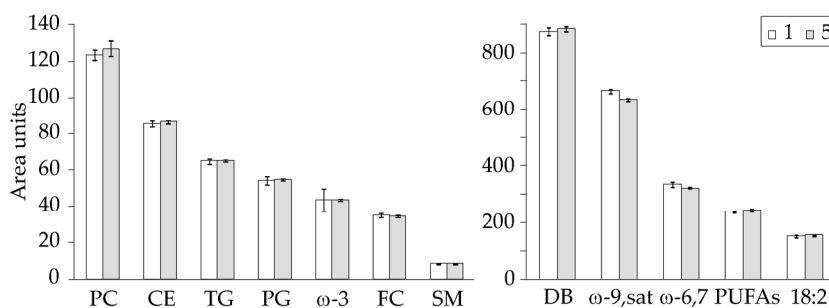
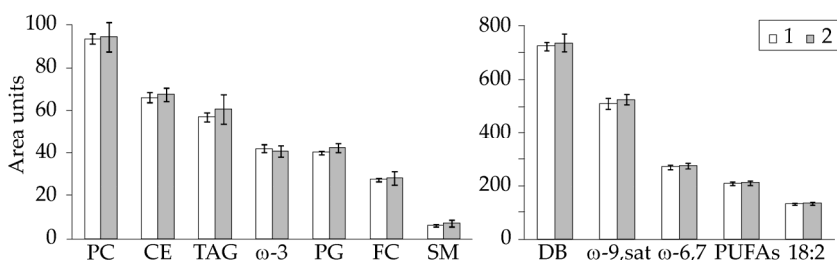**Figure 31.** *Signal areas (in area units) and standard deviations of the selected lipid species from the ^{1}H NMR spectra of serum lipid extracts calculated from triplicates. The numbering of the columns refers to the extraction procedures in Table 13. For the abbreviations, see Figure 28.*

4.4 QUANTIFICATION PROTOCOL FOR SERUM LIPIDS

The ^{1}H NMR spectra of complex lipid mixtures, such as serum, contain many closely located lines, and some of them can be strongly overlapping. Thus, the determination of signal areas by traditional integration methods from this kind of spectrum is difficult and more sophisticated methods are required.

4.4.1 Constrained total-line-shape fitting

Deconvolution is a method to determine signal areas by fitting lines under spectral signals (Laatikainen et al. 1996b). Each line has four parameters including frequency, width, intensity, and lineshape. These parameters are iterated to yield as good fit as possible. In order to get areas for signals that are formed from several lines, the lines are assorted into a group, called complex, so that the program automatically calculates the total area. The formation of complexes is especially important when the statistics of the areas is required (Soininen et al. 2005).

If there is prior knowledge available for the signal structures or shapes, it is possible to use CTLS fitting method. In the CTLS, the structures of the multiplets are given in the form of linear equations for the total-line-shape fitting algorithm (Soininen et al. 2005). Then, the spectral parameters are iterated, enabling the CTLS algorithm to automatically adapt to small changes in the signal intensities and positions (Jukarainen et al. 2008).

The constraints for the fitting can be defined in different ways. For example, it is possible to form a symmetric multiplet, e.g. a triplet with intensity ratio 1:2:1. The use of a multiplet structure minimizes the number of the parameters to be optimized since only the total intensity, the midpoint of the multiplet, usually only one splitting, and one linewidth are optimized instead of fitting many line positions, intensities, and linewidths (Soininen et al. 2005). In addition, it is possible to use "soft constraints" that include linear equations for signal positions, areas, intensities, and linewidths (Soininen et al. 2005; Jukarainen et al. 2008). For example, the linewidths of separate multiplets can be set equal. After defining the constraints, they

can be weighted. The less strict the rule, the smaller is the weight for the constraint. If absolutely strict constraints are needed, one can use a "structure" that is created by defining a list of spectral lines with characteristic positions, intensities, and linewidths (Jukarainen et al. 2008). During the iteration, the structure is exactly preserved, and only the relative intensities, positions, and linewidths of the lines constructing the structure are optimized.

Commonly the fitting has to be performed in parts since the maximum number of parameters that can be simultaneously optimized for one spectral part is 500 (Jukarainen et al. 2008). The other reason for fitting in parts is that the baseline is usually not similar in each part of the spectrum. The number of lines and baseline function terms are chosen so that a good fit is obtained (i.e. there is only a small variation between the observed and calculated spectra) for each part to be fitted (Soininen et al. 2005).

The aim of this subproject was to find out how well the NMR-based lipid concentrations and percentage values correspond to the values obtained by other methods. The samples from the chocolate study (Mursu et al. 2004) were suitable for this purpose since several lipid species were analyzed from the samples previously by GC or by an enzymatic colorimetric test.

The constraints used in the CTLS analysis of the ^{1}H NMR spectra of the lipid extract samples were built up on the basis of the model spectra (Figures 25–27). The spectra were fitted in 13 parts, each of which independently. The spectral region of 0.84–1.40 ppm is a good example of the use of different constraints since that area contains a lot of severely overlapping multiplets (Figure 32), and thus, forms a challenge for the quantification protocol.
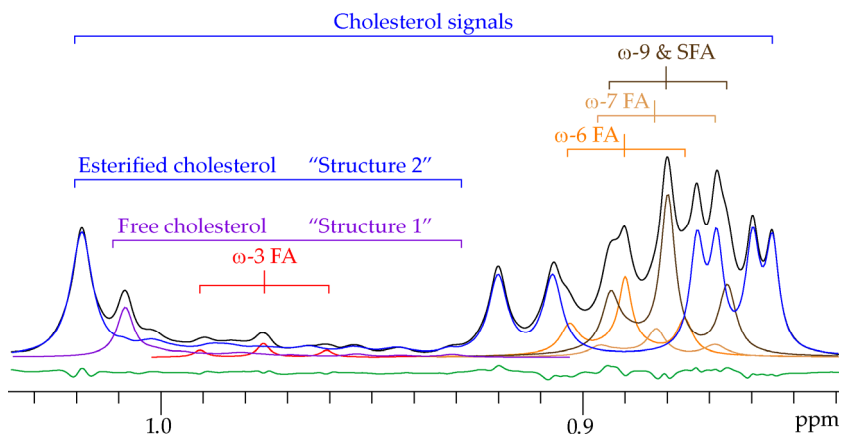
Figure 32. *A part of the ¹H NMR spectrum of extracted serum showing the observed spectrum (black line), the fitted signals (colored lines), and the difference between the observed spectrum and the fitted signals (green line).*

In the CTLS fitting protocol, the methyl signal of the ω-3 FAs was defined as a triplet with intensity ratio 1:2:1. The coupling constant of the triplet was also set as a constraint. To prevent the signal from broadening, the linewidth was bound to the linewidth of the line from the ω-6 FA signal (Table 14). The methyl signals of the ω-6, ω-7, and ω-9 and SFAs were described with four lines (Figure 33), and their frequencies, linewidths, and intensities were defined with equations shown in Table 14. Several signals arising from free and esterified cholesterol at 0.93–1.3 ppm were defined as structures (Figure 32).

Figure 33. *Construction of the methyl signals of the ω-6 (ω-6_1–4), ω-7 (ω-7_1–4), and ω-9 and saturated fatty acids (ω-9,SFA_1–4).*

Table 14. Constraint equations and weighting factors used in the quantification of the signals arising from methyl protons of ω-3, ω-6, ω-7, and ω-9 fatty acids (FAs) and saturated fatty acids (SFAs). The numbering of the lines is the same as in Figure 33.

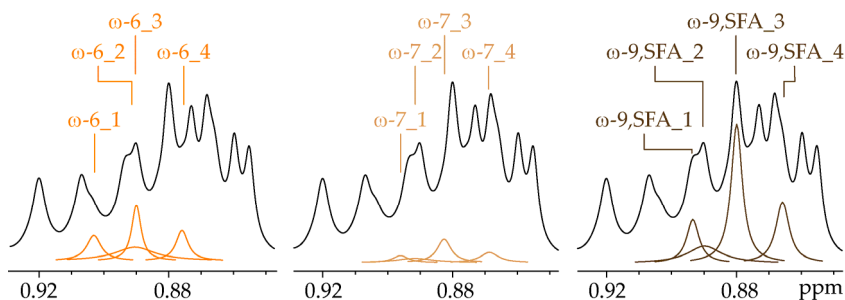| Signal	Parameter	Equation	Weight
	Frequency	1.0 × ω-6_1 = 1.0 × ω-6_3 + 6.5950	99.0
	Frequency	1.0 × ω-6_2 = 1.0 × ω-6_3 + 0.2860	99.0
	Frequency	1.0 × ω-6_4 = 1.0 × ω-6_3 - 7.0470	99.0
	Width	1.0 × ω-6_1 = 0.3550 × ω-6_2	99.0
ω-6 FAs	Width	1.0 × ω-6_3 = 0.2320 × ω-6_2	99.0
	Width	1.0 × ω-6_4 = 0.3010 × ω-6_2	99.0
	Intensity	1.0 × ω-6_1 = 0.4560 × ω-6_3	99.0
	Intensity	1.0 × ω-6_2 = 0.2450 × ω-6_3	99.0
	Intensity	1.0 × ω-6_4 = 0.5460 × ω-6_3	99.0
	Frequency	1.0 × ω-7_1 = 1.0 × ω-7_3 + 6.7270	99.0
	Frequency	1.0 × ω-7_2 = 1.0 × ω-7_3 + 4.4890	99.0
	Frequency	1.0 × ω-7_4 = 1.0 × ω-7_3 - 6.9680	99.0
	Width	1.0 × ω-7_1 = 0.4110 × ω-7_2	99.0
ω-7 FAs	Width	1.0 × ω-7_3 = 0.3730 × ω-7_2	99.0
	Width	1.0 × ω-7_4 = 0.4830 × ω-7_2	99.0
	Intensity	1.0 × ω-7_1 = 0.2960 × ω-7_3	99.0
	Intensity	1.0 × ω-7_2 = 0.1770 × ω-7_3	99.0
	Intensity	1.0 × ω-7_4 = 0.4370 × ω-7_3	99.0
	Frequency	1.0 × ω-9,SFA_1 = 1.0 × ω-9,SFA_3 + 6.7760	99.0
	Frequency	1.0 × ω-9,SFA_2 = 1.0 × ω-9,SFA_3 + 4.9610	99.0
	Frequency	1.0 × ω-9,SFA_4 = 1.0 × ω-9,SFA_3 - 7.0590	99.0
ω-9 &	Width	1.0 × ω-9,SFA_1 = 0.3710 × ω-9,SFA_2	99.0
SFAs	Width	1.0 × ω-9,SFA_3 = 0.3330 × ω-9,SFA_2	99.0
	Width	1.0 × ω-9,SFA_4 = 0.3910 × ω-9,SFA_2	99.0
	Intensity	1.0 × ω-9,SFA_1 = 0.3130 × ω-9,SFA_3	99.0
	Intensity	1.0 × ω-9,SFA_2 = 0.1230 × ω-9,SFA_3	99.0
	Intensity	1.0 × ω-9,SFA_4 = 0.4410 × ω-9,SFA_3	99.0
	Width	1.0 × ω-3 = 1.0 × ω-6_3	10.0
	Width	1.0 × ω-9,SFA_3 = 1.2130 × ω-6_3	10.0
	Width	1.0 × ω-7_3 = 1.210 × ω-9,SFA_3	10.0
	Splitting	1.0 × ω-3 = 7.50	10.0
	Frequency	1.0 × ω-7_3 = 1.0 × ω-9,SFA_3 + 1.3642	1.0

The percentage values and concentrations of various lipids determined by CTLS were compared with the corresponding measures determined by an enzymatic colorimetric test (TAGs) or by GC (FAs) in the chocolate study (Mursu et al. 2004) (Figures 34 and 35). To change the signal areas obtained from the NMR spectra into absolute concentrations, the signal areas were scaled using the total cholesterol concentration determined from the native serum by an enzymatic colorimetric test.
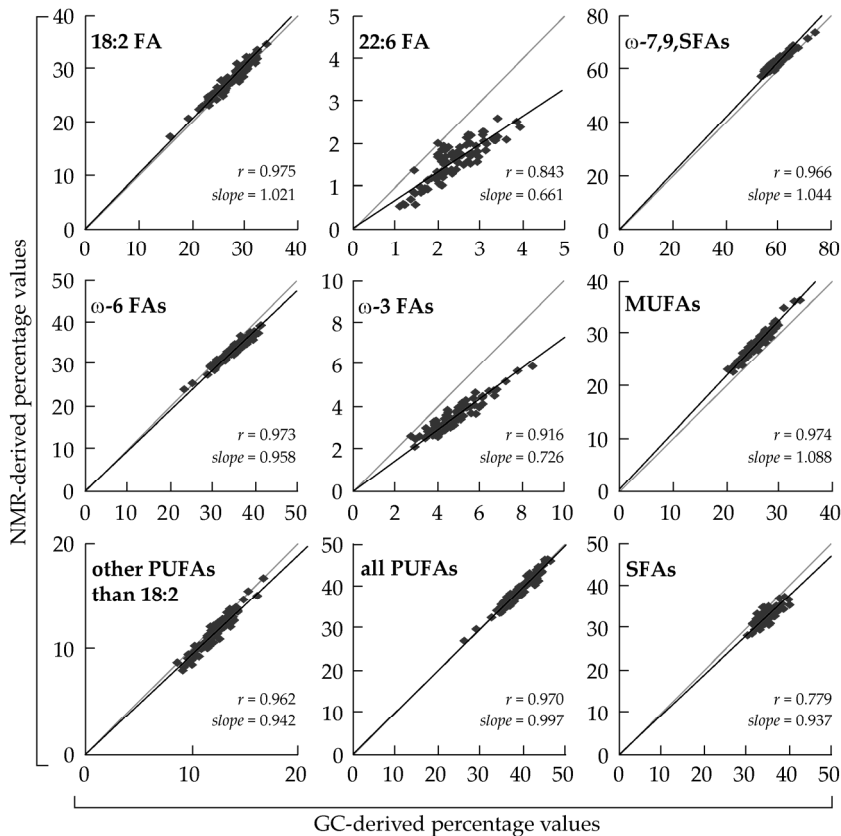
Figure 34. The percentage values of several fatty acid (FA) variables determined both by NMR (y-axis) and gas chromatography (x-axis). Pearson's or Spearman's correlation coefficients (r) are shown for each variable. All the correlations are statistically significant (p < 0.001). The grey line describes the situation in which the values determined by the two different methods are equal. 18:2 FA, linoleic acid; 22:6 FA, docosahexaenoic acid; MUFA, monounsaturated FA; PUFA, polyunsaturated FA; SFA, saturated FA

114
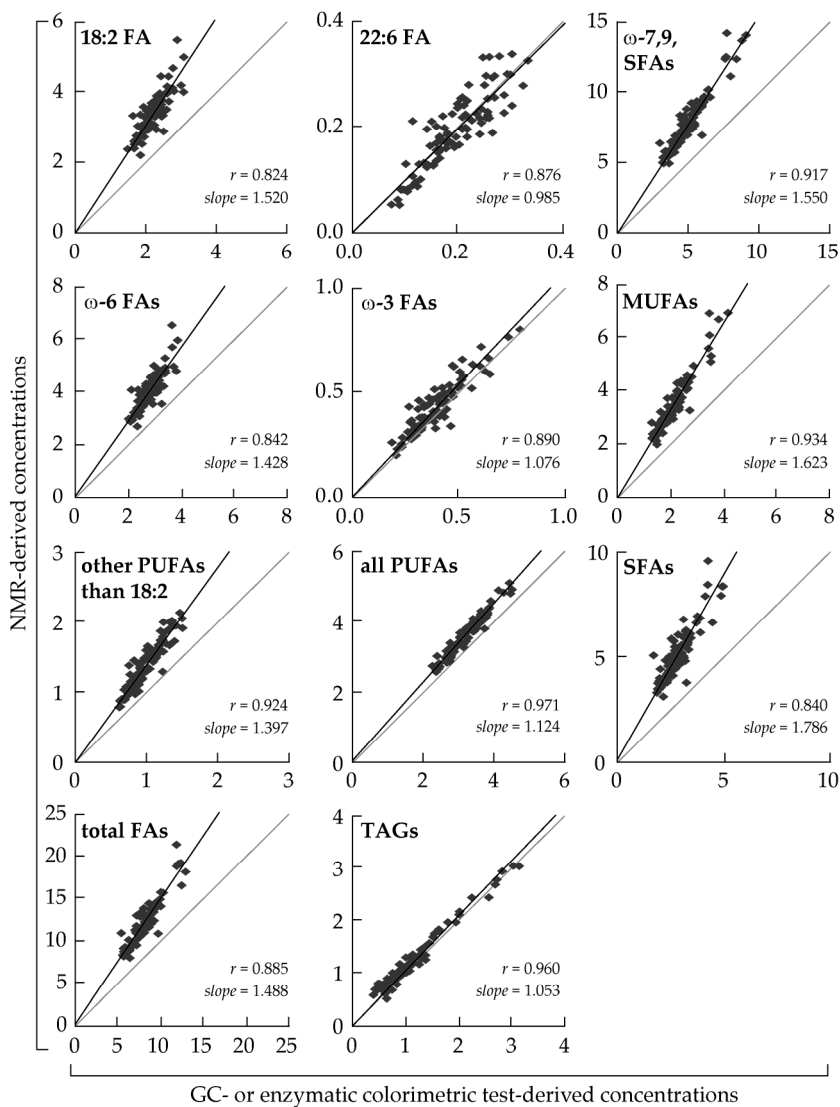
Figure 35. *The concentrations (mM) of several fatty acid (FA) variables determined both by NMR (y-axis) and gas chromatography or, in the case of triacylglycerides (TAGs), an enzymatic colorimetric test (x-axis). Pearson's or Spearman's correlation coefficients (r) are shown for each variable. All the correlations are statistically significant (p < 0.001). The grey line describes the situation in which the values determined by the two different methods are equal. 18:2 FA, linoleic acid; 22:6 FA, docosahexaenoic acid; MUFA, monounsaturated FA; PUFA, polyunsaturated FA; SFA, saturated FA*

115

Figure 35 shows that the TAG concentrations determined by NMR compare well with the concentrations obtained by an enzymatic colorimetric test (Spearman's correlation 0.960, $p < 0.001$). The concentrations of total FAs obtained by NMR are approximately 50% higher than those determined by GC (Figure 35). This difference can be partly due to the fact that some FAs that are present in serum in small amounts were not included into the GC analysis. However, the values obtained by these two methods correlate strongly (Figure 35).

Two individual FAs, linoleic acid and DHA, can be quantified directly from the ^{1}H NMR spectrum of the extracted serum. The NMR-based absolute concentrations for linoleic acid are higher than those determined by GC (Figure 35). However, the percentage values (Figure 34) are in good agreement (Pearson's correlation coefficient 0.975, $p < 0.001$). For DHA, the concentration values obtained by NMR and GC are quite similar (Pearson's correlation 0.876, $p < 0.001$) but the NMR-derived percentage values are a bit smaller than those determined by GC (Spearman's correlation 0.843, $p < 0.001$).

The NMR-based absolute concentrations for total ω-6 and ω-3 FAs are slightly higher than the corresponding GC values (Figure 35). The percentage values of ω-6 FAs are very similar (Figure 34) and the correlation is strong (Pearson's correlation 0.973, $p < 0.001$). NMR gives lower percentage values for ω-3 FAs than GC but there is still quite strong correlation between the values (Spearman's correlation 0.916, $p < 0.001$).

The ω-7 FAs and ω-9 and SFAs give methyl resonances close to each other and there are also other resonances overlapping them (Figure 32) which makes their fitting challenging. The 500 MHz spectrum does not have enough information for the reliable quantification of the ω-7 FAs separately, and thus, in the results, the amount of ω-7 FAs and ω-9 and SFAs are combined. The sum of the concentrations of ω-7, ω-9 and SFAs correlates well with the sum of corresponding FAs obtained by GC analysis (Spearman's correlation 0.917, $p < 0.001$), and the correlation between their percentage values is even stronger (Pearson's correlation 0.966, $p < 0.001$).

PUFAs that have more than two double bonds have different amounts of bisallylic protons, and this piece of information is used to calculate the concentration of other PUFAs than linoleic acid. The value representing the average number of bisallylic protons in serum PUFA pool excluding linoleic acid is six, and it could be estimated using the average concentrations of various PUFAs presented in Table 2. The percentage values of MUFAs, other PUFAs than linoleic acid, and all PUFAs determined both by NMR and GC are almost equal and they correlate strongly (Figure 34). When looking at the concentration values, the NMR method yields a bit higher concentrations for all these.

The amount of SFAs cannot be directly obtained from the ^{1}H NMR spectrum of the serum lipid extract but it can be calculated by subtracting the percentage values of MUFAs and PUFAs from 100%. Most of the NMR and GC derived percentage values for SFAs are quite similar but the dispersion of the values lowers the correlation (Spearman's correlation 0.779, $p < 0.001$). The correlation for the concentration values is higher (Spearman's correlation 0.840, $p < 0.001$) but the NMR method yields again higher values compared with GC (Figure 35Figure 34).

In general, the correlations between the percentage values are higher than the correlations between the absolute concentrations. The biggest variations in the percentage values are in the values of DHA and ω-3 FAs which are present in serum in low amounts. The extraction protocols used for GC (Mursu et al. 2004) and NMR samples were slightly different and may have caused different yields that can be seen in the amounts of total FA concentrations. By using GC method, it is possible to obtain absolute concentrations and percentage values for several individual FAs whereas NMR can separate only DHA and linoleic acid and the others are obtained as sums. However, to get reliable results, the GC method requires a standard compound for each FA to be measured and also calibration of the equipment, and thus, the GC method is more time consuming when compared with NMR.

4.5 NMR OXIDATION PROTOCOL (IV)

The objective of this project was to develop a method to study the oxidation susceptibility of serum lipids by ^{1}H NMR spectroscopy. Previously, NMR spectroscopy has been applied to study lipid peroxidation of LDL (Lodge et al. 1993; Lodge et al. 1995; Corso et al. 1997; Soininen et al. 2007). However, an NMR-based oxidation method for the lipids from whole serum is lacking.

4.5.1 Development and optimization of the NMR oxidation assay

PUFAs are prone to oxidation, and thus, the oxidation reaction can be followed from a ^{1}H NMR spectrum of extracted serum by looking at the signals arising from the bisallylic protons of PUFAs at 2.74–2.88 ppm that decrease when the oxidation reaction proceeds (Figure 36). In developing the oxidation protocol, several copper concentrations and incubation times were tested. The oxidation reaction is rapid with copper concentrations of 1–4 mM whereas the copper concentration of 0.5 mM provides milder oxidation conditions and the oxidation proceeds slower (Figure 37A). The largest variance between the percentage values describing the amount of oxidized PUFAs appeared to be at the time point of six hours (Figure 37B). Furthermore, at this point, the speed of the oxidation reaction has slowed down which allows slight differences in the incubation times without affecting the results. Oxidation of five replicate samples from three subjects (Figure 37B) proved that the NMR oxidation protocol yields repeatable results (standard deviations vary between 0.4 and 4.3 percentage units).
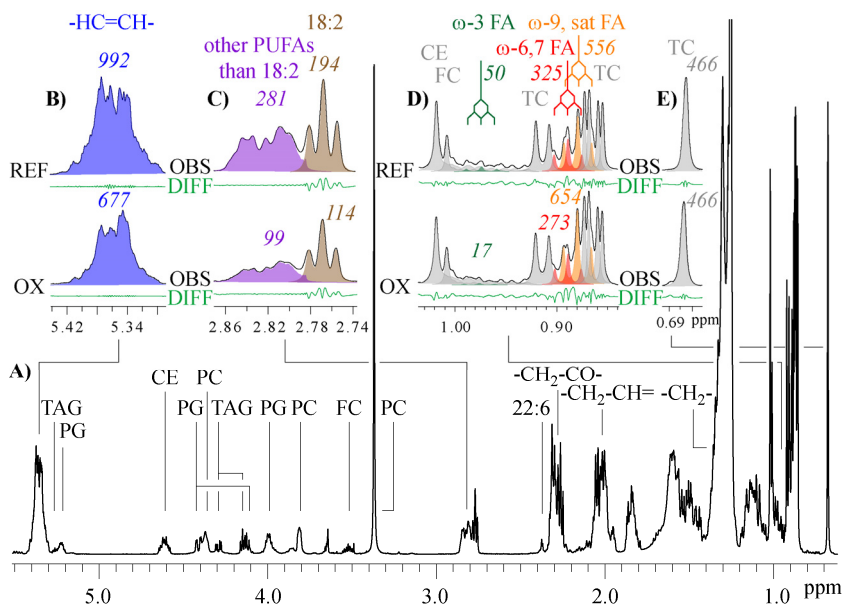
Figure 36. *A ¹H NMR spectrum of extracted serum with signal assignments (A). Some essential parts of the spectra (B–E) before (REF) and after (OX) the oxidation are shown at the top of the figure. CE, cholesteryl ester; FA, fatty acid; FC, free cholesterol; PC, phosphatidylcholine; PG, phosphoglyceride; sat, saturated; PUFA, polyunsaturated fatty acid; TC, total cholesterol; TAG, triacylglyceride*
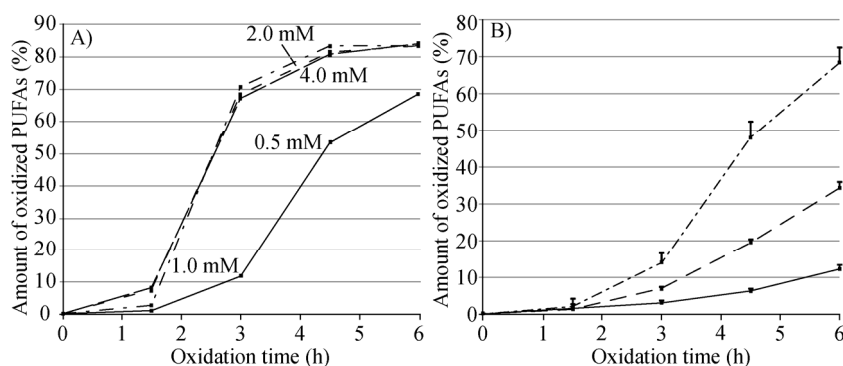
Figure 37. *The amounts of oxidized PUFAs during the copper induced oxidation with four different copper concentrations (A) and with a copper concentration of 0.5 mM for three subjects (B). Each data point in (B) is a mean of five determinations.*

4.5.2 Comparison of the NMR oxidation assay with commonly used oxidation method

The oxidation susceptibility of serum lipids has been commonly determined with a spectrophotometric method in which the oxidation reaction is initiated with copper. Oxidation leads to the formation of conjugated dienic hydroperoxides that absorb in the UV range, and thus, the reaction can be monitored spectrophotometrically (Schnitzer et al. 1998; Spranger et al. 1998; Delimaris et al. 2007). The result is usually expressed as the lag time preceding oxidation that describes the time before the maximal reaction rate of diene accumulation has been reached (Delimaris et al. 2008). If a sample is very susceptible to oxidation, the lag time is short. By using the NMR method, this is seen as a high amount of oxidized PUFAs.

Figure 38A shows that the baseline and end-point oxidation susceptibility values determined by ^{1}H NMR correlate strongly with the corresponding lag time values obtained spectrophotometrically. However, even though the baseline and end-point values of these two methods correlate, the change values (end-baseline) do not have a correlation (Figure 38B).
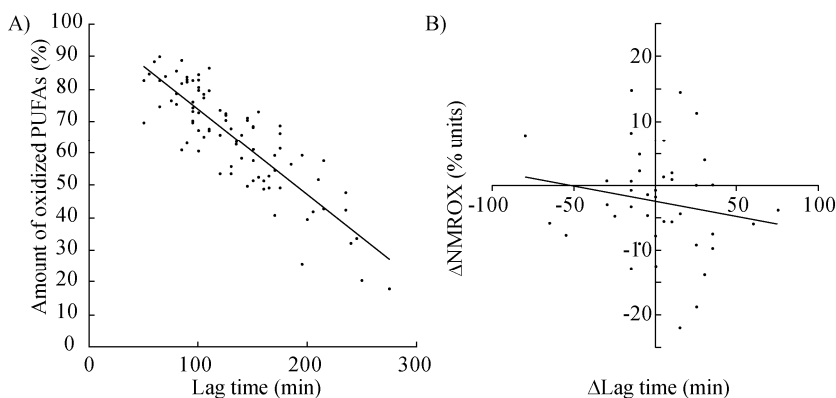
Figure 38. A) The amounts of oxidized PUFAs after the copper induced oxidation determined by the NMR oxidation method plotted against the corresponding lag time values obtained spectrophotometrically from the chocolate study samples. The regression line is y = -0.2665x + 100.4, r = 0.825. B) The end-baseline NMR oxidation values (ΔNMROX) plotted against the corresponding lag time values (ΔLag time). The regression line is y = 0.0462x + 2.3803, r = 0.158.

120

The different settings of the NMR and spectrophotometric assays explain, at least to some extent, the different results obtained with these two methods. Firstly, the NMR method observes the overall oxidation reaction considering both the early and later stages of the reaction whereas the spectrophotometric assay focuses only on the early stages of the oxidation reaction. Secondly, different incubation temperatures (37°C for the NMR protocol and 30°C for the spectrophotometric method) can affect the kinetics of the oxidation reaction as has been shown previously (Ramos et al. 1995). There are also different copper-to-serum ratios (0.5 mM/300 µl for the NMR method and 0.05 mM/13.4 µl for the spectrophotometric assay) which may have some effect on the oxidation reactions. Thirdly, there are no disturbing signals in the ^{1}H NMR spectrum overlapping with the signals arising from PUFAs whereas in the spectrophotometric assay also albumin and some oxysterols absorb at the same wavelength as conjugated dienes (Schnitzer et al. 1998).

4.6 APPLICATION OF THE NMR LIPID ANALYSIS TO CLINICAL STUDIES

4.6.1 Lipid abnormalities in MCI (II)

MCI is a neuropsychological diagnosis indicating severely increased risk for AD. There is evidence suggesting that systemic metabolite and lipid levels are associated with the development of AD (Shobab et al. 2005; Kivipelto & Solomon 2006). The purpose of this study was to find new molecular insights on the potential early changes in systemic metabolism that relate to MCI, and thus, to high risk for AD.

The self-organizing map (SOM) analysis used in this study was based on the combination of the three spectra that were measured from each serum sample (^{1}H NMR spectrum of native serum revealing information about lipoprotein subclasses, T_2 edited ^{1}H NMR spectrum of native serum yielding concentrations of low-molecular-weight metabolites, and [1]H

NMR spectrum of extracted serum that gives information about different serum lipids). According to the analysis, the MCI samples cluster on the southeast part of the SOM ($p < 0.05$) (Figure 39) suggesting that there is a link between systemic metabolism and MCI. However, the distribution of MCI samples is not inclusive which probably reflects the complex link between the serum biochemistry and cognitive decline, as well as potentially various differing biochemical pathways behind MCI. This is also supported by the analyses at individual time points since none of the serum metabolites showed statistically significant changes between the control and MCI groups or between the different time points. Nevertheless, the holistic SOM analysis based on the multi-metabolite information in the ^{1}H NMR spectra of serum did define statistically significant metabolic associations for the MCI, indicating that the combined changes of several metabolites can be descriptive while the changes in the individual metabolites are not.

Diabetes and obesity (high BMI) have been associated with MCI (Martins et al. 2006), and this was recognized also in this study since all these three conditions have quite similar color distributions in the SOM (Figure 39). Thus, the NMR data reveals the link between vascular factors and cognitive decline and a risk for dementia.
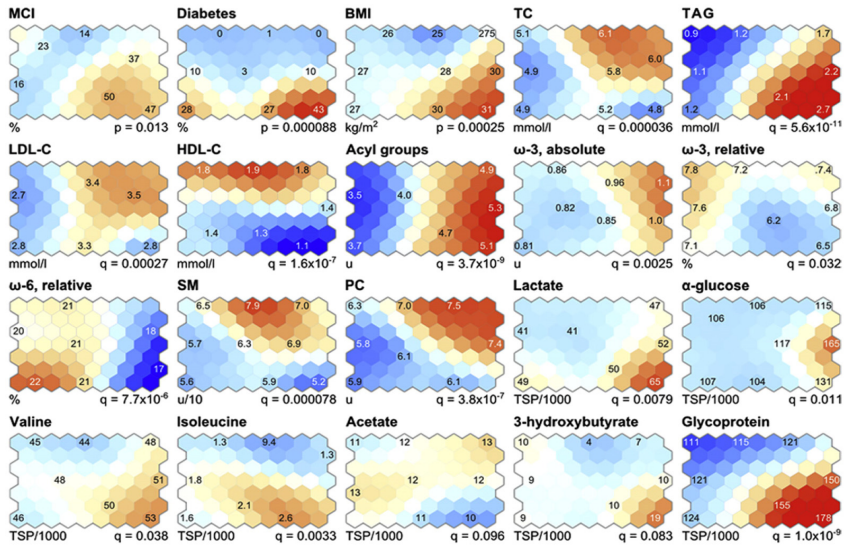
Figure 39. *Statistical colorings of the clinical and biochemical variables in the self-organizing map (SOM) analysis including 176 serum samples. Due to the SOM analysis the samples are positioned so that the multi-metabolite differences between nearby samples are minimized. Acyl groups, total amount of -CH3 groups in serum lipids; BMI, body mass index; HDL-C, high-density lipoprotein cholesterol; LDL-C, low-density lipoprotein cholesterol; MCI, mild cognitive impairment; PC, phosphatidylcholine; SM, sphingomyelin; TC, serum total cholesterol; TAG, serum triacylglycerides; ω-3 absolute, the absolute amount of serum ω-3 fatty acids; ω-3 relative, the ratio of ω-3 fatty acids and total fatty acids; ω-6 relative, the ratio of ω-6 fatty acids and total fatty acids*

Serum cholesterol has been suggested to be a risk factor for AD (Shobab et al. 2005; Kivipelto & Solomon 2006). Here, the highest total cholesterol values concentrate on the northeast corner of the SOM (Figure 39). The LDL cholesterol values follow the total cholesterol with only slight differences. It is also notable that the low HDL cholesterol clearly associates with high TAGs in the southeast corner suggesting that there is an association between the metabolic syndrome and MCI. Thus, within the current limited data set, it appears that metabolic syndrome would be more associated with MCI than high total cholesterol as such.

Since cholesterol and TAGs are abundant in serum and they contain acyl groups (except free cholesterol) it is logical that the highest amounts of acyl groups are found from the samples that have a lot of cholesterol or TAGs (Figure 39). The lowest absolute concentrations of ω-3 FAs concentrate on the western side of the SOM whereas the lowest relative amounts of ω-3 FAs coincide remarkably well with MCI in the southeast corner of the map. These results suggest that a low relative amount of ω-3 FAs would be more indicative of high risk for AD than low serum ω-3 concentration as such (Martins et al. 2006).

It has been suggested that serum sphingomyelin may be a good pre-clinical predictor of memory impairment (Mielke et al. 2010). In this study, the highest amounts of sphingomyelin and PC concentrate on the northeast corner of the SOM, similarly with total cholesterol (Figure 39). The lowest amounts of sphingomyelin cluster on the southeast corner and overlap with MCI samples (Figure 39).

To conclude, the application in cognitive impairment suggests that systemic lipid metabolism, especially the metabolic syndrome and the relative amount of serum ω-3 FAs, has a distinct role in the risk assessment of AD. The results from this pilot study also justify more extensive applications of serum NMR metabonomics in neurological disorders.

4.6.2 Lipid abnormalities in type 1 diabetic patients having kidney disease (III)

Diabetic kidney disease is a symptom of chronic vascular injury in diabetes and it is associated with dyslipidemia and increased mortality. The aim of this study was to find out which lipid variables are related with diabetic kidney disease.

The univariate logistic regression analysis revealed that sphingomyelin and large HDL lipids have the strongest association with diabetic kidney disease and only commonly known biomarkers such as serum creatinine, serum cystatin-C, serum urea, and glomerular filtration rate have higher regression coefficients (Figure 40). Also various lipids of large

and extra large VLDL particles are related with kidney disease. (Figure 40)

Since 24 h-AER values describe the continuous renal status, also correlations between lipid variables and 24 h-AER were studied. Sphingomyelin has the largest correlation coefficient but also TAGs, large VLDL cholesterol, large HDL cholesterol, and HDL cholesterol have strong correlations (Table 15). Sphingomyelin, TAGs, and large VLDL cholesterol are directly correlated with 24 h-AER, whereas large HDL cholesterol and HDL cholesterol are inversely correlated (Table 15).
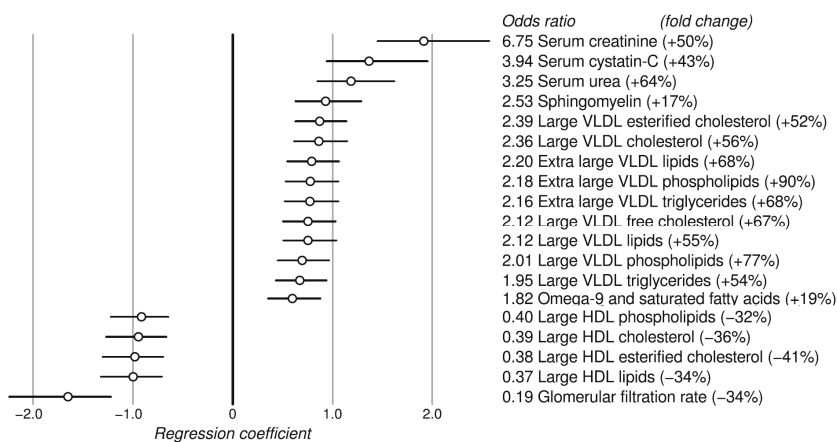
Figure 40. Odds ratios for diabetic kidney disease (adjusted by diabetes duration, age, and gender). The circles indicate logarithmic odds ratios (regression coefficients in the logistic model) and the horizontal lines show the 95% interval. The fold change was calculated by dividing the median concentration difference (after adjustments) between the cases and controls by the median concentration in the control group. Only those variables that reached Bonferroni multiple testing significance are included (p < 0.00038).

Table 15. *Lipid variables that are significantly correlated with 24 h-AER.*

	Adjusted		Unadjusted	
	Correlation	***p***	**Correlation**	***p***
Sphingomyelin	0.42	1.5×10^{-14}	0.43	6.7×10^{-16}
TAGs	0.30	3.7×10^{-7}	0.38	1.6×10^{-10}
Large VLDL cholesterol	0.30	1.2×10^{-7}	0.29	1.4×10^{-7}
Free cholesterol	0.29	3.0×10^{-7}	0.32	9.2×10^{-9}
ω-9 and sat FAs	0.26	3.3×10^{-6}	0.33	1.8×10^{-9}
ω-6 and ω-7 FAs	0.26	5.3×10^{-6}	0.26	4.3×10^{-6}
IDL TAGs	0.22	0.00011	0.27	1.8×10^{-6}
Phosphoglycerides	0.12	0.036	0.16	0.0041
PC	-0.02	0.71	0.00	0.96
ω-3 FAs	-0.05	0.39	-0.03	0.60
FA length	-0.20	0.00040	-0.25	6.6×10^{-6}
Medium HDL cholesterol	-0.25	1.2×10^{-5}	-0.28	5.7×10^{-7}
HDL cholesterol	-0.31	2.1×10^{-7}	-0.27	4.9×10^{-6}
Large HDL cholesterol	-0.33	3.6×10^{-9}	-0.32	7.7×10^{-9}

Correlation was measured by the Spearman coefficient and the Bonferroni multiple testing limit is at $p < 0.00038$.

FA, fatty acid; HDL, high-density lipoprotein; IDL, intermediate-density lipoprotein; PC, phosphatidylcholine; sat, saturated; TAG, triacylglyceride; VLDL, very-low-density lipoprotein

Multivariate linear regression was used to explain the covariance between sphingomyelin and 24 h-AER. For this purpose, two sets of variables were chosen. Set 1 included sphingomyelin, duration of type 1 diabetes, metabolic syndrome, glomerular filtration, and glucose disposal rate (Table 16). Set 2 involved measures that are diagnostic for some disease states. For example, blood pressure is associated with hypertension and TAGs and HDL cholesterol are related to dyslipidemia (Table 16). Sphingomyelin was shown to be a statistically significant variable in both models (Table 16) suggesting that sphingomyelin has an important role in albuminuria.

Table 16. *Regression coefficients for the two models of 24 h-AER.*

Model 1	Beta	p	Model 2	Beta	p
Sphingomyelin	0.22	1.8×10^{-5}	Sphingomyelin	0.22	1.1×10^{-5}
T1DM duration	0.011	0.42	T1DM duration	0.19	0.00013
MetS	0.12	0.0042	Male gender	0.0012	0.50
eGDR	-0.32	1.4×10^{-10}	Waist	0.057	0.173
eGFR	-0.28	5.6×10^{-6}	Systolic BP	0.087	0.047
			Hemoglobin A1c	0.15	0.0011
			TAGs	0.031	0.33
			HDL cholesterol	-0.13	0.0046
			Creatinine	0.30	7.8×10^{-6}

Models 1 and 2 explained 44.1 and 41.9% of 24 h-AER variance, respectively. Without sphingomyelin the explanation percentages were 40.5 and 38.8, respectively. AER, urinary albumin excretion rate; BP, blood pressure; eGDR, efficient glucose disposal rate; eGFR, estimated glomerular filtration rate; HDL, high-density lipoprotein; MetS, Metabolic syndrome; T1DM, type 1 diabetes mellitus; TAG, triacylglyceride

A recent animal study supports the role of sphingomyelin in kidney disease. In the study, untreated mice on a high-fat diet developed insulin resistance and albuminuria but the inhibition of the conversion of sphingomyelin into ceramide significantly decreased glomerular injury and restored AER to normal range (Boini et al. 2010).

It is also possible that excess circulating sphingomyelin is a by-product of the disease process and not an initiator. In fact, excess SFAs may be the underlying cause since SFAs are substrates for sphingolipid synthesis. SFAs promote lipotoxicity through the production of ceramides and they are also linked to insulin resistance (Kennedy et al. 2009; Yang et al. 2009; Bunn et al. 2010). The correlations between the sum of ω-9 and saturated FAs and kidney disease (Figure 40) and 24 h-AER (Table 15) support this view.

In conclusion, sphingomyelin was shown to be associated both with diabetic kidney disease and AER. The results are supported by animal data, which suggests that sphingolipids

may reflect some of the molecular links between microvascular injury, insulin resistance, and SFAs. Further research is required to confirm the role of sphingomyelin in diabetic kidney disease.

4.7 APPLICATION OF THE NMR OXIDATION ASSAY TO CHOCOLATE STUDY SAMPLES (IV)

The NMR oxidation assay was applied to fasting serum samples from the chocolate study. The oxidation susceptibility of serum lipids decreased in the HPC group ($p = 0.016$) after the chocolate consumption but there were no significant changes in the DC ($p = 0.407$) or WC ($p = 0.758$) groups. The change in the NMR oxidation susceptibility was significantly different between the WC and HPC groups ($p = 0.031$). Since the baseline values of the HPC group are lower than in the WC and DC groups (Table 17), the analyses were also performed by adjusting the baseline values of the variables but the changes between the groups were significantly different also after the adjustment ($p = 0.043$). Interestingly, statistically significant changes between the study groups were not observed when the oxidation susceptibility was determined using the spectrophotometric method (Table 17) (Mursu et al. 2004).

Table 17. The NMR oxidation susceptibility and the lag time before (baseline) and after (change) the consumption of the study chocolates.

Parameter		NMR oxidation susceptibility (%)	Lag time (min)
WC	Baseline	72 ± 14	118 ± 43
	Change	0 ± 5	6 ± 31
DC	Baseline	71 ± 10	122 ± 35
	Change	-2 ± 8	4 ± 32
HPC	Baseline	64 ± 17	160 ± 61
	Change	7 ± 10	-3 ± 28
p		0.033	0.711

4.7.1 Determinants of oxidation susceptibility

Random forest regression was used to find out if there is a set of variables that would explain the differences in the NMR oxidation susceptibility values. The variables included into the analyses consisted of previously measured variables (Mursu et al. 2004) and a total of 23 lipid variables obtained by NMR. The previously measured variables involved several FAs and other lipid measures, some common serum parameters such as hemoglobin and hematocrit, as well as vitamins and polyphenols.

The analysis included the baseline and end-point values of the variables described above. Random forest regression was able to explain 60% of the NMR oxidation susceptibility values with nine variables, and most of them are lipid measures (Figure 41). According to the variable importance measures, arachidonic acid and DHA are the most important determinants of NMR oxidation susceptibility (Figure 41). This is logical since the NMR oxidation protocol measures the amount of oxidized PUFAs.
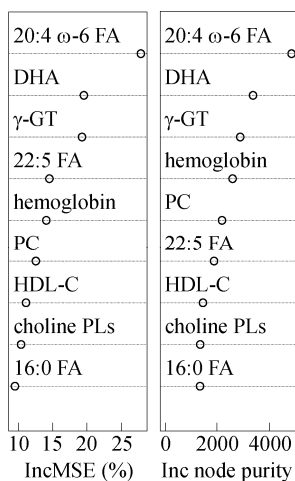
Figure 41. Increase in mean square error (IncMSE) (%) and increase in node purity (Inc node purity) values for each variable obtained from the random forest regression when modeling the oxidation susceptibility values. 20:4 ω-6 FA, arachidonic acid; DHA, docosahexaenoic acid; FA, fatty acid; γ-GT, gamma-glutamyl transferase; HDL-C, high-density lipoprotein cholesterol; PC, phosphatidylcholine; PL, phospholipid

Previously, vitamin C, urate, α-tocopherol, albumin, and HDL concentration have been proposed to be determinants of oxidation susceptibility (Nyyssönen et al. 1997). HDL cholesterol was also among our descriptors. Our data included also vitamin C and α-tocopherol values that were calculated

based on a 4 day food record but they were not regarded as determinants of oxidation susceptibility. However, considering that our data lacked serum urate and albumin concentrations, the explanation percentage of the model trying to explain the NMR oxidation susceptibility values (60%) is quite high.

4.7.2 Lipid changes induced by the chocolate consumption

The study chocolates had similar amounts of FAs, excluding behenic acid, but the amounts of cocoa and polyphenols were different. The main difference between the DC and HPC chocolates was the amount of polyphenols; HPC chocolate contained approximately 1.5 times more polyphenols than the DC chocolate.

The random forest method allowed clustering of the WC, DC, and HPC groups with six variables (Figure 42). The analysis included the change (end-baseline) values of the variables described above. Behenic acid was excluded from the analysis since the HPC chocolate contained ten-fold amount of behenic acid compared with other study chocolates.
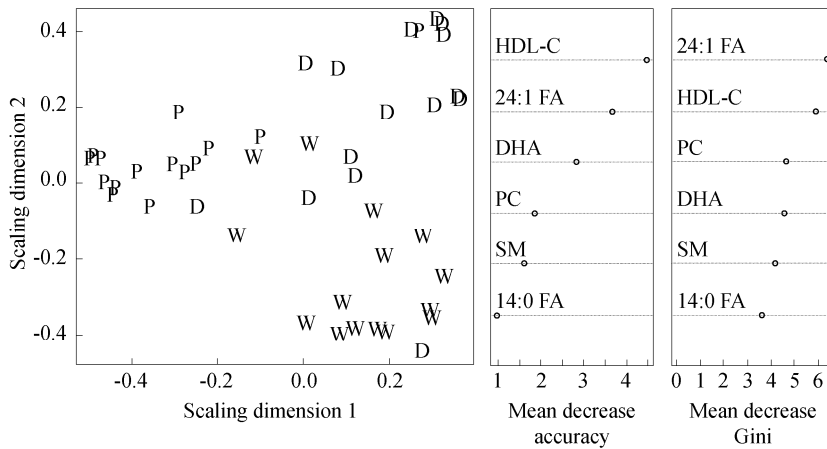
Figure 42. Random forest clustering was obtained with six end-baseline variables. The variable importance measures, mean decrease in accuracy and mean decrease in Gini index, are shown for each of these variables. D, dark chocolate; DHA, docosahexaenoic acid; FA, fatty acid; HDL-C, high-density lipoprotein cholesterol; P, high-polyphenol chocolate; PC, phosphatidylcholine; SM, sphingomyelin; W, white chocolate

All the clustering variables are lipid measures (Figure 42) and three of them are same as those obtained by random forest regression (Figure 41). It seems that the consumption of the HPC chocolate induces different changes to the amounts of HDL cholesterol, nervonic acid, DHA, PC, sphingomyelin, and myristic acid than the consumption of the WC or DC chocolates as can be seen from the variable profiles (Figure 43). Since the main difference between the study chocolates was the amount of polyphenols, it is likely that they have induced the metabolic changes in the HPC group. However, on the grounds of this study it is impossible to identify the mechanisms of action.
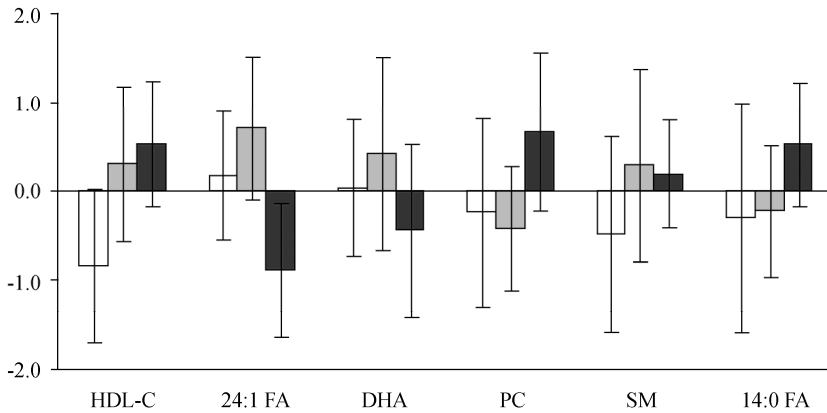
Figure 43. *The profiles of the variable changes for the white chocolate (white), dark chocolate (light grey), and high-polyphenol chocolate (dark grey) groups. The values are expressed as standard deviation units from the mean of the whole study population. DHA, docosahexaenoic acid; FA, fatty acid; HDL-C, high-density lipoprotein cholesterol; PC, phosphatidylcholine; SM, sphingomyelin*

5 Conclusions and future aspects

In the present study, NMR protocols for analysis of serum lipids were developed and assessed.

Quantum mechanical spectral analyses of ^{1}H NMR spectra of *n*-alkanes were performed to be able to understand the conformational behavior of CH_2-fragments, common structural units in lipids, in a solution state. According to the coupling constant information, the proportion of the *trans* conformation increases when the hydrocarbon chain is lengthened (Paper I). Chemical environment was shown to have only minor effects on the conformational equilibrium (Paper I). Quantum mechanical spectral analysis was also performed for a short fatty acid, and its spectral parameters greatly resembled those of *n*-alkanes.

We developed an assay that allows the extraction of lipids from about 100 serum samples in a day, as well as a constrained total-line-shape fitting method for the quantification of lipids from the ^{1}H NMR spectra of serum lipid extracts. The lipid analysis protocol was applied to two clinical studies. The results from the study involving patients with MCI revealed that a low relative amount of ω-3 FAs is more indicative of MCI than low serum ω–3 concentration as such (Paper II). The other study, involving type 1 diabetic patients, indicated that sphingomyelin is associated with kidney disease in type 1 diabetic patients (Paper III).

Also, an NMR-based oxidation method for serum lipids was developed and the protocol was applied to serum samples from a dietary intervention. The results showed that the consumption of high-polyphenol chocolate decreased the oxidation susceptibility of serum lipids (Paper IV). This could not be detected by using the conventional spectrophotometric method,

even though the values obtained by these two oxidation methods correlated (Paper IV).

So far, NMR lipid analysis has been used in several clinical studies covering various disease states such as subclinical atherosclerosis (Würtz et al. 2011; Würtz et al. 2012), cardiovascular disease (International Consortium for Blood Pressure Genome-Wide Association Studies 2011), and metabolic syndrome (Vanhala et al. 2012), as well as in studies dealing with associations of human serum metabolite levels and genetic loci (Inouye et al. 2010; Chambers et al. 2011; Kettunen et al. 2012; Tukiainen et al. 2012). In the future, one aim is to further optimize the protocol to decrease solvent consumption and to be able to increase the number of lipid measures obtained from a spectrum. Regarding the NMR oxidation assay, it would be interesting to apply this method to clinical studies in order to explore the applicability of the assay in assessing the oxidation susceptibility of serum lipids in disease states.

6 References

Adibhatla R M & Hatcher J F (2010) Lipid oxidation and peroxidation in CNS health and disease: From molecular mechanisms to therapeutic opportunities. *Antioxidants & Redox Signaling* 12: 125-169.

Adiels M, Olofsson S-O, Taskinen M-R & Borén J (2008) Overproduction of very low-density lipoproteins is the hallmark of the dyslipidemia in the metabolic syndrome. *Arteriosclerosis, Thrombosis, and Vascular Biology* 28: 1225-1236.

Ahima R S (2011) Digging deeper into obesity. *The Journal of Clinical Investigation* 121: 2076-2079.

Ala-Korpela M, Korhonen A, Keisala J, Hörkkö S, Korpi P, Ingman L P, Jokisaari J, Savolainen M J & Kesäniemi Y A (1994) ^{1}H NMR-based absolute quantitation of human lipoproteins and their lipid contents directly from plasma. *Journal of Lipid Research* 35: 2292-2304.

Ala-Korpela M (1995) ^{1}H NMR spectroscopy of human blood plasma. *Progress in Nuclear Magnetic Resonance Spectroscopy* 27: 475-554.

Ala-Korpela M, Lankinen N, Salminen A, Suna T, Soininen P, Laatikainen R, Ingman P, Jauhiainen M, Taskinen M-R, Héberger K & Kaski K (2007) The inherent accuracy of ^{1}H NMR spectroscopy to quantify plasma lipoproteins is subclass dependent. *Atherosclerosis* 190: 352-358.

Ascherio A (2006) Trans fatty acids and blood lipids. *Atherosclerosis Supplements* 7: 25-27.

Assies J, Pouwer F, Lok A, Mocking R J T, Bockting C L H, Visser I, Abeling N G G M, Duran M & Schene A H (2010) Plasma and erythrocyte fatty acid patterns in patients with recurrent depression: A matched case-control study. *Plos One* 5: Article ID e10635.

Bagatolli L A, Ipsen J H, Simonsen A C & Mouritsen O G (2010) An outlook on organization of lipids in membranes: Searching for a realistic connection with the organization of biological membranes. *Progress in Lipid Research* 49: 378-389.

Barberger-Gateau P, Samieri C, Féart C & Plourde M (2011) Dietary Omega 3 Polyunsaturated Fatty Acids and Alzheimer's Disease:

Interaction with Apolipoprotein E Genotype. *Current Alzheimer Research* 8: 479-491.

Basu S (2010) Fatty acid oxidation and isoprostanes: Oxidative strain and oxidative stress. *Prostaglandins Leukotrienes and Essential Fatty Acids* 82: 219-225.

Beger R, Schnackenberg L, Holland R, Li D & Dragan Y (2006) Metabonomic models of human pancreatic cancer using 1D proton NMR spectra of lipids in plasma. *Metabolomics* 2: 125-134.

Betteridge D J (2011) Lipid control in patients with diabetes mellitus. *Nature reviews. Cardiology* 8: 278-290.

Beyer T, Diehl B & Holzgrabe U (2010) Quantitative NMR spectroscopy of biologically active substances and excipients. *Bioanalytical Reviews* 2: 1-22.

Bhabak K P & Mugesh G (2010) Functional Mimics of Glutathione Peroxidase: Bioinspired Synthetic Antioxidants. *Accounts of Chemical Research* 43: 1408-1419.

Bicalho B, David F, Rumplel K, Kindt E & Sandra P (2008) Creating a fatty acid methyl ester database for lipid profiling in a single drop of human blood using high resolution capillary gas chromatography and mass spectrometry. *Journal of Chromatography A* 1211: 120-128.

Black D D (2007) Development and physiological regulation of intestinal lipid absorption. I. Development of intestinal lipid absorption: cellular events in chylomicron assembly and secretion. *American Journal of Physiology - Gastrointestinal and Liver Physiology* 293: G519-G524.

Bligh E G & Dyer W J (1959) A rapid method of total lipid extraction and purification. *Canadian Journal of Biochemistry and Physiology* 37: 911-917.

Boini K M, Zhang C, Xia M, Poklis J L & Li P-L (2010) Role of Sphingolipid Mediator Ceramide in Obesity and Renal Injury in Mice Fed a High-Fat Diet. *Journal of Pharmacology and Experimental Therapeutics* 334: 839-846.

Bondia-Pons I, Morera-Pons S, Castellote A I & López-Sabater M C (2006) Determination of phospholipid fatty acids in biological samples by solid-phase extraction and fast gas chromatography. *Journal of Chromatography A* 1116: 204-208.

Bornfeldt K E & Tabas I (2011) Insulin Resistance, Hyperglycemia, and Atherosclerosis. *Cell Metabolism* 14: 575-585.

Bradamante S, Barenghi L, Giudici G A & Vergani C (1992) Free radicals promote modifications in plasma high-density lipoprotein: nuclear magnetic resonance analysis. *Free Radical Biology and Medicine* 12: 193-203.

Brufau G, Groen A K & Kuipers F (2011) Reverse Cholesterol Transport Revisited Contribution of Biliary Versus Intestinal Cholesterol Excretion. *Arteriosclerosis, Thrombosis, and Vascular Biology* 31: 1726-1733.

Bunn R C, Cockrell G E, Ou Y, Thrailkill K M, Lumpkin C K & Fowlkes J L (2010) Palmitate and insulin synergistically induce IL-6 expression in human monocytes. *Cardiovascular Diabetology* 9: 73.

Bunney T D & Katan M (2011) PLC regulation: emerging pictures for molecular mechanisms. *Trends in Biochemical Sciences* 36: 88-96.

Burdge G C, Wright P, Jones A E & Wootton S A (2000) A method for separation of phosphatidylcholine, triacylglycerol, non-esterified fatty acids and cholesterol esters from plasma by solid-phase extraction. *The British Journal of Nutrition* 84: 781-787.

Burke J & Dennis E (2009) Phospholipase A_2 Biochemistry. *Cardiovascular Drugs and Therapy* 23: 49-59.

Castro-Perez J M, Kamphorst J, DeGroot J, Lafeber F, Goshawk J, Yu K, Shockcor J P, Vreeken R J & Hankemeier T (2010) Comprehensive LC-MSE Lipidomic Analysis using a Shotgun Approach and Its Application to Biomarker Detection and Identification in Osteoarthritis Patients. *Journal of Proteome Research* 9: 2377-2389.

Cequier-Sánchez E, Rodríguez C, Ravelo Á G & Zárate R (2008) Dichloromethane as a solvent for lipid extraction and assessment of lipid classes and fatty acids from samples of different natures. *Journal of Agricultural and Food Chemistry* 56: 4297-4303.

Chalfant C E & Spiegel S (2005) Sphingosine 1-phosphate and ceramide 1-phosphate: expanding roles in cell signaling. *Journal of Cell Science* 118: 4605-4612.

Chambers J C, Zhang W, Sehmi J, Li X, Wass M N, Van der Harst P, Holm H, Sanna S, Kavousi M, Baumeister S E, Coin L J, Deng G, Gieger C, Heard-Costa N L, Hottenga J J, Kühnel B, Kumar V, Lagou V, Liang L, Luan J, Vidal P M, Leach I M, O'Reilly P F, Peden J F, Rahmioglu N, Soininen P, Speliotes E K, Yuan X, Thorleifsson G, Alizadeh B Z, Atwood L D, Borecki I B, Brown M J, Charoen P, Cucca F, Das D, de Geus E J C, Dixon A L, Döring A, Ehret G,

Eyjolfsson G I, Farrall M, Forouhi N G, Friedrich N, Goessling W, Gudbjartsson D F, Harris T B, Hartikainen A L, Heath S, Hirschfield G M, Hofman A, Homuth G, Hyppönen E, Janssen H L A, Johnson T, Kangas A J, Kema I P, Kühn J P, Lai S, Lathrop M, Lerch M M, Li Y, Liang T J, Lin J P, Loos R J F, Martin N G, Moffatt M F, Montgomery G W, Munroe P B, Musunuru K, Nakamura Y, O'Donnell C J, Olafsson I, Penninx B W, Pouta A, Prins B P, Prokopenko I, Puls R, Ruokonen A, Savolainen M J, Schlessinger D, Schouten J N L, Seedorf U, Sen-Chowdhry S, Siminovitch K A, Smit J H, Spector T D, Tan W, Teslovich T M, Tukiainen T, Uitterlinden A G, Van der Klauw M M, Vasan R S, Wallace C, Wallaschofski H, Wichmann H E, Willemsen G, Würtz P, Xu C, Yerges-Armstrong L M, Abecasis G R, Ahmadi K R, Boomsma D I, Caulfield M, Cookson W O, van Duijn C M, Froguel P, Matsuda K, McCarthy M I, Meisinger C, Mooser V, Pietiläinen K H, Schumann G, Snieder H, Sternberg M J E, Stolk R P, Thomas H C, Thorsteinsdottir U, Uda M, Waeber G, Wareham N J, Waterworth D M, Watkins H, Whitfield J B, Witteman J C M, Wolffenbuttel B H R, Fox C S, Ala-Korpela M, Stefansson K, Vollenweider P, Völzke H, Schadt E E, Scott J, Järvelin M R, Elliott P & Kooner J S (2011) Genome-wide association study identifies loci influencing concentrations of liver enzymes in plasma. *Nature Genetics* 43: 1131-1138.

Chan D I & Vogel H J (2010) Current understanding of fatty acid biosynthesis and the acyl carrier protein. *Biochemical Journal* 430: 1-19.

Chatterjee C & Sparks D L (2011) Hepatic Lipase, High Density Lipoproteins, and Hypertriglyceridemia. *The American Journal of Pathology* 178: 1429-1433.

Choi S H & Ginsberg H N (2011) Increased very low density lipoprotein (VLDL) secretion, hepatic steatosis, and insulin resistance. *Trends in Endocrinology & Metabolism* 22: 353-363.

Claridge T D W (1999) *High-Resolution NMR Techniques in Organic chemistry*. Pergamon, Amsterdam.

Coleman R A & Lee D P (2004) Enzymes of triacylglycerol synthesis and their regulation. *Progress in Lipid Research* 43: 134-176.

Connor W E, Lin D S & Colvis C (1996) Differential mobilization of fatty acids from adipose tissue. *Journal of Lipid Research* 37: 290-298.

Corso G, Trivellone E, Motta A, Postiglione A, Mancinia F P, Carbone V & Napoli C (1997) Effect of low density lipoprotein fatty acid composition on copper-induced peroxidation: [1]H-nuclear magnetic resonance analysis. *Clinica Chimica Acta* 258: 193-200.

Cremesti A E, Goni F M & Kolesnick R (2002) Role of sphingomyelinase and ceramide in modulating rafts: do biophysical properties determine biologic outcome? *FEBS Letters* 531: 47-53.

Cunnane S C, Plourde M, Pifferi F, Bégin M, Féart C & Barberger-Gateau P (2009) Fish, docosahexaenoic acid and Alzheimer's disease. *Progress in Lipid Research* 48: 239-256.

Daniels T F, Killinger K M, Michal J J, Wright R W & Jiang Z (2009) Lipoproteins, cholesterol homeostasis and cardiac health. *International Journal of Biological Sciences* 5: 474-488.

Das U N (2008) Essential fatty acids and their metabolites could function as endogenous HMG-CoA reductase and ACE enzyme inhibitors, anti-arrhythmic, anti-hypertensive, anti-atherosclerotic, anti-inflammatory, cytoprotective, and cardioprotective molecules. *Lipids in Health and Disease* 7: Article ID 37.

de Castro S H, Castro-Faria-Neto H C & Gomes M B (2005) Association of Postprandial Hyperglycemia with in Vitro LDL Oxidation in Non-Smoking Patients with Type 1 Diabetes - a Cross-Sectional Study. *The Review of Diabetic Studies* 2: 157-164.

de Hoffmann E & Stroobant V (1999) *Mass spectrometry: principles and applications*. John Wiley & Sons, LTD, Chichester.

Delimaris I, Faviou E, Antonakos G, Stathopoulou E, Zachari A & Dionyssiou-Asteriou A (2007) Oxidized LDL, serum oxidizability and serum lipid levels in patients with breast or ovarian cancer. *Clinical Biochemistry* 40: 1129-1134.

Delimaris I, Georgopoulos S, Kroupis C, Zachari A, Liberi M, Bastounis E & Dionyssiou-Asteriou A (2008) Serum oxidizability, total antioxidant status and albumin serum levels in patients with aneurysmal or arterial occlusive disease. *Clinical Biochemistry* 41: 706-711.

Devaraj S & Jialal I (2012) Dysfunctional Endothelial Progenitor Cells in Metabolic Syndrome. *Experimental Diabetes Research* 2012: Article ID 585018.

Di Paolo G & Kim T-W (2011) Linking lipids to Alzheimer's disease: cholesterol and beyond. *Nature Reviews Neuroscience* 12: 284-296.

Ding J, Sorensen C M, Jaitly N, Jiang H L, Orton D J, Monroe M E, Moore R J, Smith R D & Metz T O (2008) Application of the accurate mass and time tag approach in studies of the human blood lipidome. *Journal of Chromatography B-Analytical Technologies in the Biomedical and Life Sciences* 871: 243-252.

Dodds E, McCoy M, Rea L & Kennish J (2005) Gas chromatographic quantification of fatty acid methyl esters: Flame ionization detection vs. Electron impact mass spectrometry. *Lipids* 40: 419-428.

Eyster K M (2007) The membrane and lipids as integral participants in signal transduction: lipid signal transduction for the non-lipid biochemist. *Advances in Physiology Education* 31: 5-16.

Fahy E, Subramaniam S, Brown H A, Glass C K, Merrill A H, Murphy R C, Raetz C R H, Russell D W, Seyama Y, Shaw W, Shimizu T, Spener F, van Meer G, VanNieuwenhze M S, White S H, Witztum J L & Dennis E A (2005) A comprehensive classification system for lipids. *Journal of Lipid Research* 46: 839-862.

Fernandez-Panchon M S, Villano D, Troncoso A M & Garcia-Parrilla M C (2008) Antioxidant activity of phenolic compounds: From in vitro results to in vivo evidence. *Critical Reviews in Food Science and Nutrition* 48: 649-671.

Fernández-Quintela A, Churruca I & Portillo M P (2007) The role of dietary fat in adipose tissue metabolism. *Public Health Nutrition* 10: 1126-1131.

Fessenden R J, Fessenden J S & Logue M W (1998) *Organic chemistry*. Brooks/Cole Publishing company, Pacific Grove.

Flegal K M, Carroll M D, Ogden C L & Curtin L R (2010) Prevalence and Trends in Obesity Among US Adults, 1999-2008. *JAMA: The Journal of the American Medical Association* 303: 235-241.

Folch J, Lees M & Sloan Stanley G H (1957) A simple method for the isolation and purification of total lipides from animal tissues. *Journal of Biological Chemistry* 226: 497-509.

Fonseca A C R G, Resende R, Oliveira C R & Pereira C M F (2010) Cholesterol and statins in Alzheimer's disease: Current controversies. *Experimental Neurology* 223: 282-293.

Fraga C G, Galleano M, Verstraeten S V & Oteiza P I (2010) Basic biochemical mechanisms behind the health benefits of polyphenols. *Molecular Aspects of Medicine* 31: 435-445.

Fuchs B, Süß R, Nimptsch A & Schiller J (2009) MALDI-TOF-MS directly combined with TLC: A review of the current state. *Chromatographia* 69: S95-S105.

Fuchs B, Süß R & Schiller J (2010) An update of MALDI-TOF mass spectrometry in lipid research. *Progress in Lipid Research* 49: 450-475.

Fuchs B, Süß R, Teuber K, Eibisch M & Schiller J (2011) Lipid analysis by thin-layer chromatography--A review of the current state. *Journal of Chromatography A* 1218: 2754-2774.

Fuller M (2010) Sphingolipids: the nexus between Gaucher disease and insulin resistance. *Lipids in Health and Disease* 9: Article ID 113.

Galleano M, Verstraeten S V, Oteiza P I & Fraga C G (2010) Antioxidant actions of flavonoids: Thermodynamic and kinetic analysis. *Archives of Biochemistry and Biophysics* 501: 23-30.

Gangoiti P, Camacho L, Arana L, Ouro A, Granado M H, Brizuela L, Casas J, Fabriás G, Abad J L, Delgado A & Gómez-Muñoz A (2010) Control of metabolism and signaling of simple bioactive sphingolipids: Implications in disease. *Progress in Lipid Research* 49: 316-334.

Gebauer S K, Psota T L & Kris-Etherton P M (2007) The diversity of health effects of individual trans fatty acid isomers. *Lipids* 42: 787-799.

German J B, Smilowitz J T & Zivkovic A M (2006) Lipoproteins: When size really matters. *Current Opinion in Colloid & Interface Science* 11: 171-183.

Gillingham L, Harris-Janz S & Jones P (2011) Dietary monounsaturated fatty acids are protective against metabolic syndrome and cardiovascular disease risk factors. *Lipids* 46: 209-228.

Glaser C, Demmelmair H & Koletzko B (2010) High-Throughput Analysis of Total Plasma Fatty Acid Composition with Direct In Situ Transesterification. *Plos One* 5: Article ID e12045.

Goodman B E (2010) Insights into digestion and absorption of major nutrients in humans. *Advances in Physiology Education* 34: 44-53.

Gross J L, de Azevedo M J, Silveiro S P, Canani L H, Caramori M L & Zelmanovitz T (2005) Diabetic Nephropathy: Diagnosis, Prevention, and Treatment. *Diabetes Care* 28: 164-176.

Grundy S M, Cleeman J I, Daniels S R, Donato K A, Eckel R H, Franklin B A, Gordon D J, Krauss R M, Savage P J, Smith S C, Jr., Spertus J A & Costa F (2005) Diagnosis and management of the metabolic

syndrome: An american heart association/national heart, lung, and blood institute scientific statement. *Circulation* 112: 2735-2752.

Guillou H, Zadravec D, Martin P G P & Jacobsson A (2010) The key roles of elongases and desaturases in mammalian fatty acid metabolism: Insights from transgenic mice. *Progress in Lipid Research* 49: 186-199.

Gulati S, Liu Y, Munkacsi A B, Wilcox L & Sturley S L (2010) Sterols and sphingolipids: Dynamic duo or partners in crime? *Progress in Lipid Research* 49: 353-365.

Günther H (1995) *NMR Spectroscopy. Basic principles, concepts, and applications in chemistry*. John Wiley & Sons, Chichester.

Han X, Yang K & Gross R W (2012) Multi-dimensional mass spectrometry-based shotgun lipidomics and novel strategies for lipidomic analyses. *Mass Spectrometry Reviews* 31: 134-178.

Hannun Y A & Obeid L M (2008) Principles of bioactive lipid signalling: lessons from sphingolipids. *Nature Reviews Molecular Cell Biology* 9: 139-150.

Hardwick J P, Osei-Hyiaman D, Wiland H, Abdelmegeed M A & Song B J (2009) PPAR/RXR Regulation of Fatty Acid Metabolism and Fatty Acid ω-Hydroxylase (CYP4) Isozymes: Implications for Prevention of Lipotoxicity in Fatty Liver Disease. *Ppar Research* 2009: Article ID 952734.

Hartmann T, Kuchenbecker J & Grimm M O W (2007) Alzheimer's disease: the lipid connection. *Journal of Neurochemistry* 103: S159-S170.

He X, Huang Y, Li B, Gong C-X & Schuchman E H (2010) Deregulation of sphingolipid metabolism in Alzheimer's disease. *Neurobiology of Aging* 31: 398-408.

Henry S L, Bensley J G, Wood-Bradley R J, Cullen-McEwen L A, Bertram J F & Armitage J A (2012) White adipocytes: More than just fat depots. *The International Journal of Biochemistry & Cell Biology* 44: 435-440.

Hodson L, Skeaff C M & Fielding B A (2008) Fatty acid composition of adipose tissue and blood in humans and its use as a biomarker of dietary intake. *Progress in Lipid Research* 47: 348-380.

Holland W L & Summers S A (2008) Sphingolipids, insulin resistance, and metabolic disease: New insights from in vivo manipulation of sphingolipid metabolism. *Endocrine Reviews* 29: 381-402.

Hornstra G, Al M D M, von Houwelingen A C & Foreman-van Drongelen M M H P (1995) Essential Fatty-Acids in Pregnancy and Early Human-Development. *European Journal of Obstetrics Gynecology and Reproductive Biology* 61: 57-62.

Houten S M & Wanders R J A (2010) A general introduction to the biochemistry of mitochondrial fatty acid β-oxidation. *Journal of Inherited Metabolic Disease* 33: 469-477.

Hu C, van der Heijden R, Wang M, van der Greef J, Hankemeier T & Xu G (2009) Analytical strategies in lipidomics and applications in disease biomarker discovery. *Journal of Chromatography B* 877: 2836-2846.

Hu C, van Dommelen J, van der Heijden R, Spijksma G, Reijmers T H, Wang M, Slee E, Lu X, Xu G, van der Greef J & Hankemeier T (2008) RPLC-ion-trap-FTMS method for lipid profiling of plasma: Method validation and application to p53 mutant mouse model. *Journal of Proteome Research* 7: 4982-4991.

Hui D Y, Labonté E D & Howles P N (2008) Development and Physiological Regulation of Intestinal Lipid Absorption. III. Intestinal transporters and cholesterol absorption. *American Journal of Physiology - Gastrointestinal and Liver Physiology* 294: G839-G843.

Hänninen T, Hallikainen M, Tuomainen S, Vanhanen M & Soininen H (2002) Prevalence of mild cognitive impairment: a population-based study in elderly subjects. *Acta Neurologica Scandinavica* 106: 148-154.

Inouye M, Kettunen J, Soininen P, Silander K, Ripatti S, Kumpula L S, Hämäläinen E, Jousilahti P, Kangas A J, Männistö S, Savolainen M J, Jula A, Leiviskä J, Palotie A, Salomaa V, Perola M, Ala-Korpela M & Peltonen L (2010) Metabonomic, transcriptomic, and genomic variation of a population cohort. *Molecular Systems Biology* 6: Article ID 441.

International Consortium for Blood Pressure Genome-Wide Association Studies (2011) Genetic variants in novel pathways influence blood pressure and cardiovascular disease risk. *Nature* 478: 103-109.

Iqbal J & Hussain M M (2009) Intestinal lipid absorption. *American Journal of Physiology-Endocrinology and Metabolism* 296: E1183-E1194.

Jakobsson A, Westerberg R & Jacobsson A (2006) Fatty acid elongases in mammals: Their regulation and roles in metabolism. *Progress in Lipid Research* 45: 237-249.

Jang J-H, Lee C S, Hwang D & Ryu S H (2012) Understanding of the roles of phospholipase D and phosphatidic acid through their binding partners. *Progress in Lipid Research* 51: 71-81.

Jeyarajah E J, Cromwell W C & Otvos J D (2006) Lipoprotein particle analysis by nuclear magnetic resonance spectroscopy. *Clinics in Laboratory Medicine* 26: 847-870.

Jicha G A & Markesbery W R (2010) Omega-3 fatty acids: potential role in the management of early Alzheimer´s disease. *Clinical Interventions in Aging* 5: 45-61.

Jukarainen N M, Korhonen S P, Laakso M P, Korolainen M A, Niemitz M, Soininen P P, Tuppurainen K, Vepsäläinen J, Pirttilä T & Laatikainen R (2008) Quantification of H-1 NMR spectra of human cerebrospinal fluid: a protocol based on constrained total-line-shape analysis. *Metabolomics* 4: 150-160.

Jump D B & Clarke S D (1999) Regulation of gene expression by dietary fat. *Annu. Rev. Nutr.* 19: 63-90.

Jump D B (2004) Fatty acid regulation of gene transcription. *Critical Reviews in Clinical Laboratory Sciences* 41: 41-78.

Kaluzny M A, Duncan L A, Merritt M V & Epps D E (1985) Rapid separation of lipid classes in high yield and purity using bonded phase columns. *Journal of Lipid Research* 26: 135-140.

Kang D W, Choi K-Y & Min D S (2011) Phospholipase D Meets Wnt Signaling: A New Target for Cancer Therapy. *Cancer Research* 71: 293-297.

Karantonis H C, Nomikos T & Demopoulos C A (2009) Triacylglycerol metabolism. *Current Drug Targets* 10: 302-319.

Kawashima A, Sugawara S, Okita M, Akahane T, Fukui K, Hashiuchi M, Kataoka C & Tsukamoto I (2009) Plasma fatty acid composition, estimated desaturase activities, and intakes of energy and nutrient in Japanese men with abdominal obesity or metabolic syndrome. *Journal of Nutritional Science and Vitaminology* 55: 400-406.

Kennedy A, Martinez K, Chuang C-C, LaPoint K & McIntosh M (2009) Saturated Fatty Acid-Mediated Inflammation and Insulin Resistance in Adipose Tissue: Mechanisms of Action and Implications. *Journal of Nutrition* 139: 1-4.

Kettunen J, Tukiainen T, Sarin A P, Ortega-Alonso A, Tikkanen E, Lyytikainen L P, Kangas A J, Soininen P, Würtz P, Silander K, Dick D M, Rose R J, Savolainen M J, Viikari J, Kähönen M, Lehtimäki T,

Pietiläinen K H, Inouye M, McCarthy M I, Jula A, Eriksson J, Raitakari O T, Salomaa V, Kaprio J, Järvelin M-R, Peltonen L, Perola M, Freimer N B, Ala-Korpela M, Palotie A & Ripatti S (2012) Genome-wide association study identifies multiple loci influencing human serum metabolite levels. *Nature Genetics* 44: 269-U65.

Khalil M B, Hou W, Zhou H, Elisma F, Swayne L A, Blanchard A P, Yao Z, Bennett S A L & Figeys D (2010) Lipidomics era: Accomplishments and challenges. *Mass Spectrometry Reviews* 29: 877-929.

Khan A, Tania M, Zhang D & Chen H (2010) Antioxidant enzymes and cancer. *Chinese Journal of Cancer Research* 22: 87-92.

Kivipelto M & Solomon A (2006) Cholesterol as a risk factor for Alzheimer's disease – epidemiological evidence. *Acta Neurologica Scandinavica* 114 (Suppl. 185): 50-57.

Kolter T & Sandhoff K (2006) Sphingolipid metabolism diseases. *Biochimica et Biophysica Acta* 1758: 2057-2079.

Kolter T & Sandhoff K (2010) Lysosomal degradation of membrane lipids. *FEBS Letters* 584: 1700-1712.

Kontush A & Chapman M J (2010) Lipidomics as a tool for the study of lipoprotein metabolism. *Current Atherosclerosis Reports* 12: 194-201.

Kotronen A, Seppänen-Laakso T, Westerbacka J, Kiviluoto T, Arola J, Ruskeepää A L, Yki-Järvinen H & Orešic M (2010) Comparison of Lipid and Fatty Acid Composition of the Liver, Subcutaneous and Intra-abdominal Adipose Tissue, and Serum. *Obesity* 18: 937-944.

Kriat M, Vion-Dury J, Confort-Gouny S, Favre R, Viout P, Sciaky M, Sari H & Cozzone P J (1993) Analysis of Plasma-Lipids by Nmr-Spectroscopy - Application to Modifications Induced by Malignant-Tumors. *Journal of Lipid Research* 34: 1009-1019.

Laatikainen R, Niemitz M, Weber U, Sundelin J, Hassinen T & Vepsäläinen J (1996a) General strategies for total-lineshape-type spectral analysis of NMR spectra using integral-transform iterator. *Journal of Magnetic Resonance, Series A* 120: 1-10.

Laatikainen R, Niemitz M, Malaisse W J, Biesemans M & Willem R (1996b) A computational strategy for the deconvolution of NMR spectra with multiplet structures and constraints: Analysis of overlapping C-13-H-2 multiplets of C-13 enriched metabolites from cell suspensions incubated in deuterated media. *Magnetic Resonance in Medicine* 36: 359-365.

Laatikainen R, Niemitz M, Korhonen S-P, Hassinen T & Venäläinen T (2011) *PERCH NMR Software,* http://www.perchsolutions.com.

Lafontan M & Langin D (2009) Lipolysis and lipid mobilization in human adipose tissue. *Progress in Lipid Research* 48: 275-297.

Langeveld M & Aerts J M F G (2009) Glycosphingolipids and insulin resistance. *Progress in Lipid Research* 48: 196-205.

Leaf A (2001) Plasma nonesterified fatty acid concentration as a risk factor for sudden cardiac death: The Paris prospective study. *Circulation* 104: 744-745.

Leopold J A & Loscalzo J (2009) Oxidative risk for atherothrombotic cardiovascular disease. *Free Radical Biology and Medicine* 47: 1673-1706.

Li T & Chiang J Y L (2009) Regulation of Bile Acid and Cholesterol Metabolism by PPARs. *Ppar Research* 2009: Article ID 501739.

Liaw A & Wiener M (2002) Classification and regression by randomForest. *R News* 2: 18-22.

Linderborg K M & Kallio H P T (2005) Triacylglycerol fatty acid positional distribution and postprandial lipid metabolism. *Food Reviews International* 21: 331-355.

Liu Y, Chen T, Qiu Y, Cheng Y, Cao Y, Zhao A & Jia W (2011) An ultrasonication-assisted extraction and derivatization protocol for GC/TOFMS-based metabolite profiling. *Analytical and Bioanalytical Chemistry* 400: 1405-1417.

Lodge J K, Patel S U & Sadler P J (1993) Aldehydes from metal ion- and lipoxygenase-induced lipid peroxidation: detection by [1]H-n.m.r. spectroscopy. *Biochemical Journal* 289: 149-153.

Lodge J K, Sadler P J, Kus M L & Winyard P G (1995) Copper-induced LDL peroxidation investigated by ^{1}H-NMR spectroscopy. *Biochimica et Biophysica Acta* 1256: 130-140.

Lotito S B & Frei B (2006) Consumption of flavonoid-rich foods and increased plasma antioxidant capacity in humans: Cause, consequence, or epiphenomenon? *Free Radical Biology and Medicine* 41: 1727-1746.

Lounila J, Hiltunen Y, Tuppurainen K, Pulkkinen A & Laatikainen R (1999) Solvent dependence of rotational energetics and formyl-proton long-range spin-spin coupling behavior of 2,6-dichloro- and 2,6-dinitrobenzaldehydes using dipolar couplings and temperature

dependence of long-range couplings. *Canadian Journal of Chemistry-Revue Canadienne de Chimie* 77: 1788-1796.

Lusis A J (2000) Atherosclerosis. *Nature* 407: 233-241.

Lusis A J, Fogelman A M & Fonarow G C (2004) Genetic Basis of Atherosclerosis: Part I. *Circulation* 110: 1868-1873.

Lusis A J & Pajukanta P (2008) A treasure trove for lipoprotein biology. *Nature Genetics* 40: 129-130.

Mäkinen V-P, Soininen P, Forsblom C, Parkkonen M, Ingman P, Kaski K, Groop P H & Ala-Korpela M (2008) H-1 NMR metabonomics approach to the disease continuum of diabetic complications and premature death. *Molecular Systems Biology* 4: Article ID 167.

Mäkinen V-P, Tynkkynen T, Soininen P, Peltola T, Kangas A, Forsblom C, Thorn L, Kaski K, Laatikainen R, Ala-Korpela M & Groop P-H (2012a) Metabolic diversity of progressive kidney disease in 325 patients with type 1 diabetes (the FinnDiane Study). *Journal of Proteome Research* 11: 1782-1790.

Mäkinen V-P, Tynkkynen T, Soininen P, Forsblom C, Peltola T, Kangas A, Groop P-H & Ala-Korpela M (2012b) Sphingomyelin is associated with kidney disease in type 1 diabetes (The FinnDiane Study). *Metabolomics* 8: 369-375.

Mallat Z & Tedgui A (2001) Current Perspective on the Role of Apoptosis in Atherothrombotic Disease. *Circulation Research* 88: 998-1003.

Manach C, Scalbert A, Morand C, Rémésy C & Jiménez L (2004) Polyphenols: food sources and bioavailability. *American Journal of Clinical Nutrition* 79: 727-747.

Mangge H, Almer G, Truschnig-Wilders M, Schmidt A, Gasser R & Fuchs D (2010) Inflammation, Adiponectin, Obesity and Cardiovascular Risk. *Current Medicinal Chemistry* 17: 4511-4520.

Mansbach C M & Gorelick F (2007) Development and physiological regulation of intestinal lipid absorption. II. Dietary lipid absorption, complex lipid synthesis, and the intracellular packaging and secretion of chylomicrons. *American Journal of Physiology - Gastrointestinal and Liver Physiology* 293: G645-G650.

Martins I J, Hone E, Foster J K, Sünram-Lea S I, Gnjec A, Fuller S J, Nolan D, Gandy S E & Martins R N (2006) Apolipoprotein E, cholesterol metabolism, diabetes, and the convergence of risk factors

for Alzheimer's disease and cardiovascular disease. *Molecular Psychiatry* 11: 721-736.

Mathew A, Yoshida Y, Maekawa T & Sakthi Kumar D (2011) Alzheimer's disease: Cholesterol a menace? *Brain Research Bulletin* 86: 1-12.

Matyash V, Liebisch G, Kurzchalia T V, Shevchenko A & Schwudke D (2008) Lipid extraction by methyl-tert-butyl ether for high-throughput lipidomics. *Journal of Lipid Research* 49: 1137-1146.

Maxfield F R & Tabas I (2005) Role of cholesterol and lipid organization in disease. *Nature* 438: 612-621.

Mensink R P (2005) Metabolic and health effects of isomeric fatty acids. *Current Opinion in Lipidology* 16: 27-30.

Mensink R P & Nestel P (2009) Trans fatty acids and cardiovascular risk markers: does the source matter? *Current Opinion in Lipidology* 20: 1-2.

Meyer zu Heringdorf D, Himmel H M & Jakobs K H (2002) Sphingosylphosphorylcholine--biological functions and mechanisms of action. *Biochimica et Biophysica Acta* 1582: 178-189.

Mielke M M, Bandaru V V R, Haughey N J, Rabins P V, Lyketsos C G & Carlson M C (2010) Serum sphingomyelins and ceramides are early predictors of memory impairment. *Neurobiology of Aging* 31: 17-24.

Mladenka P, Zatloukalová L, Filipský T & Hrdina R (2010) Cardiovascular effects of flavonoids are not caused only by direct antioxidant activity. *Free Radical Biology and Medicine* 49: 963-975.

Moore K J & Tabas I (2011) Macrophages in the Pathogenesis of Atherosclerosis. *Cell* 145: 341-355.

Mozaffarian D (2006) Trans fatty acids - Effects on systemic inflammation and endothelial function. *Atherosclerosis Supplements* 7: 29-32.

Mu H & Høy C-E (2004) The digestion of dietary triacylglycerols. *Progress in Lipid Research* 43: 105-133.

Mukherji M, Schofield C J, Wierzbicki A S, Jansen G A, Wanders R J A & Lloyd M D (2003) The chemical biology of branched-chain lipid metabolism. *Progress in Lipid Research* 42: 359-376.

Mursu J, Voutilainen S, Nurmi T, Rissanen T H, Virtanen J K, Kaikkonen J, Nyyssönen K & Salonen J T (2004) Dark chocolate consumption increases HDL cholesterol concentration and chocolate

fatty acids may inhibit lipid peroxidation in healthy humans. *Free Radical Biology and Medicine* 37: 1351-1359.

Müller M, Schiller J, Petkovic M, Oehrl W, Heinze R, Wetzker R, Arnold K & Arnhold J (2001) Limits for the detection of (poly-)phosphoinositides by matrix-assisted laser desorption and ionization time-of-flight mass spectrometry (MALDI-TOF MS). *Chemistry and Physics of Lipids* 110: 151-164.

Nakajima K, Nakano T, Tokita Y, Nagamine T, Inazu A, Kobayashi J, Mabuchi H, Stanhope K L, Havel P J, Okazaki M, Ai M & Tanaka A (2011) Postprandial lipoprotein metabolism: VLDL vs chylomicrons. *Clinica Chimica Acta* 412: 1306-1318.

Nelson D L & Cox M M (2000) *Lehninger principles of biochemistry*. Worth, New York.

Niki E, Yoshida Y, Saito Y & Noguchi N (2005) Lipid peroxidation: Mechanisms, inhibition, and biological effects. *Biochemical and Biophysical Research Communications* 338: 668-676.

Niki E (2009) Lipid peroxidation: Physiological levels and dual biological effects. *Free Radical Biology and Medicine* 47: 469-484.

Niot I, Poirier H, Tran T T T & Besnard P (2009) Intestinal absorption of long-chain fatty acids: Evidence and uncertainties. *Progress in Lipid Research* 48: 101-115.

Nixon G F, Mathieson F A & Hunter I (2008) The multi-functional role of sphingosylphosphorylcholine. *Progress in Lipid Research* 47: 62-75.

Novgorodtseva T P, Karaman Y K, Zhukova N V, Lobanova E G, Antonyuk M V & Kantur T A (2011) Composition of fatty acids in plasma and erythrocytes and eicosanoids level in patients with metabolic syndrome. *Lipids in Health and Disease* 10: Article ID 82.

Nyyssönen K, Porkkala-Sarataho E, Kaikkonen J & Salonen J T (1997) Ascorbate and urate are the strongest determinants of plasma antioxidative capacity and serum lipid resistance to oxidation in Finnish men. *Atherosclerosis* 130: 223-233.

Ogura T, Takada H, Okuno M, Kitade H, Matsuura T, Kwon M, Arita S, Hamazaki K, Itomura M & Hamazaki T (2010) Fatty acid composition of plasma, erythrocytes and adipose: Their correlations and effects of age and sex. *Lipids* 45: 137-144.

Olofsson S-O, Stillemark-Billton P & Asp L (2000) Intracellular assembly of VLDL - Two major steps in separate cell compartments. *Trends in Cardiovascular Medicine* 10: 338-345.

Oostendorp M, Engelke U F H, Willemsen M A A P & Wevers R A (2006) Diagnosing inborn errors of lipid metabolism with proton nuclear magnetic resonance spectroscopy. *Clinical Chemistry* 52: 1395-1405.

Opara E C (2006) Oxidative stress. *Disease-a-Month* 52: 183-198.

Ordovas J M (2003) Lipoproteins. In Benjamin C (Ed) *Encyclopedia of Food Sciences and Nutrition (Second Edition)*. Academic Press, Oxford, pp. 3543-3552.

Orešic M, Simell S, Sysi-Aho M, Näntö-Salonen K, Seppänen-Laakso T, Parikka V, Katajamaa M, Hekkala A, Mattila I, Keskinen P, Yetukuri L, Reinikainen A, Lähde J, Suortti T, Hakalax J, Simell T, Hyöty H, Veijola R, Ilonen J, Lahesmaa R, Knip M & Simell O (2008) Dysregulation of lipid and amino acid metabolism precedes islet autoimmunity in children who later progress to type 1 diabetes. *The Journal of Experimental Medicine* 205: 2975-2984.

Otieno A C & Mwongela S M (2008) Capillary electrophoresis-based methods for the determination of lipids - A review. *Analytica Chimica Acta* 624: 163-174.

Otvos J D, Jeyarajah E J, Bennett D W & Krauss R M (1992) Development of a proton nuclear magnetic resonance spectroscopic method for determining plasma lipoprotein concentrations and subspecies distributions from a single, rapid measurement. *Clinical Chemistry* 38: 1632-1638.

Panda T, Basak T, Saraswathi G & Théodore T (2011) Kinetic Mechanisms of Cholesterol Synthesis: A Review. *Industrial & Engineering Chemistry Research* 50: 12847-12864.

Pang L-Q, Liang Q-L, Wang Y-M, Ping L & Luo G-A (2008) Simultaneous determination and quantification of seven major phospholipid classes in human blood using normal-phase liquid chromatography coupled with electrospray mass spectrometry and the application in diabetes nephropathy. *Journal of Chromatography B-Analytical Technologies in the Biomedical and Life Sciences* 869: 118-125.

Patel P S, Sharp S J, Jansen E, Luben R N, Khaw K T, Wareham N J & Forouhi N G (2010) Fatty acids measured in plasma and erythrocyte-membrane phospholipids and derived by food-frequency questionnaire and the risk of new-onset type 2 diabetes: a pilot study in the European Prospective Investigation into Cancer and Nutrition

(EPIC)–Norfolk cohort. *American Journal of Clinical Nutrition* 92: 1214-1222.

Peterson B L & Cummings B S (2006) A review of chromatographic methods for the assessment of phospholipids in biological samples. *Biomedical Chromatography* 20: 227-243.

Pietiläinen K H, Sysi-Aho M, Rissanen A, Seppänen-Laakso T, Yki-Järvinen H, Kaprio J & Orešic M (2007) Acquired Obesity Is Associated with Changes in the Serum Lipidomic Profile Independent of Genetic Effects - A Monozygotic Twin Study. *Plos One* 2: Article ID e218.

Pollesello P, Eriksson O & Höckerstedt K (1996) Analysis of total lipid extracts from human liver by C-13 and H-1 nuclear magnetic resonance spectroscopy. *Analytical Biochemistry* 236: 41-48.

Poudyal H, Panchal S K, Diwan V & Brown L (2011) Omega-3 fatty acids and metabolic syndrome: Effects and emerging mechanisms of action. *Progress in Lipid Research* 50: 372-387.

Prescott S M, Zimmerman G A, Stafforini D M & McIntyre T M (2000) Platelet-activating factor and related lipid mediators. *Annual Review of Biochemistry* 69: 419-445.

Quehenberger O, Armando A M, Brown A H, Milne S B, Myers D S, Merrill A H, Bandyopadhyay S, Jones K N, Kelly S, Shaner R L, Sullards C M, Wang E, Murphy R C, Barkley R M, Leiker T J, Raetz C R H, Guan Z, Laird G M, Six D A, Russell D W, McDonald J G, Subramaniam S, Fahy E & Dennis E A (2010) Lipidomics reveals a remarkable diversity of lipids in human plasma. *Journal of Lipid Research* 51: 3299-3305.

Quehenberger O & Dennis E A (2011) Mechanisms of Disease the Human Plasma Lipidome. *New England Journal of Medicine* 365: 1812-1823.

Quehenberger O, Armando A M & Dennis E A (2011) High sensitivity quantitative lipidomics analysis of fatty acids in biological samples by gas chromatography–mass spectrometry. *Biochimica et Biophysica Acta* 1811: 648-656.

R Development Core Team (2008) *R: A language and environment for statistical computing*. R Foundation for Statistical Computing, Vienna.

Raclot T (2003) Selective mobilization of fatty acids from adipose tissue triacylglycerols. *Progress in Lipid Research* 42: 257-288.

Rader D J & Daugherty A (2008) Translating molecular discoveries into new therapies for atherosclerosis. *Nature* 451: 904-913.

Rains J L & Jain S K (2011) Oxidative stress, insulin signaling, and diabetes. *Free Radical Biology and Medicine* 50: 567-575.

Ramos P, Gieseg S P, Schuster B & Esterbauer H (1995) Effect of temperature and phase-transition on oxidation resistance of low-density-lipoprotein. *Journal of Lipid Research* 36: 2113-2128.

Ratnayake W M N & Galli C (2009) Fat and fatty acid terminology, methods of analysis and fat digestion and metabolism: A background review paper. *Annals of Nutrition & Metabolism* 55: 8-43.

Reddy J K & Hashimoto T (2001) Peroxisomal β-oxidation and peroxisome proliferator-activated receptor α: An adaptive metabolic system. *Annual Review of Nutrition* 21: 193-230.

Redgrave T G (2004) Chylomicron metabolism. *Biochemical Society Transactions* 32: 79-82.

Reid P C, Urano Y, Kodama T & Hamakubo T (2007) Alzheimer's Disease: cholesterol, membrane rafts, isoprenoids and statins. *Journal of Cellular and Molecular Medicine* 11: 383-392.

Richmond G S & Smith T K (2011) Phospholipases A_1. *International Journal of Molecular Sciences* 12: 588-612.

Rinaldo P, Matern D & Bennett M J (2002) Fatty acid oxidation disorders. *Annual Review of Physiology* 64: 477-502.

Risé P, Eligini S, Ghezzi S, Colli S & Galli C (2007) Fatty acid composition of plasma, blood cells and whole blood: Relevance for the assessment of the fatty acid status in humans. *Prostaglandins Leukotrienes and Essential Fatty Acids* 76: 363-369.

Risérus U, Willett W C & Hu F B (2009) Dietary fats and prevention of type 2 diabetes. *Progress in Lipid Research* 48: 44-51.

Roberts L D, McCombie G, Titman C M & Griffin J L (2008) A matter of fat: An introduction to lipidomic profiling methods. *Journal of Chromatography B-Analytical Technologies in the Biomedical and Life Sciences* 871: 174-181.

Roman R J (2002) P-450 metabolites of arachidonic acid in the control of cardiovascular function. *Physiological Reviews* 82: 131-185.

Roncalli J, Smih F, Desmoulin F, Dumonteil N, Harmancey R, Hennig S, Perez L, Pathak A, Galinier M, Massabuau P, Malet-Martino M, Senard J M & Rouet P (2007) NMR and cDNA array analysis prior to heart failure reveals an increase of unsaturated lipids, a

glutamine/glutamate ratio decrease and a specific transcriptome adaptation in obese rat heart. *Journal of Molecular and Cellular Cardiology* 42: 526-539.

Ross R (1999) Atherosclerosis – An inflammatory disease. *New England Journal of Medicine* 340: 115-126.

Ruiz-Gutiérrez V & Pérez-Camino M C (2000) Update on solid-phase extraction for the analysis of lipid classes and related compounds. *Journal of Chromatography A* 885: 321-341.

Ruiz-Rodriguez A, Reglero G & Ibañez E (2010) Recent trends in the advanced analysis of bioactive fatty acids. *Journal of Pharmaceutical and Biomedical Analysis* 51: 305-326.

Rye K-A, Bursill C A, Lambert G, Tabet F & Barter P J (2009) The metabolism and anti-atherogenic properties of HDL. *Journal of Lipid Research* 50: S195-S200.

Sandra K, Pereira A D, Vanhoenacker G, David F & Sandra P (2010) Comprehensive blood plasma lipidomics by liquid chromatography/quadrupole time-of-flight mass spectrometry. *Journal of Chromatography A* 1217: 4087-4099.

Schiller J, Arnhold J, Benard S, Müller M, Reichl S & Arnold K (1999) Lipid analysis by matrix-assisted laser desorption and ionization mass spectrometry: A methodological approach. *Analytical Biochemistry* 267: 46-56.

Schiller J, Süß R, Arnhold J, Fuchs B, Leßig J, Müller M, Petkovic M, Spalteholz H, Zschörnig O & Arnold K (2004) Matrix-assisted laser desorption and ionization time-of-flight (MALDI-TOF) mass spectrometry in lipid and phospholipid research. *Progress in Lipid Research* 43: 449-488.

Schneider C, Pratt D A, Porter N A & Brash A R (2007) Control of Oxygenation in Lipoxygenase and Cyclooxygenase Catalysis. *Chemistry & Biology* 14: 473-488.

Schnitzer E, Pinchuk I, Bor A, Fainaru M, Samuni A M & Lichtenberg D (1998) Lipid oxidation in unfractionated serum and plasma. *Chemistry and Physics of Lipids* 92: 151-170.

Schupp M & Lazar M A (2010) Endogenous Ligands for Nuclear Receptors: Digging Deeper. *Journal of Biological Chemistry* 285: 40409-40415.

Shibata N & Glass C K (2010) Macrophages, oxysterols and atherosclerosis. *Circulation Journal* 74: 2045-2051.

Shindou H & Shimizu T (2009) Acyl-CoA:Lysophospholipid acyltransferases. *Journal of Biological Chemistry* 284: 1-5.

Shobab L A, Hsiung G-Y R & Feldman H H (2005) Cholesterol in Alzheimer's disease. *The Lancet Neurology* 4: 841-852.

Simons K & Vaz W L C (2004) Model systems, lipid rafts, and cell membranes. *Annual Review of Biophysics and Biomolecular Structure* 33: 269-295.

Singh A K & Jiang Y (1995) Quantitative chromatographic analysis of inositol phospholipids and related compounds. *Journal of Chromatography B: Biomedical Sciences and Applications* 671: 255-280.

Skyrme-Jones R A P, O'Brien R C, Luo M & Meredith I T (2000) Endothelial vasodilator function is related to low-density lipoprotein particle size and low-density lipoprotein vitamin E content in type 1 diabetes. *Journal of the American College of Cardiology* 35: 292-299.

Smit E N, Muskiet F A J & Boersma E R (2004) The possible role of essential fatty acids in the pathophysiology of malnutrition: a review. *Prostaglandins Leukotrienes and Essential Fatty Acids* 71: 241-250.

Smith S (1994) The animal fatty acid synthase: one gene, one polypeptide, seven enzymes. *The FASEB Journal* 8: 1248-1259.

Soininen P, Haarala J, Vepsäläinen J, Niemitz M & Laatikainen R (2005) Strategies for organic impurity quantification by ^{1}H NMR spectroscopy: Constrained total-line-shape fitting. *Analytica Chimica Acta* 542: 178-185.

Soininen P, Öörni K, Maaheimo H, Laatikainen R, Kovanen P T, Kaski K & Ala-Korpela M (2007) ^{1}H NMR at 800 MHz facilitates detailed phospholipid follow-up during atherogenic modifications in low density lipoproteins. *Biochemical and Biophysical Research Communications* 360: 290-294.

Soininen P, Kangas A J, Würtz P, Tukiainen T, Tynkkynen T, Laatikainen R, Järvelin M R, Kähönen M, Lehtimäki T, Viikari J, Raitakari O T, Savolainen M J & Ala-Korpela M (2009) High-throughput serum NMR metabonomics for cost-effective holistic studies on systemic metabolism. *The Analyst* 134: 1781-1785.

Sommer U, Herscovitz H, Welty F K & Costello C E (2006) LC-MS-based method for the qualitative and quantitative analysis of complex lipid mixtures. *Journal of Lipid Research* 47: 804-814.

Sorensen C M, Ding J, Zhang Q B, Alquier T, Zhao R, Mueller P W, Smith R D & Metz T O (2010) Perturbations in the lipid profile of individuals with newly diagnosed type 1 diabetes mellitus: Lipidomics analysis of a Diabetes Antibody Standardization Program sample subset. *Clinical Biochemistry* 43: 948-956.

Spranger T, Finckh B, Fingerhut R, Kohlschütter A, Beisiegel U & Kontush A (1998) How different constituents of human plasma and low density lipoprotein determine plasma oxidizability by copper. *Chemistry and Physics of Lipids* 91: 39-52.

Srivastava N K, Pradhan S, Mittal B & Gowda G A N (2010a) High resolution NMR based analysis of serum lipids in Duchenne muscular dystrophy patients and its possible diagnostic significance. *NMR in Biomedicine* 23: 13-22.

Srivastava N K, Pradhan S, Gowda G A N & Kumar R (2010b) In vitro, high-resolution ^{1}H and ^{31}P NMR based analysis of the lipid components in the tissue, serum, and CSF of the patients with primary brain tumors: one possible diagnostic view. *NMR in Biomedicine* 23: 113-122.

Srivastava S & Govil G (2001) Application of NMR to the study of cells and body fluids. *Current Organic Chemistry* 5: 1039-1057.

Stübiger G, Pittenauer E, Belgacem O, Rehulka P, Widhalm K & Allmaier G (2009) Analysis of human plasma lipids and soybean lecithin by means of high-performance thin-layer chromatography and matrix-assisted laser desorption/ionization mass spectrometry. *Rapid Communications in Mass Spectrometry* 23: 2711-2723.

Suna T, Salminen A, Soininen P, Laatikainen R, Ingman P, Mäkelä S, Savolainen M J, Hannuksela M L, Jauhiainen M, Taskinen M-R, Kaski K & Ala-Korpela M (2007) ^{1}H NMR metabonomics of plasma lipoprotein subclasses: elucidation of metabolic clustering by self-organising maps. *NMR in Biomedicine* 20: 658-672.

Taskinen M-R (2003) Diabetic dyslipidaemia: from basic research to clinical practice. *Diabetologia* 46: 733-749.

Thomas L L, Christakis T J & Jorgensen W L (2006) Conformation of Alkanes in the Gas Phase and Pure Liquids. *The Journal of Physical Chemistry B* 110: 21198-21204.

Thompson A K, Minihane A M & Williams C M (2011) Trans fatty acids, insulin resistance and diabetes. *European Journal of Clinical Nutrition* 65: 553-564.

Torsdottir G, Kristinsson J, Snaedal J, Sveinbjörnsdóttir S, Gudmundsson G, Hreidarsson S & Jóhannesson T (2010) Case-control studies on ceruloplasmin and superoxide dismutase (SOD1) in neurodegenerative diseases: A short review. *Journal of the Neurological Sciences* 299: 51-54.

Touchstone J C (1995) Thin-Layer Chromatographic Procedures for Lipid Separation. *Journal of Chromatography B-Biomedical Applications* 671: 169-195.

Tukiainen T, Tynkkynen T, Mäkinen V-P, Jylänki P, Kangas A, Hokkanen J, Vehtari A, Gröhn O, Hallikainen M, Soininen H, Kivipelto M, Groop P H, Kaski K, Laatikainen R, Soininen P, Pirttilä T & Ala-Korpela M (2008) A multi-metabolite analysis of serum by H-1 NMR spectroscopy: Early systemic signs of Alzheimer's disease. *Biochemical and Biophysical Research Communications* 375: 356-361.

Tukiainen T, Kettunen J, Kangas A J, Lyytikäinen L P, Soininen P, Sarin A P, Tikkanen E, O'Reilly P F, Savolainen M J, Kaski K, Pouta A, Jula A, Lehtimäki T, Kähönen M, Viikari J, Taskinen M-R, Jauhiainen M, Eriksson J G, Raitakari O, Salomaa V, Järvelin M-R, Perola M, Palotie A, Ala-Korpela M & Ripatti S (2012) Detailed metabolic and genetic characterization reveals new associations for 30 known lipid loci. *Human Molecular Genetics* 21: 1444-1455.

Uppu R M, Cueto R, Squadrito G L & Pryor W A (1995) What Does Ozone React with at the Air Lung Interface? Model Studies Using Human Red Blood Cell Membranes. *Archives of Biochemistry and Biophysics* 319: 257-266.

van Heyningen C (2005) Lipid metabolism: lipoproteins in the metabolic syndrome and subclass sex and age differences. *Current Opinion in Lipidology* 16: 119-120.

Vanhala M, Saltevo J, Soininen P, Kautiainen H, Kangas A J, Ala-Korpela M & Mäntyselkä P (2012) Serum omega-6 polyunsaturated fatty acids and the metabolic syndrome: A longitudinal population-based cohort study. *American Journal of Epidemiology* (in press).

Vehtari A, Mäkinen V-P, Soininen P, Ingman P, Mäkela S M, Savolainen M J, Hannuksela M L, Kaski K & Ala-Korpela M (2007) A novel Bayesian approach to quantify clinical variables and to determine their spectroscopic counterparts in ^{1}H NMR metabonomic data. *BMC Bioinformatics* 8: Article ID S8.

Vergès B (2009a) Lipid disorders in type 1 diabetes. *Diabetes & Metabolism* 35: 353-360.

Vergès B (2009b) Lipid modification in type 2 diabetes: the role of LDL and HDL. *Fundamental & Clinical Pharmacology* 23: 681-685.

Vessby B, Gustafsson I B, Tengblad S, Boberg M & Andersson A (2002) Desaturation and elongation of fatty acids and insulin action. *Annals of the New York Academy of Sciences* 967: 183-195.

Vessby B (2003) Dietary fat, fatty acid composition in plasma and the metabolic syndrome. *Current Opinion in Lipidology* 14: 15-19.

Wallis J G, Watts J L & Browse J (2002) Polyunsaturated fatty acid synthesis: what will they think of next? *Trends in Biochemical Sciences* 27: 467-473.

Wanders R J A, Jansen G A & Lloyd M D (2003) Phytanic acid alpha-oxidation, new insights into an old problem: a review. *Biochimica et Biophysica Acta* 1631: 119-135.

Wanders R J A & Waterham H R (2006) Biochemistry of mammalian peroxisomes revisited. *Annual Review of Biochemistry* 75: 295-332.

Wanders R J A, Komen J & Kemp S (2011) Fatty acid omega-oxidation as a rescue pathway for fatty acid oxidation disorders in humans. *Febs Journal* 278: 182-194.

Wang Y, Krull I S, Liu C & Orr J D (2003) Derivatization of phospholipids. *Journal of Chromatography B* 793: 3-14.

Warensjö E, Öhrvall M & Vessby B (2006) Fatty acid composition and estimated desaturase activities are associated with obesity and lifestyle variables in men and women. *Nutrition Metabolism and Cardiovascular Diseases* 16: 128-136.

Weggemans R M, Rudrum M & Trautwein E A (2004) Intake of ruminant versus industrial trans fatty acids and risk of coronary heart disease ΓÇô what is the evidence? *European Journal of Lipid Science and Technology* 106: 390-397.

Wenk M R (2005) The emerging field of lipidomics. *Nature Reviews Drug Discovery* 4: 594-610.

White T, Bursten S, Federighi D, Lewis R A & Nudelman E (1998) High-resolution separation and quantification of neutral lipid and phospholipid species in mammalian cells and sera by multi-one-dimensional thin-layer chromatography. *Analytical Biochemistry* 258: 109-117.

Wiesner P, Leidl K, Boettcher A, Schmitz G & Liebisch G (2009) Lipid profiling of FPLC-separated lipoprotein fractions by electrospray ionization tandem mass spectrometry. *Journal of Lipid Research* 50: 574-585.

Willker W & Leibfritz D (1998) Assignment of mono- and polyunsaturated fatty acids in lipids of tissues and body fluids. *Magnetic Resonance in Chemistry* 36: S79-S84.

Wright E, Scism-Bacon J L & Glass L C (2006) Oxidative stress in type 2 diabetes: the role of fasting and postprandial glycaemia. *International Journal of Clinical Practice* 60: 308-314.

Würtz P, Soininen P, Kangas A J, Mäkinen V-P, Groop P-H, Savolainen M J, Juonala M, Viikari J S, Kähönen M, Lehtimäki T, Raitakari O T & Ala-Korpela M (2011) Characterization of systemic metabolic phenotypes associated with subclinical atherosclerosis. *Molecular BioSystems* 7: 385-393.

Würtz P, Raiko J R, Magnussen C G, Soininen P, Kangas A J, Tynkkynen T, Thomson R, Laatikainen R, Savolainen M J, Laurikka J, Kuukasjärvi P, Tarkka M, Karhunen P J, Jula A, Viikari J S, Kähönen M, Lehtimäki T, Juonala M, Ala-Korpela M & Raitakari O T (2012) High-throughput quantification of circulating metabolites improves prediction of subclinical atherosclerosis. *European Heart Journal* (in press).

Yang G, Badeanlou L, Bielawski J, Roberts A J, Hannun Y A & Samad F (2009) Central role of ceramide biosynthesis in body weight regulation, energy metabolism, and the metabolic syndrome. *American Journal of Physiology-Endocrinology and Metabolism* 297: E211-E224.

Yatomi Y, Ohmori T, Rile G, Kazama F, Okamoto H, Sano T, Satoh K, Kume S, Tigyi G, Igarashi Y & Ozaki Y (2000) Sphingosine 1-phosphate as a major bioactive lysophospholipid that is released from platelets and interacts with endothelial cells. *Blood* 96: 3431-3438.

Yen C-L E, Stone S J, Koliwad S, Harris C & Farese R V (2008) Thematic review series: Glycerolipids. DGAT enzymes and triacylglycerol biosynthesis. *Journal of Lipid Research* 49: 2283-2301.

Yin H Y & Porter N A (2005) New insights regarding the autoxidation of polyunsaturated fatty acids. *Antioxidants & Redox Signaling* 7: 170-184.

Yin H, Xu L & Porter N A (2011) Free radical lipid peroxidation: Mechanisms and analysis. *Chemical Reviews* 111: 5944-5972.

Yu Z H, Kastenmüller G, He Y, Belcredi P, Möller G, Prehn C, Mendes J, Wahl S, Roemisch-Margl W, Ceglarek U, Polonikov A, Dahmen N, Prokisch H, Xie L, Li Y, Wichmann H E, Peters A, Kronenberg F, Suhre K, Adamski J, Illig T & Wang-Sattler R (2011) Differences between Human Plasma and Serum Metabolite Profiles. *Plos One* 6: Article ID e21230.

Yuen A K L, Lafon O, Charpentier T, Roy M, Brunet F, Berthault P, Sakellariou D, Robert B, Rimsky S, Pillon F, Cintrat J-C & Rousseau B (2010) Measurement of Long-Range Interatomic Distances by Solid-State Tritium-NMR Spectroscopy. *Journal of the American Chemical Society* 132: 1734-1735.

Zechner R, Kienesberger P C, Haemmerle G, Zimmermann R & Lass A (2009) Adipose triglyceride lipase and the lipolytic catabolism of cellular fat stores. *Journal of Lipid Research* 50: 3-21.

Zehethofer N & Pinto D M (2008) Recent developments in tandem mass spectrometry for lipidomic analysis. *Analytica Chimica Acta* 627: 62-70.

Zeleniuch-Jacquotte A, Chajès V, Van Kappel A, Riboli E & Toniolo P (2000) Reliability of fatty acid composition in human serum phospholipids. *European Journal of Clinical Nutrition* 54: 367-372.

Zhu C, Hu P, Liang Q-L, Wang Y-M & Luo G-A (2009) Recent advances in lipidomics. *Chinese Journal of Analytical Chemistry* 37: 1390-1396.

Zlatanos S N, Laskaridis K & Sagredos A (2008) Conjugated linoleic acid content of human plasma. *Lipids in Health and Disease* 7: Article ID 34.

Tuulia Tynkkynen
¹H NMR Analysis of Serum Lipds

To deepen our understanding of the complex human lipid metabolism, simple, fast, and cost-effective methods to study the serum lipid profile are needed. This thesis presents a nuclear magnetic resonance (NMR) spectroscopy -based high-throughput method for the quantification of serum lipids, as well as a protocol to study the oxidation susceptibility of serum. The applications of the developed methods to clinical and nutritional studies are also discussed.

UNIVERSITY OF
EASTERN FINLAND